Molecular Substrate Design for the Selective Adhesion, Proliferation and Differentiation of Marrow Connective Tissue Progenitors

By

Ada Au

B.A.Sc. (Hon.) Engineering Science, University of Toronto, 1999

Submitted to the Biological Engineering Division in partial fulfillment of the requirements for the degree of

Doctor of Philosophy

at the

Massachusetts Institute of Technology

June, 2005
[September 2005]

Signature of author: _____
Biological Engineering Division

Certified by: _____
Linda Griffith, Professor of Biological and Mechanical Engineering, Thesis Advisor

Accepted by: _____
Douglas Lauffenburger, Professor and Director of Biological Engineering Division

Molecular Substrate Design for the Selective Adhesion, Proliferation and Differentiation of Marrow Connective Tissue Progenitors

by

Ada Au

Submitted to the Biological Engineering Division on June 10th, 2005 in Partial Fulfillment of the Requirements for the Degree of Doctor of Philosophy in Bioengineering

Abstract

A multi-faceted approach was applied to the molecular design of substrates for the selective adhesion, proliferation and differentiation of connective tissue progenitors (CTPs) from human bone marrow aspirates. The basic premise of the thesis is that integrin-specific adhesion peptides, when presented in a biophysically appropriate spatial arrangement against an inert background, allow enrichment of CTPs *in vitro*. Comb copolymer comprising a methyl methacrylate backbone with 10-mer poly(oxyethylene) sidechains was selected as the vehicle to present small adhesion peptides at the surface. This polymer shows excellent performance in cell resistance studies and offers sufficient functionalizable sites to create high local densities of ligands. Methods for preparing comb copolymer substrates with peptides in ~300 nm^2 clusters with inter-ligand spacings closer than integrins were developed. This nanometer-scale clustered presentation was favorable to integrin binding. Cells were more spread on RGD peptide substrates with a higher degree of nanoscale clustering but of the same overall peptide surface density as comparable substrates with lower degree of peptide clustering. We evaluated adhesion peptides for their ability to support CFU formation of marrow-derived CTPs using colony forming unit (CFU) assay. The results, analyzed with a statistical model implemented to capture characteristics of CFU assay, showed that while RGD substrates supported a moderate amount of alkaline phosphatase -positive CFU (CFU-AP) formation, the bone sialoprotein peptide FHRRIKA, and two $\alpha_4\beta_1$ peptides demonstrated the best performance in promoting CFU-AP formation. Patient variability in CFU data could be partially explained by the variations in marrow aspirate cell integrin expression, particularly α_5 and $\alpha_v\beta_3$. The high level of ECM protein association seen with aspirate cells, as revealed by immunoblotting, may inhibit cell adhesion and account for the fairly low CFU counts observed. Treatments of marrow aspirate with phosphate saline buffer (PBS) and RGD solution reduced a significant amount of protein

association. A comprehensive study showed that patients' marrow aspirates were naturally partitioned into two groups of very different colony formation behavior and integrin and AP expressions but consistency was observed within each group. Upon treatment of marrow cells with divalent ion-free PBS, CFU-AP formation on RGD substrates drastically increased in one group of patients. The designs and assays developed in this thesis could be applied for the further understanding of marrow aspirates, such as their interaction with a high-affinity $\alpha_5\beta_1$ peptide, and with that knowledge, further optimize the surface design of bone marrow grafts.

Thesis Advisor: Linda Griffith
Title: Professor of Biological and Mechanical Engineering

Acknowledgements

"Be warned, my son, of anything in addition to them. Of making many books there is no end, and much study wearies the body." (Ecclesiastes 12:12) Despite the weariness my body has endured as a result of this dissertation, I am thankful that my scientific pursuit as a doctoral student in MIT has been a journey of personal growth, for which I am indebted to many.

First, thank you to my advisor, Linda Griffith for giving me the many opportunities to learn and grow and the freedom to try and err. Your support during the last 6 months of my Ph.D. has been especially valuable and without which this thesis would not have happened. I also thank my thesis committee, Dane Wittrup, Anne Mayes and George Muschler for their invaluable suggestions and advices and critical reading of my thesis drafts. I would like to extend my special thanks to George Muschler, for all his insightful suggestions and comments during our video- or teleconference discussions, his thoroughness in going through experiment plans and data, and his hospitality during my visits to Cleveland were essential to the completion of this thesis. (Also thanks to Cathy for her gorgeous cooking when I was in Cleveland!)

I had the privilege to work with Cynthia Boehm of the Muschler lab. She is an individual who deserves one of my sincerest thanks. She has assisted me with the most tedious part of the bone marrow experiments. Without her, this thesis will not be possible and I really appreciate her efforts and carefulness. Past and present members of the Griffith and Lauffenburger Lab not only provided a terrific working environment but also essential research and personal support. Lily Koo always reminded me that God loves us for who we are and not what we do and I thank her very much for all the encouragement, support and prayers. Maria Ufret not only shared with me her expertise in peptides and chemistry, but we also shared a fun time in and outside of the lab. I am indebted to Will Kuhlman who knows almost everything in the lab and for sharing with me his comb polymers. Special thanks to Peter Woolf for the fruitful discussions and help in developing the statistical model for CFU assays. Also, it makes a big difference to have someone to graduate around the same time as I do - thanks to Ley Richardson for the mutual encouragement as we were cranking out the last sets of experiments and writing up our theses. I would also like to thank the several UROPs I had, Victoria Fan, Robert Leke, Christine Chiu and Mahreen Khan. Their hard work (especially in spincoating) and diligence allowed me to focus on the planning and interpretation of experiments. Staff from various MIT labs had provided invaluable technical help and support for my experiments. I would like to acknowledge Glenn Paradis for help with FACS experiments, staff from the Biopolymers Lab for peptide synthesis and Libby Shaw for help in x-ray photoelectron spectroscopy. Special thanks to Harutsugi Abukawa of the Vacanti Lab in MGH for harvesting and isolating the pig mesenchymal stem cells.

I am incredibly grateful to Yu-Ling Cheng and Michael Sefton of the University of Toronto for introducing me to research and giving me the confidence to go to MIT. Thanks particularly to Yu-Ling for her continual support and counsel all these years.

I also owe a deep thank you to the MIT Department of Music and Theater Arts, especially to William Cutter and David Deveau. Before I came to MIT, I never imagined I could pursue my musical interest at such a sophisticated level here. Thanks very much, Bill, for having so much faith in me and for the tremendous help and encouragement along my conducting quest. You have trained me from knowing almost nothing about conducting, to being accepted by the best graduate conducting programs in North America. David, thanks a lot for taking me into your studio and for all the music and times we have shared.

My deepest thanks go to my brothers and sisters in Christ who have given me much support in the Lord and prayed for me during all these years. The unfailing love and support from past and present members of the MIT HKSBS, especially Pearl (who is also my thesis delivery person in London!), Lotty, Becky, Edmond, Ernie, Connie, Bak-Fun and Mei-Kee have given me the strength to go through the valleys for the past 5.5 years. Pastor Joe Kok and Prisca, Pastor Perry Chow and in particular Peggy "c mo", you deserve a big thank you from the bottom of my heart! Not only you have nourished me with the Word of God, encouraged me to follow Christ, your love and support really warmed my heart. I also want to thank brothers and sisters from Boston Chinese Evangelical Church and Zion Alliance Church in Toronto for their friendship and prayers.

Mom and Dad, I cannot even find the words to express my deepest gratitude to you. You are always there for me, no matter where I go and in what I do. You have been a constant source of support to me in Christ. You have shown me a glimpse of how much God loves me. Grandma and Auntie Jocelyn, I wish you were here for this day. I miss both of you dearly.

"Through many dangers, toils and snares,
I have already come;
'Tis grace hath brought me safe thus far,
And grace will lead me home.

The Lord has promised good to me,
His Word my hope secures;
He will my Shield and Portion be,
As long as life endures."

Soli Deo Gloria

Table of Contents

Chapter 1

Introduction and background

1.1 Current bone graft technology

Over 1 million bone grafting procedures are performed annually in the United States to treat acute fractures, bone defects, fracture non-union and other problems associated with bone. Roughly fifty percent of these procedures involve the use of autogenous bone graft. Autogenous bone has proved to be highly successful due to the transfer of osteoprogenitor cells, its osteoinductive and osteoconductive capacity, as well as its mechanical properties (Burwell, 1994a). However, the lack of sufficient material, difficulties in shaping the bone graft to fill the defect, and the significant morbidity associated with the harvest of autogenous bone, including blood loss and infection risk, all preclude the universal use of autogenous bone for orthopaedic applications. As a result, surgeons turn to allograft bone and synthetic materials for alternatives. The risk of disease transmission and the potential danger of cell-mediated immune responses of allografts has led many researchers to search for other methods to repair skeletal defects. Synthetic polymers such as poly(methyl methacrylate) had been used as grafting material to fix implants to bone or to graft bone defects but they are not osteoconductive and non-degradable. Some possess mechanical properties incompatible with those of bone, leading to stress shielding and bone resorption. Another class of materials, calcium phosphate ceramics, such as β-tricalcium phosphate and hydroxyapatite (HA), provide an effective scaffold for bone ingrowth but their poor mechanical properties make them difficult to use for load-bearing applications.

The success of bone graft materials in stimulating new bone formation is highly dependent on the presence of a sufficient number of cells that possess the potential to

repopulate the graft, the osteoblastic progenitors. Burwell showed that primitive osteogenic cells in bone marrow were responsible for much of the biologic efficacy of cancellous bone graft (Burwell, 1994b). In many cases, the performance of bone grafts is limited by the scarcity of the local progenitor population and therefore bone grafts providing an exogenous source of progenitors can improve the grafts' efficacy (Ohgushi et al., 1989; Muschler et al., 1996). Bone marrow aspirates have proven to be a practical cell source (Muschler et al., 1997) and the efficacy of a bone marrow graft can be significantly enhanced by rapid intraoperative concentration of bone marrow derived cells using allograft or HA matrices as surfaces for attachment (Matsukura et al., 2000; Muschler et al., 2003).

1.2 Bone marrow as the cell source for bone grafting

The drastic improvement of graft efficacy provided by implanting exogenous bone marrow at the grafting site is due to the heterogeneous population of stem and progenitor cells in bone marrow. These progenitor cells possess different potentials to proliferate and differentiate into osteoblasts which play an important role in bone formation, such as extracellular matrix (ECM) maturation and mineralization. It had been demonstrated that some mesenchymal stem cells, also known as marrow stromal cells, present at a concentration of 200 - 1000 per mL of bone marrow, are pluripotent and can differentiate, under the appropriate conditions, into the chondrocyte lineage, the adipocyte lineage, the osteoblast lineage and possibly others (Owen, 1985; Muschler et al., 1997; Pittenger et al., 1999). In this proposal, the term connective tissue progenitors (CTPs) refers to these cells, a heterogeneous population of cells including fully pluripotent as well as undifferentiated progenitors at various stages of commitment to connective tissue or adipocyte lineages. Progenitors and even mature cells in these three lineages exhibit some level of plasticity. Some of these cells can be trans-differentiated into cells of other lineages (Figure 1.1). As a progenitor becomes more differentiated, its

proliferative ability drastically decreases. As illustrated in Figure 1.2, when a multipotential stem cell becomes an osteoprogenitor, its self-renewal ability is limited but it can still undergo extensive proliferation. However, mature osteoblasts and osteocytes are post-mitotic. Figure 1.2 also shows the sequence of steps of osteoblast differentiation. A proliferative phase is followed by the upregulation of Type I collagen, osteopontin, osteonectin, and alkaline phosphatase (AP). Mineralization follows, accompanied by the downregulation of AP and upregulation of osteocalcin (OC) and bone sialoprotein (BSP). The expression of these markers permits a rough identification of the stage of differentiation of the cells. In natural bone formation and remodelling, osteoprogenitor recruitment is a crucial step in which migration, attachment, and proliferation play roles just as significant as subsequent differentiation. In addition, once matured to a late differentiation stage, cell proliferation can no longer occur. In light of all these models, the attachment of sufficient cells and their proliferation before differentiation is extremely important in the success of repopulating the grafting site. In fact, Muschler et al. have shown, using the canine spinal fusion model, a 4-fold concentration of bone marrow derived connective tissue progenitors could be obtained when allograft matrices were used as surfaces for selective attachment. The union rate and quality of spinal fusion were also much improved compared to the use of fresh bone marrow without concentrating the CTPs (Muschler et al., 2003). The studies showed that even a modest increase in the number of osteoprogenitors in a bone graft using a matrix as a surface for attachment could drastically improve the biologic result. Preliminary data from the Muschler laboratory demonstrated that coralline hydroxyapatite (HA) and allograft cancellous bone chips (3x3x3 mm^3) can provide a 2 to 1 selection of CTPs over other marrow cells (~40% of nucleated marrow cells and ~80% of CTPs attached to the matrices). These studies suggested the feasibility of bone formation enhancement by matrices, although the poor mechanical properties of HA and the risk of disease transmission and limited supply of allograft cancellous bone make both materials suboptimal for bone grafting. Therefore, there is a need to develop a synthetic material that is capable of selecting and concentrating osteoprogenitor cells

from marrow. This material should have the capability to be easily incorporated to bone grafting devices as the surface material, making it possible to separate surface and bulk properties of bone grafts. Utilizing the advantage of the osteoprogenitor cell concentrating ability of this synthetic coating material as well as the architectural and mechanical properties of the bulk.

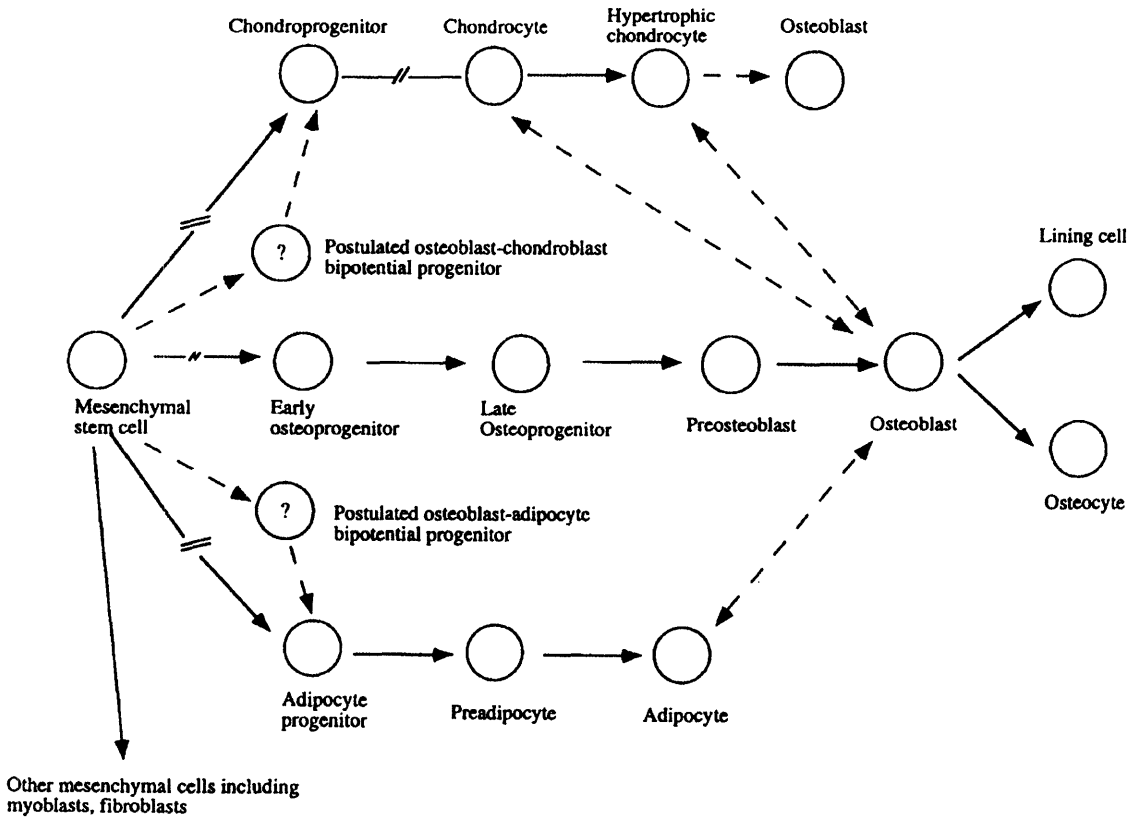

Figure 1.1 Postulated steps in the osteoblast lineage outlining some of the potential commitment and restriction points and plasticity. (Adapted from Aubin. (Aubin, 1998))

To develop such an osteoprogenitor cell selective material, an understanding of the mechanistic basis for osteoprogenitor attachment and function via interaction with ECM molecules would be valuable. The cells of interest are human marrow-derived CTPs which grow to form clonogenic cell clusters of connective tissue lineage known as colony forming units (CFUs) in *in vitro* assays. CTPs have been a challenge to identify from the

mixed population of marrow. The mean prevalence of these cells is about 1 per 20,000 cells in human bone marrow (Majors et al., 1997; Muschler et al., 1997). In addition, a marker or a set of markers that can definitively single out only this cell population had not been identified. STRO-1, an IgM antibody that labels all CTPs, was a marker used to concentrate CTPs using fluorescence activated cell sorting (FACS). About 7% of all human marrow cells express the STRO-1 antigen and of all the colonies formed by STRO-1+ cells, essentially all exhibit osteoblastic potential. About 50% exhibit adipocytic potential (Gronthos et al., 1994). Based on the cell surface molecular profile of human mesenchymal stem cells, researchers had used a combination of molecules present and absent on these cells in an attempt to identify them, for example, $CD105^{+}CD45^{-}$ (Meinel et al., 2004), $CD105^{+}CD45^{-}$ with the addition of $GlyA^{-}$ (Lodie et al., 2002), $CD49a^{+}CD45^{med,low}$ (Deschaseaux et al., 2003), $STRO\text{-}1^{high}VCAM\text{-}1^{+}$ (De Ugarte et al., 2003). However, in many of these studies, the mesenchymal stem cells assayed had been plated or expanded in culture and therefore their surface molecular profiles may have changed compared to when they were first isolated. This may be especially a problem for the expression profile of cell adhesion molecules such as integrins.

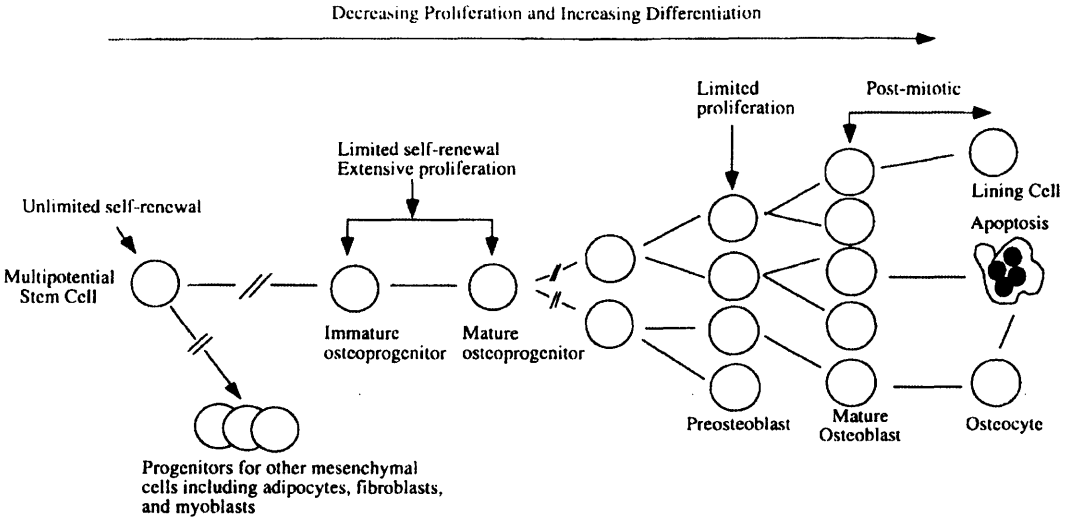

Figure 1.2 Postulated steps in the osteoblast lineage implying recognizable stages of proliferation and differentiation as detectable from *in vitro* and *in vivo* experiments. (Adapted from Aubin et al. (Aubin and Heersche, 2000))

1.3 Integrin-mediated cell adhesion

Integrins constitute the principal class of cell adhesion molecules that mediate cell-matrix adhesion. These transmembrane receptors are heterodimers that are composed of α and β subunits (Hynes, 1992; Hynes, 2002). In mammals, there exist at least 18 types of α subunits and 8 types of β subunits. Permutations of α and β subunits generate at least 24 known distinct integrin heterodimers that bind to different ligands. This diversity of integrins and their ability to bind to various ligands, such as ECM molecules, allow cells to express a combination of integrins, in order to recognize different adhesion molecules. This is essential in enabling cells to migrate to their correct location in tissue morphogenesis. The extracellular binding of integrins to ligands activates these transmembrane receptors to associate with various cytoplasmic proteins and thereby initiates multiple signalling pathways that regulate cell functions such as survival, motility, proliferation and differentiation (Huttenlocher et al., 1996; Palecek et al., 1997; Bourdoulous et al., 1998; Davey et al., 1999; Scott et al., 2003; Onodera et al., 2005). In addition, cells that express integrins that bind to the same ligands can selectively regulate the density and activity of each type to elicit certain cell function through fine-tuning their interaction with the matrix. For example, a decrease in the number of $\alpha_4\beta_1$ integrins at the late stage of hematopoietic cell differentiation is believed to allow mature blood cells to detach from bone marrow stroma (Kronenwett et al., 2000).

Integrins, however, bind to their ligands at relatively low affinities (dissociation constants K_D are typically between 10^{-6} and 10^{-8} M) compared to cell-surface hormone receptors (K_D between 10^{-9} to 10^{-11}M) (Lodish et al., 1999). Therefore, biophysical parameters play an important role in mediating cell-matrix interactions via integrin binding. On one hand, because individual binding is weak, migrating cells can break individual contacts with the matrix and cell motility can be regulated through the cell-substratum adhesion by varying substratum ECM surface density. On the other hand, due to the multi-hundreds or thousands of integrins that are present, these weak binding forces can be combined

together to anchor a cell firmly to the matrix. In fact, upon binding to extracellular ligands, integrins form nanoscale clusters which enable the assembly of multiple cytoplasmic regulatory and structural proteins at sites of aggregated integrin cytoplasmic domains, activating intracellular signalling pathways. Structurally, the formation of integrin clusters strengthens the adhesion of cells to their underlying substrata by enhancing connection to the cytoskeleton with the formation of actin-rich stress fibers that are attached through adapter proteins to the β subunit of integrins (Schoenwaelder and Burridge, 1999). On the cell-signaling level, accumulating data show that both ligand binding and receptor clustering are needed to elicit full cellular responses mediated by receptor-signaling-protein interactions (Miyamoto et al., 1995a; Miyamoto et al., 1995b). Previous studies in our lab have shown that clustered presentation of the RGD peptides was more effective in promoting cell adhesion and migration. (List of abbreviations of amino acids can be found in Appendix A.) Surfaces coated with synthetic star-configured polyethylene oxide polymer with more YGRGD peptides grafted on each star molecule (i.e., more peptides per polymer cluster) were more effective in promoting cell adhesion. Not only cell attachment but also full spreading and haptokinetic, as well as chemokinetic, motility was observed. At the same time, even with the same overall peptide density, fibroblast migration was impaired on unclustered peptide surfaces (Maheshwari et al., 2000). Koo et al. also showed an increase in adhesion force by fibroblasts on surfaces with RGD peptides presented as clusters by comb-shaped copolymer with poly(methyl methacrylate) backbone and poly(oxyethylene) side chains (P(MMA-r-POEM)) (Koo et al., 2002). Thus, both the biochemical recognition of ligands by integrins and the biophysical presentation of ligands plays an important role in eliciting full cellular responses.

In bone marrow biology, reports of integrin expression profile of CTPs are quite conflicting. This may in part be due to the difference in cell source (animal vs. human, calvarial bone vs. marrow aspiration etc) and in part due to the various methods of culture and different expansion. As mentioned above, one of the major difficulties is the

impossibility of analyzing a cell molecular profile while assaying for its ability to form colonies. Once a cell adheres to a surface *in vitro*, its molecular profile will likely have been changed. Mesenchymal stem cells have been shown in culture to express ECM molecules such as fibronectin, laminin, collagens, hyaluronan (Chichester et al., 1993; Conget and Minguell, 1999; Minguell et al., 2001) and it is generally believed that they secrete these matrix molecules *in vivo* to make up the stroma in bone marrow. In Chapter 6, the ECM and integrin profile of bone marrow aspirates, both the overall as well as particular subpopulations, is reported in attempt to elucidate an understanding of these cells. In addition to integrins, there are other transmembrane receptors that mediate cell adhesion. Cell surface proteoglycans are of particular interest in bone biology. Proteoglycans consist of a transmembrane core protein and an extracellular domain containing polysaccharide chains that can also bind to ECM molecules such as fibronectin and bone sialoprotein. This class of cell adhesion molecules is of growing interest as proteoglycans such as hyaluronan which is present in marrow can stimulate the proliferation of bone marrow mesenchymal stem cells (Zou et al., 2004).

1.4 Rational design for *in vivo* cell-based tissue engineering

In recent years, the discipline of bone regeneration and its related fields have progressed very rapidly. Bone development biology has provided a better understanding of mesenchymal stem cells and the cues needed for their cell function, including differentiation into bone. Cellular engineering to enhance bone graft efficacy utilizing bone marrow has greatly advanced. Previously, in order to transplant sufficient mesenchymal stem cells into the grafting site, an *ex vivo* expansion of mesenchymal stem cells was considered the principle strategy for the enhancement of CTPs. Now clinical strategies in intraoperative aspiration and concentration of CTPs as well as delivery of these cells to the grafting site have been developed. At the same time, the technologies in tissue engineering have advanced immensely. The use of biomaterials has grown from

the traditional concept of a bio-inert space-holder to constructs providing an environment both conductive and inductive to regenerating the original tissue structure and function. This progress is made feasible by the advance in technologies allowing the capabilities of manipulating the architectural, mechanical and surface properties of tissue engineering scaffolds. Rational design of tissue engineering scaffolds is therefore possible, and much needed to facilitate three- dimensional tissue development. Scaffolds with the desirable mechanical properties can be achieved by the use of the appropriate polymer and architecture. A careful architectural design also takes into account all of the nano-, micro- and macro-scale aspects which allow spatial control in tissue formation at the molecular, cellular and tissue-length scale respectively. The scaffold not only provides a void space for cells to proliferate, vascularize and form new tissues. It provides a pathway for diffusion and mass transport of oxygen and nutrients. Solid-form fabrication techniques, such as the Three-Dimensional Printing™ process (Park et al., 1998; Griffith, 2002), allow precise control in implementing these architectural designs and the separation of bulk and surface material properties of tissue engineering scaffolds. Surface design is crucial for the success of tissue engineering scaffolds as the surface is the interface at which cells and the scaffold interact. Bio-molecules presented by covalent-linking to a surface can provide an appropriate chemical environment for the adhesion and function of specific cell types. In this regard, a comb-shaped polymer recently developed by our laboratory was shown to be protein- and cell-resistant but small peptides can be covalently attached to the side-chains of the polymer and be presented at a surface in submicron clusters to induce specific cell function (Irvine et al., 2001a; Irvine et al., 2001b). This polymer is discussed in detail in the next chapter. Despite the development of all these tools in tissue engineering, an integral design of scaffolds has not been widely applied to *in vivo* bone tissue engineering. A lot of the earlier works have been aimed to seed cells in scaffolds and grow them *in vitro* before implanting them back to the host and in *in vivo* studies, only simple scaffolds with undefined pore size and architecture, such as those made by freeze-drying, have been used. On the other hand, in developing clinical strategies in enhancing the efficiency of

bone marrow grafts, the focus on optimizing the acquisition and concentration of CTPs has allowed the possibility for this procedure to be done intraoperatively. However, so far, only naturally occurring materials and hydroxyapatite have been used as the carrier of these progenitor cells and the matrix in which these cells are concentrated and grown. Bringing the aforementioned technologies in tissue engineering into the design of bone graft scaffolds would free the development of bone marrow grafts from being precluded by the limitations of the matrices currently used. Taking the best from both the field of engineering design and clinical cellular engineering, the rational design of a tissue engineering scaffold that is tailored for the intraoperative concentration of CTPs from bone marrow and for the proliferation and differentiation of CTPs into bone would bring bone graft technology to a new dimension.

1.5 Scope of thesis and objectives

This thesis focuses on the molecular design of bone graft surfaces. While the overall aim of engineering bone marrow graft is to develop a matrix with defined architecture and surface chemistry to enhance the rapid intraoperative concentration of connective tissue progenitors from bone marrow aspirates, the objective of this dissertation is to develop and implement the design of a synthetic polymer system that is capable of enriching CTPs from whole bone marrow and can be incorporated into the surface of bone grafts by 3DP™. A perfect selectivity for CTPs is not needed, in fact may not be desired due to the possible co-operative interactions between CTPs and other marrow cells. Thus, our approach is to use the P(MMA-r-POEM) comb copolymer to strategically present small adhesion peptides to facilitate a two-fold "enrichment" - the positive concentration and function of CTPs, and the negative selection of other marrow cells in the aspirate. In particular, this dissertation encompassed three specific aims:

1. Design of surfaces for bone grafts by the design of the base surface material, the biophysical and biochemical presentation of small adhesion peptides. And in particular,
    a. Improving the protein- and cell-resistance of comb copolymer, the base surface material
    b. Preparation of comb copolymer surfaces with covalently-bound peptides
    c. Selecting a short list of peptides based on critical literature reviews and empirically identifying peptide-substrates that enhance the selective colony formation of CTPs
    d. Enhancing the efficacy of peptides in mediating cell functions by biophysical presentation of peptides
2. Developing and standardizing marrow aspirate assays to evaluate and understand the colony formation of CTPs.
3. Enhancing the interaction of bone marrow cells and graft surface by cell-preloading treatments

It is our hope that not only the molecular design of substrates for selective adhesion and proliferation of CTPs in this thesis would be incorporated into the overall design of bone marrow grafts, but the knowledge gained in this dissertation on marrow cells, especially the CTPs, provide a better understanding in the behavior and molecular profile of these cells.

1.6 References

Aubin, J. (1998). "Bone stem cells." Journal of Cellular Biochemistry Supplements **30/31**: 73-82.

Aubin, J. and Heersche, J.N.M. (2000). "Osteoprogenitor cell differentiation to mature bone-forming osteoblasts." Drug Development Research **49**: 206-215.

Bourdoulous, S., Orend, G., MacKenna, D.A., Pasqualini, R. and Ruoslahti, E. (1998). "Fibronectin matirx regulates activation of Rho and Cdc42 GTPases and cell cycle progression." Journal of Cell Biology **143**: 267-276.

Burwell, R.G. (1994a). History of bone grafting and bone substitutes with special reference to osteogenic induction. Bone Grafts, Derivatives and Substitutes. M. R. Urist, Burwell, R.G. Oxford, Butterworth-Heinemann Ltd**:** 3-102.

Burwell, R.G. (1994b). The Burwell theory on the importance of bone marrow in bone grafting. Bone Grafts, Derivatives and Substitutes. M. R. Urist, Burwell, R.G. Oxford, Butterworth-Heinemann Ltd**:** 103-155.

Chichester, C.O., Fernandez, M. and Minguell, J.J. (1993). "Extracellular-matrix gene-expression by human bone-marrow stroma and by marrow fibroblasts." Cell Adhesion and Communication **2**: 93-99.

Conget, P.A. and Minguell, J.J. (1999). "Phenotypical and functional properties of human bone marrow mesenchymal progenitor cells." Journal of Cell Physiology **181**: 67-73.

Davey, G., Buzzai, M. and Assoian, R.K. (1999). "Reduced expression of $\alpha_5\beta_1$ integrin prevents spreading-dependent cell proliferation." Journal of Cell Science **112**: 4663-4672.

De Ugarte, D.A., Alfonso, Z., Zuk, P.A., Elbarbary, A., Zhu, M., Ashjian, P., Benhaim, P., Hedrick, M.H. and Fraser, J.K. (2003). "Differential expression of stem cell mobilization-associated molecules on multi-lineage cells from adipose tissue and bone marrow." Immunology Letters **89**(2-3): 267-270.

Deschaseaux, F., Gindraux, F., Saadi, R., Obert, L., Chalmers, D. and Herve, P. (2003). "Direct selection of human bone marrow mesenchymal stem cells using an anti-CD49a antibody reveals their CD45(med,low) phenotype." British Journal of Haematology **122**(3): 506-517.

Griffith, L.G. (2002). "Emerging design principles in biomaterials and scaffolds for tissue engineering." Ann NY Acad Sci **961**: 83-95.

Gronthos, S., Graves, S.E., Ohta, S. and Simmons, P.J. (1994). "The STRO-1+ fraction of adult human bone marrow contains the osteogenic precursors." Blood **84**(12): 4164-4173.

Huttenlocher, A., Ginsberg, M.H. and Horwitz, A.F. (1996). "Modulation of cell migration by integrin-mediated cytoskeletal linkages and ligand-binding affinity." Journal of Cell Biology **134**: 1551-1562.

Hynes, R.O. (1992). "Integrins - versatility, modulation, and signaling in cell-adhesion." Cell **69**: 11-25.

Hynes, R.O. (2002). "Integrins: Bidirectional, allosteric signaling machines." Cell **110**(6): 673-687.

Irvine, D.J., Mayes, A.M. and Griffith, L.G. (2001a). "Nanoscale clustering of RGD peptides at surfaces using comb polymers. 1. Synthesis and characterization of comb thin films." Biomacromolecules **2**(1): 85-94.

Irvine, D.J., Ruzette, A.V.G., Mayes, A.M. and Griffith, L.G. (2001b). "Nanoscale clustering of RGD peptides at surfaces using comb polymers. 2. Surface segregation of comb polymers in polylactide." Biomacromolecules **2**(2): 545-556.

Koo, L.Y., Irvine, D.J., Mayes, A.M., Lauffenburger, D.A. and Griffith, L.G. (2002). "Co-regulation of cell adhesion by nanoscale RGD organization and mechanical stimulus." Journal of Cell Science **115**(7): 1423-1433.

Kronenwett, R., Martin, S. and Haas, R. (2000). "The role of cytokines and adhesion molecules for mobilization of peripheral blood stem cells." Stem Cells **18**(5): 320-330.

Lodie, T.A., Blickarz, C.E., Devarakonda, T.J., He, C.F., Dash, A.B., Clarke, J., Gleneck, K., Shihabuddin , L. and Tubo, R. (2002). "Systematic analysis of reportedly distinct populations of multipotent bone marrow-derived stem cells reveals a lack of distinction." Tissue Engineering **8**(5): 739-751.

Lodish, H., Berk, A., Zipursky, A.L., Matsudaira, P., Baltimore, D. and Darnell, J. (1999). Molecular Cell Biology. New York, USA, W.H. Freeman and Company.

Maheshwari, G., Brown, G., Lauffenburger, D.A., Wells, A. and Griffith, L.G. (2000). "Cell adhesion and motility depend on nanoscale RGD clustering." Journal of Cell Science **113**: 1677-1686.

Majors, A.K., Boehm, C., Nitto, H., Midura, R.J. and Muschler, G.F. (1997). "Characterization of human bone marrow stromal cells with respect to osteoblastic differentiation." Journal of Orthopaedic Research **15**: 546-557.

Matsukura, Y., Boehm, C., Valdevit, A., Kambic, H., Davros, W., Easley, K. and Muschler, G. (2000). "Concentration of bone marrow derived osteoprogenitors for spinal fusion." Journal of Bone and Mineral Research **15**(M199 Suppl. 1): S504-S504.

Meinel, L., Karageorgiou, V., Fajardo, R., Snyder, B., Shinde-Patil, V., Zichner, L., Kaplan, D., Langer, R. and Vunjak-Novakovic, G. (2004). "Bone tissue engineering using human mesenchymal stem cells: Effects of scaffold material and medium flow." Annals of Biomedical Engineering **32**(1): 112-122.

Minguell, J.J., Erices, A. and Conget, P. (2001). "Mesenchymal stem cells." Experimental Biology and Medicine **226**(6): 507-520.

Miyamoto, S., Akiyama, S.K. and Yamada, K.M. (1995a). "Synergistic roles for receptor occupancy and aggregation in integrin transmembrane function." Science **167**: 883.

Miyamoto, S., Teramoto, H., Coso, O.A., Gutkind, S.J., Burbelo, P.D., Akiyama, S.K. and Yamada, K.M. (1995b). "Integrin function: Molecular hierarchies of cytoskeletal and signalling molecules." Journal of Cell Biology **131**: 791-805.

Muschler, G.F., Boehm, C. and Easley, K. (1997). "Aspiration to obtain osteoblastic progenitor cells from human bone marrow: the influence of aspiration volume." Journal of Bone and Joint Surgery (Am) **79**: 1699-1709.

Muschler, G.F., Negami, S., Easley, K. and Kambic, H. (1996). "The evaluation of collagen and ceramic composites as bone graft materials in a canine posterior segmental spinal fusion model." Clinical orthopaedics and related research **328**: 250-260.

Muschler, G.F., Nitto, H., Matsukura, Y., Boehm, C., Valdevit, A., Kambic, H., Davros, W., Powell, K. and Easley, K. (2003). "Spine fusion using cell matrix composites enriched in bone marrow-derived cells." Clinical orthopaedics and related research **407**: 102-118.

Ohgushi, H., Goldberg, V.M. and Caplan, A.I. (1989). "Repair of bone defects with marrow-cells and porous ceramic-Experiments in rats." Acta Orthopaedica Scandinavica **60**(3): 334-339.

Onodera, K., Takahashi, I., Sasano, Y., Bae, J.W., Mitani, H., Kagayama, M. and Mitani, H. (2005). "Stepwise mechanical stretching inhibits chondrogenesis through cell-matrix adhesion mediated by integrins in embryonic rat limb-bud mesenchymal cells." European Journal of Cell Biology **84**(1): 45-58.

Owen, M. (1985). "Lineage of osteogenic cells and their relationship to the stromal system." Journal of Bone and Mineral Research **3**.

Palecek, S.P., Loftus, J.C., Ginsberg, M.H., Lauffenburger, D.A. and Horwitz, A.F. (1997). "Integrin-ligand binding properties govern cell migration speed through cell-substratum adhesiveness." Nature **385**(537-540).

Park, A., Wu, B. and Griffith, L.G. (1998). "Integration of surface modification and 3D fabrication techniques to prepare patterned poly(L-lactide) substrates allowing regionally selective cell adhesion." Journal of Biomaterials Science - Polymer Edition **9**(2): 89-110.

Pittenger, M.F., Mackay, A.M., Beck, S.C., Jaiwal, R.K., Douglas, R., Mosca, J.D., Moorman, M.A., Simonetti, S.W., Craig, S. and Marshak, D.R. (1999). "Multilineage Potential of Adult Human Mesenchymal Stem Cells." Science **284**(5411): 143-147.

Schoenwaelder, S.M. and Burridge, K. (1999). "Bidirectional signaling between the cytoskeleton and integrins." Current Opinion in Cell Biology **11**(2): 274-286.

Scott, L.M., Priestley, G.V. and Papayannopoulou, T. (2003). "Deletion of alpha 4 integrins from adult hematopoietic cells reveals roles in homeostasis, regeneration, and homing." Molecular and Cellular Biology **23**(24): 9349-9360.

Zou, X.N., Li, H.S., Chen, L., Baatrup, A., Bunger, C. and Lind, M. (2004). "Stimulation of porcine bone marrow stromal cells by hyaluronan, dexamethasone and rhBMP-2." Biomaterials **25**(23): 5375-5385.

Chapter 2

Design of Base Material for the Surface of Bone Grafts

2.1 Introduction

To design a suitable surface material that presents biomolecules to target specific cells and their function in bone grafts, several properties of the material have to be considered. The stability of the material in an aqueous environment, protein and cell resistance, and the availability and sufficiency of sites for covalently coupling biomolecules to engender cell response, are all important design criteria. In addition, another favorable property is facile incorporation onto the surface of bone grafts, by for example, three-dimensional printing (3DP™). In choosing a base material candidate, a biomaterial intrinsically resistant to protein adsorption and cell adhesion is needed. With a cell and protein resistant base material, any interactions between cells and the material, such as adhesion and proliferation, are engendered by specific receptor-mediated interactions with biomolecules covalently coupled to the material, rather than to proteins non-specifically adsorbed from the culture or grafting environment, such as serum, cellular secretion, exogenous factors, etc. In this regard, the class of comb copolymers that consist of a hydrophobic backbone of poly(methyl methacrylate) (PMMA) and short poly(ethylene oxide) (PEO) side chains (Figure 2.1) were chosen to test for their protein and cell resistance ability. One comb copolymer in the class with side chains of 6-9 ethylene oxide units has been previously tested to be completely resistant to non-specific adhesion of wtNR6 fibroblasts, even in the presence of serum (Irvine et al., 2001a). The hydrophobic PMMA backbone imparts stability to the comb polymer surface in contact with aqueous solution while the hydrophilic PEO side chains are extended and segregate at the water-polymer interface to provide protein and cell resistance as well as sites for peptide coupling (Figure 2.2). The segregation of POEM sidechains is due to both

entropic forces – the enrichment of chain-ends at the surface (Walton and Mayes, 1996), and enthalpic forces – the formation of hydrogen bonds between POEM sidechains and water molecules (Irvine et al., 2001b).

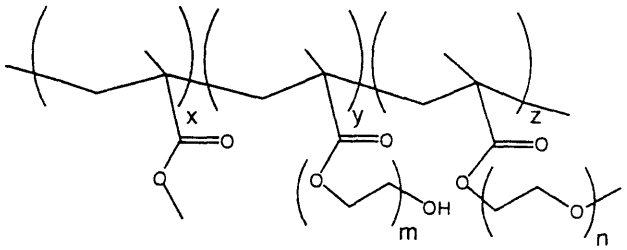

Figure 2.1 Basic comb copolymer structure. Repeat units are *x* – methyl methacrylate (MMA), *y* – poly(oxyethylene) methacrylate (HPOEM), and *z* – methoxy-poly(oxyethylene) methacrylate (MPOEM). Side chain lengths are presented as *m* and *n*.

Several attributes of the comb copolymer play a role in giving the material its protein and cell resistance - the proportion of PEO in the polymer, length of side chains and side chain end-groups. These parameters were systematically varied to render the comb copolymer more effective as a bone graft surface material. Previous work gave us an idea of the range of PEO content we could vary — comb copolymer (6-9 ethylene oxide unit side chains) with greater than 30 wt% PEO content is generally NR6 fibroblast resistant while the same polymer with greater than 40 wt% PEO was soluble in aqueous solution (Irvine, 2000). We tested a set of comb copolymers within this range of PEO content to determine what properties yielded the greatest resistance to marrow aspirates, which consist of various cell types as well as a significant amount of associated proteins from the marrow environment. Different surface chemical groups of biomaterials have also been known to impart different degrees of cell inertness (Ratner et al., 2004). For the comb copolymer, it has been shown that certain combs with more methoxy ($-OCH_3$) side chain ends are more resistant than those with more hydroxyl (-OH) chain ends (Hester, 2000; Irvine, 2000). However, only the hydroxyl side chain ends are functionalizable for downstream peptide-coupling. Hence, in this study, we varied the sidechain end-groups to obtain good cell resistance and at the same time maximize the

amount of functionalizable end-groups. The length of side chains also plays a role in determining whether the comb polymer is protein and cell resistant. Increasing the length of the side chains while maintaining the same PEO content would mean fewer side chains in the comb and hence the average spacing between side chains would increase (Figure 2.3). Greater spacings may reduce protein resistance, as the PEO side chain in the PEO brush layer may not be able to fan the underlying PMMA backbones.

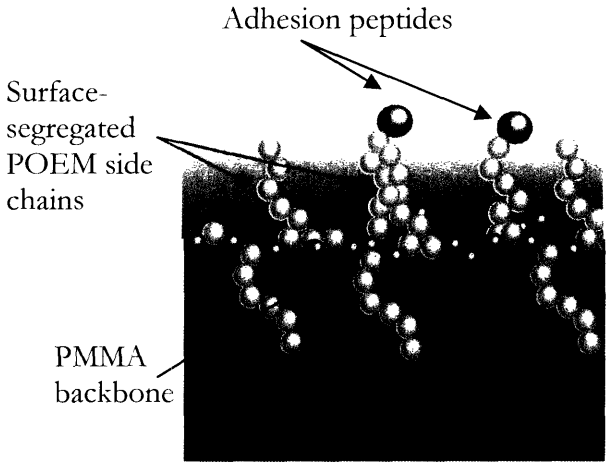

Figure 2.2 A schematic of comb copolymer structure at the water-polymer interface. Hydrophilic POEM sidechains (yellow), being enthalpically and entropically driven, segregated at the aqueous interface while the backbone PMMA stays in the bulk.

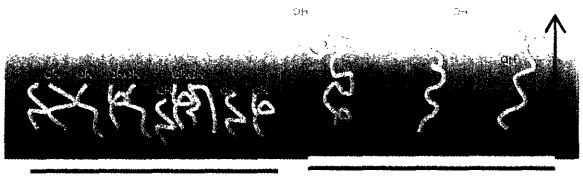

Figure 2.3 A schematic showing the relationship between sidechain length and spacing between sidechains. With the same POEM content, increasing the length of POEM sidechains increases the spacing in between.

The same can happen when the side chains are too short. In addition, long side chains provide fewer functional groups in a comb molecule. Therefore, in this chapter, the objective of the work was to evaluate a set of polymers to identify parameters giving the maximum functionalizable chain-ends without compromising protein and cell resistance. This was achieved by varying the PEO content of the comb, side chain lengths and side chain end-groups, and testing empirically with both wtNR6 fibroblasts, one of the most adhesive cells in our experience, and human marrow aspirates. Protein adsorption

studies with ^{125}I -BSA were conducted to determine if comb copolymers were protein resistant. The water insoluble comb polymer with the optimal protein and cell resistance and sufficient functionalizable chain ends will be used as the base polymer for our subsequent studies.

This work was done in collaboration with William Kuhlman, who synthesized and provided some of the comb copolymers used in these studies.

2.2 Materials and Methods

2.2.1 Cells and Culture

2.2.1.1 wt NR6 fibroblast cell line and culture

The wtNR6 fibroblast cell line, obtained from the Wells Lab (University of Pittsburgh), is a 3T3 variant that lacks endogenous EGF receptors but expresses stably-transfected human EGFR. Cells were routinely cultured in minimum essential medium-α (MEM- α) supplemented with 7.5% fetal bovine serum (FBS), 350 μg/mL Geneticin, 1 mM non-essential amino acids, 2mM L-glutamine, 1mM sodium pyruvate and 100 i.u./mL penicillin and 200 μg/mL streptomycin. All materials were obtained from Gibco, Grand Island, NY, USA. Cells were cultured at 37°C with 5% CO_2 and split when they were near 80% confluency.

2.2.1.2 Human bone marrow aspirations

Donors and patients presenting for treatment to Dr. George Muschler were recruited for assay of bone marrow immediately prior to an elective orthopaedic procedure. All subjects were enrolled with full informed consent under a protocol which was approved by the Institutional Review Board of The Cleveland Clinic Foundation. Bone marrow aspirates were obtained using a procedure described previously (Muschler et al., 2001). In brief, on the day of surgery, following induction of anesthesia and sterile skin preparation, a 3-mm stab incision was made approximately 4 cm posterior and lateral to the anterior superior iliac spine (ASIS). A bone marrow aspiration needle (Lee-Lok, Minneapolis, MN, USA) was advanced through this incision into the intramedullary cavity of the iliac crest approximately 2 cm posterior to the ASIS. A 2-ml sample of bone marrow was aspirated into a 10-ml plastic syringe containing 1 ml of saline containing 1000 units of heparin. Subsequent aspirates were taken using identical technique through separate cortical perforations separated by at least 1 cm, moving posteriorly along the

iliac crest. Four aspirates were harvested from each side, a total of eight aspirates per patient. The heparinized marrow sample from each site was suspended into 20 ml of MEMα containing 2 unit/ml Na-heparin and sealed in a 50-ml test tube for transportation to the laboratory for cell count and experiments. All samples were harvested by Dr. Muschler.

2.2.2 Comb copolymer synthesis and surface preparations

Comb copolymer was synthesized using a protocol similar to one previously described but with some modifications (Irvine, 2000; Irvine et al., 2001a). In summary, comb copolymer was synthesized by free radical polymerization of methacrylate, polyethylene glycol methacrylate (HPOEM) and polyethylene glycol methyl ether methacrylate (MPOEM) in toluene using azo(bis)isobutyronitrile (AIBN, Sigma-Aldrich, St. Louis, MO, USA) as an initiator. The polymer product was purified several times with ethanol-hexane (1:8). HPOEM of molecular weight M_n ~ 360 g/mol (6-mer PEO units) and M_n ~ 526 g/mol (9.7-mer PEO units) and MPOEM with M_n ~ 475 g/mol (9-mer PEO units) used in the polymerization were obtained from Aldrich (St. Louis, MO). Other HPOEM and MPOEM, such as 22-mer and 33-mer HPOEM and 45-mer MPOEM were synthesized by reacting polyethylene glycol (PEG) of the desired chain lengths (Aldrich) with methacryloyl-chloride (Aldrich) with triethylamine (TEA) as base. The products were purified using a C18 sephadex column.

The molecular weight and polydispersity index (PDI) of resulting comb polymers were determined by gel permeation chromatography with inline light scattering (GPC-LS, Wyatt MiniDawn) based on polystyrene standards. The weight ratio of the three monomers in the resulting polymer were determined by NMR (Bruker Avance DPX400 proton NMR running at 400 mHz) using 1% copolymer solution in deuterated chloroform. PDI of all comb polymers were less than 3.5 and other specifications of the polymers were tabulated in Table 2.1.

Comb	*m-mer* HPOEM m=	*n-mer* MPOEM n=	wt% HPOEM	wt% MPOEM	Total wt% PEO
H6M9_1	6	9	17.7%	16.3%	34.0%
H6M9_2	6	9	25.9%	11.1%	37.0%
H6M9_3	6	9	19.8%	16.2%	36.0%
H6M0	6	----	40.0%	----	40.0%
H10M0	10	----	40.0%	----	40.0%
H22M0	22	----	40.0%	----	40.0%
H33M0	33	----	40.0%	----	40.0%
H22M9	22	9	35.0%	5.0%	40.0%
H33M9	33	9	35.0%	5.0%	40.0%
H0M9	----	9	----	39.0%	39.0%
H0M45	----	45	----	50.0%	50.0%

Table 2.1 Specifications of comb copolymers tested

Comb polymer substrates used for subsequent protein and cell resistance testing were prepared by spincoating 0.2μm-filtered polymer solution on glass coverslips previously silanized with methacryloxypropyltrimethoxysilane (MPTS, Gelest Inc, PA) to render the glass surfaces more hydrophobic. To prepare for silanization, glass coverslips were first sonicated in 200 proof ethanol for 30 minutes to remove any dust and dirt. After rinsing, the coverslips were placed in a 4% solution of MPTS in 95% ethanol and 5% water (pH 4 – 5) with constant agitation for 20 minutes. After five rinses in 200 proof ethanol, the coverslips were allowed to cure in room temperature for overnight, or at 130°C for one hour. Spincoating solutions were prepared by dissolving comb copolymer in 3:1 methyl ethyl ketone to toluene solution at 20 mg/mL. Spincoated coverslips were then placed *in vacuo* at room temperature for overnight to allow the evaporation of any remaining solvents. Ellipsometry measurements indicated that the comb polymer thin films produced by this method were between 900 – 1000 Å.

2.2.3 Protein resistance experiments

To study protein resistance of comb polymer substrates, bovine serum albumin (BSA) (Sigma-Aldrich, St. Louis, MO) was used as the model protein. BSA radiolabelled with iodine-125 using iodobeads (Pierce, Rockford, IL) was used to quantify how much BSA was adsorbed on comb substrates. Comb copolymer surfaces were placed in contact with BSA solutions with concentration ranging from 0.01 to 1 mg/mL of phosphate-buffered saline (PBS) at pH 7-7.5 for 2 hours at room temperature. After 2 hours, the substrates were washed four times with PBS before gamma activity in counts per minute (cpm) was measured with the Packard Cobra II Gamma Counter. From cpm, the amount of BSA adsorbed was calculated from the standard calibration curve set up by gamma counting a series of BSA solutions with known concentrations.

2.2.4 wtNR6 fibroblast resistance studies

wtNR6 fibroblasts were used as the first pass of cell resistance studies before human marrow aspirates were used. 12mm glass coverslips spincoated with the comb copolymer to be tested were fixed in 24 well-plates with silicone rings cut out from biocompatible and non-fouling silicone tubings. Surfaces were sterilized under UV light for 30 – 45 mins and then pre-incubated with wtNR6 growth media that contained 7.5% serum overnight before 14000 cells / cm^2 were seeded with the same wtNR6 growth media. Tissue culture treated polystyrene (TCPS) was used as a positive control. Surfaces were examined under a microscope (Nikon upright, transmission mode) after 48 hours of seeding and on Day 7 and three images were taken per coverslip. Each comb polymer substrate was tested in triplicate within the same experiment and the results were from three sets of separate experiments. Images were processed using the Openlab software and cells in each image were counted manually. The cell counts from microscopy were correlated with results from Vybrant MTT assays (Molecular Probes, CA) performed on Day 7 after the images were taken.

2.2.5 Human marrow resistance studies

Comb copolymer substrates to be tested were prepared on 18mm x 18mm square glass coverslips by spincoating. Spincoated coverslips were stored at room temperature prior to use and coverslips were set in experiments no later than 4 weeks after they were first prepared. In human marrow resistance studies, coverslips were placed in 2-chamber Lab-tek glass chamber slides (Nunc, NY), sterilized under UV and were seeded with 0.5 million fresh marrow aspirate cells in DMEM with 10% FBS. Glass coverslips and Lab-tek glass slides were used as the positive control. Non-adherent cells were transferred to new Lab-tek slides after 48 hours of seeding and were replenished with new media. On day 6, all slides were washed with PBS twice and fixed. The number of colonies, defined as a cluster of 8 or more cells, and sub-colony clusters were counted for each slide and the amount of single cells were scored as + (0 – 10 cells per slip/chamber), ++ (10 – 100 cells per slip/chamber) and +++ (>100 cells per slip/chamber). Four slips/chambers were used for each type of comb copolymer surface per marrow sample and three patient samples were used in this study.

2.2.6 Statistical analysis

Results from cell resistance experiments were analyzed by single-factor analysis of variance (ANOVA) with MSExcel. Pairwise comparisons were performed by using Fisher LSD post hoc test. Confidence level was as indicated in the figures.

2.3 Results

2.3.1 Protein resistance studies – ^{125}I -BSA adsorption on comb surfaces

To determine the amount of BSA adsorbed onto various comb surfaces, adsorption isotherms were constructed for each of the comb polymers listed in Table 2.1. Results are summarized in Figure 2.4 and Figure 2.5. The BSA amounts adsorbed on all comb copolymer surfaces were substantially less than the amount adsorbed on glass. Even the highest BSA adsorption observed on comb surface was less than 13% of the amount adsorbed on glass at the same concentration of BSA solution. In most cases, the relative percentage of adsorption is less than 8% (Figure 2.5) and below 40ng/cm^2 even at the highest BSA concentration tested (1 mg/mL).

The actual amount of BSA adsorbed on glass was, however, as high as (94.9 ± 2.2) ng/cm^2 even at 0.01 mg/mL of BSA and increased to (477.5 ± 35.4) ng/cm^2 when the concentration of BSA solution used for adsorption was 1 mg /mL.

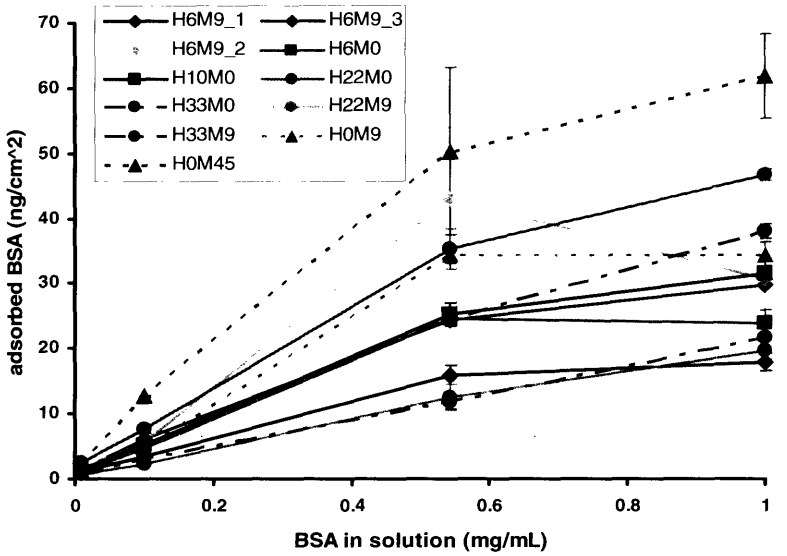

Figure 2.4 BSA adsorption isotherms for comb copolymers with various POEM content, sidechain lengths and endgroups. Absorption amount was obtained using ^{125}I -BSA.

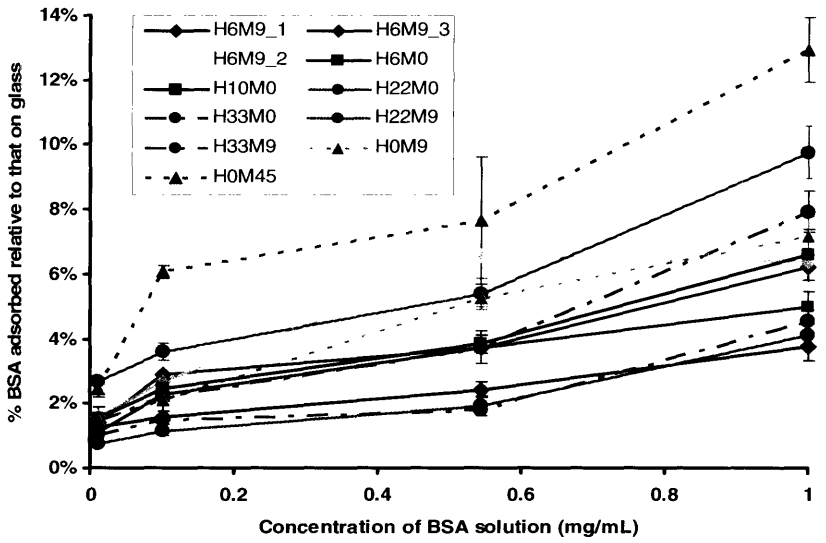

Figure 2.5 Relative percentage of BSA adsorbed on comb copolymers to that on glass. Absorption amount was obtained using ^{125}I -BSA.

Among different types of comb copolymer, there did not seem to be an apparent trend of BSA adsorption in correlation to the attributes of the comb polymer, such as sidechain end-groups, sidechain lengths, etc. H0M45 was the comb copolymer that was the least resistant to BSA adsorption. The amount adsorbed on H0M45 surfaces, (61.8 ± 1.54) ng/cm^2 at 1 mg/mL, was significantly higher than all the other comb surfaces tested while adsorption to H22M9, H33M9 and H6M9_1 was lower than the other combs. The adsorption isotherms of H6M9_2, H6M0 and H10M0 almost coincided with each other. At 1 mg/mL BSA concentration for adsorption, most comb copolymers had reached or were approaching an asymptotic maximum of BSA adsorption, with the exception of H22M9 and H33M9, both of which exhibited the lowest amount of BSA adsorption compared to the rest of the comb copolymers tested.

2.3.2 wtNR6 fibroblast resistance of comb copolymers

The wtNR6 fibroblast cell line is the most adhesive cell line we have in our experience and was therefore chosen to be used to empirically test the cell resistance of comb

copolymers in the presence of serum. All comb copolymer surfaces were inert to cell attachment even after 24 hours of serum pre-incubation and subsequent seeding with wtNR6 cells for 7 days. Figure 2.7 shows the relative percentages of wtNR6 fibroblast adhesion on various comb copolymer surfaces. Here, relative cell adhesion is defined as the ratio of number of adherent cells on comb surfaces to that on tissue-culture polystyrene (TCPS) control surfaces. Figure 2.7 showed that all comb copolymers, even the less cell resistant H22M9, H33M0 and H6M9_2, exhibit a relative cell adhesion of less than 25% in 7 days ($p < 0.001$ vs. TCPS control, Fisher LSD post hoc test). Due to this low relative cell adhesion observed, to obtain statistical significance in cell resistance performance, each comb copolymer was compared pair-wise with H6M9_1 and H22M9 as reference points. Comb polymers with only methoxy-terminated POEM sidechains, the 9-mer H0M9 and the 45-mer H0M45, as well as the 10-mer HPOEM sidechain comb H10M0 were the most cell resistant. Relative cell adhesion was only $(1.38 \pm 0.78)\%$, $(0.52 \pm 0.27)\%$ and $(2.10 \pm 0.68)\%$ respectively. These three comb copolymers were the only ones that exhibit a lower relative adhesion than H6M9_1 with $p < 0.05$ and H22M9 with $p < 0.01$. The comb polymer with 6-mer HPOEM sidechains, H6M0 and H6M9_3 (comb copolymer with a mixture of 6-mer HPOEM and 9-mer MPOEM sidechains) also exhibited excellent NR6 fibroblast cell resistance. $((2.05 \pm 1.16)\%$, and $(2.03 \pm 1.24)\%$ respectively. $p < 0.01$ vs. H22M9.) When observed under the microscope, many of these surfaces, particularly the ones that exhibited less than 3% cell adhesion, had no cells adhered on them in general. For the fibroblasts that were attached, they were either round and did not spread as they did on TCPS surfaces or they were found on visible defects on the surface, such as scratches that exposed the underlying glass to which the cells adhered. Encouraged by these results of inertness of the comb copolymer with fibroblast cell lines, we proceeded to test these comb copolymers for their resistance to human marrow aspirates.

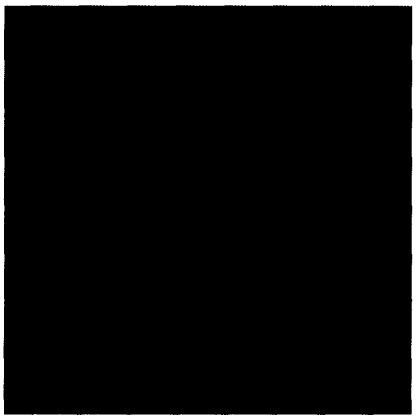

Figure 2.6 Microscopic image of H10M0 comb surface after wtNR6 has been seeded for 7 days. The image showed no apparent cell adhesion.

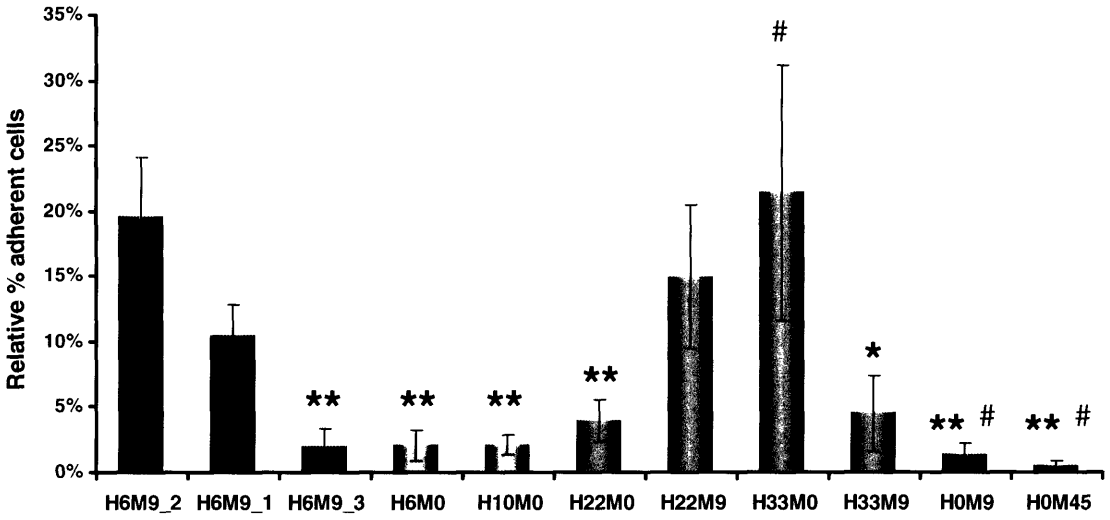

Figure 2.7 Relative ratio of adherent wtNR6 fibroblasts on comb copolymer surfaces to that on TCPS control after 7 days of culture. Note that all comb copolymers supported less than 25% of non-specific cell adhesion compared to TCPS control. H6M9_3, H6M0, H10M0 and MPOEM combs exhibited less than 5% cell adhesion. Cell adhesion was assessed by counting the number of adherent cells in microscopic images of surfaces. Results are mean ± SE of three experiments. (Error from variance of three experiments, which was larger than the technical error propagated from triplicates of each experiment (data not shown), was used here to give a more conservative error measurement.) The differences observed among the comb copolymers were significant, $p < 1x10^{-20}$ (ANOVA). Comb surfaces were compared with H6M9_1 and H22M9 using the Fisher LSD post hoc test. * $p \leq 0.05$ vs. H22M9, ** $p \leq 0.01$ vs. H22M9, and $^{\#}$ $p \leq 0.05$ vs. H6M9_1.

2.3.3 Human marrow aspirate resistance of comb copolymers

To study how resistant comb copolymers were to non-specific adhesion of bone marrow aspirates, the colony forming unit (CFU) assay was used. The number of cell colonies (cluster of 8 or more cells) and sub-colony clusters were counted and the number of single cells on the substrates was recorded on a scale of 1 (+) to 3 (+++), where + (0 – 10 cells per slip/chamber), ++ (10 – 100 cells per slip/chamber) and +++ (>100 cells per slip/chamber) of 500,000 marrow cells seeded. CFU efficiency, which is defined as the ratio of colonies formed on a test surface to that on glass or a Lab-tek control, was used to measure colony formation on comb surfaces. With the exception of H6M9_2, which supported (38 ± 15) % of CFU efficiency, all comb copolymers showed significant reduction of colony formation compared to glass control ($p < 0.001$). However, due to the lower amount of CFU formation observed, the trend among comb copolymer wasn't statistically significant. Only H6M9_1 and H6M9_3 showed significantly less CFU formation than H6M9_2 ($p < 0.05$, Fisher LSD post hoc test), suggesting good cell resistance for these two polymers. H6M0 and H0M9 seemed to show very good resistance to non-specific colony forming cell adhesion and colony formation (CFU efficiency less than 2%). However, due to the smaller sample size for these two polymers ($n = 5$, compared to $n = 12$ for H6M9 comb copolymers), statistical significance was not observed. The longer chain polymer H33M0, H33M9 and H0M45 did not seem to perform as well (CFU efficiency ranged from 9% to 14%) while the CFU efficiency of H6M9_1, H6M9_3, H10M0, H22M0 and H22M9 were less than 6% (Figure 2.8). When subcolony-clusters were taken into consideration, and the ratio of the sum of colonies and subcolony-clusters on comb surfaces to that on glass controls ($\%_{colonies+clusters}$) was plotted for each comb copolymer, we found that the longer-sidechain combs were not as resistant as the shorter sidechain ones (Figure 2.9). H22M9, H33M0 and H33M9 supported over 40% of colony and subcolony-cluster formation when compared to that on a glass control. H6M0, H10M0, H22M0 were the most resistant to non-specific colony and cluster formation ($p < 0.05$ vs. H22M9) followed by comb with only

methoxy-terminated POEM sidechains ($p < 0.1$ vs. H22M9). However, around 20% of non-specific colony and cluster formation was observed on H6M9 comb copolymers. The degree of single cell adhesion was very similar for all surfaces, comb copolymers and glass or Lab-tek slides. The average score of single cells ranged between 1.2 and 2.25. (Table 2.2)

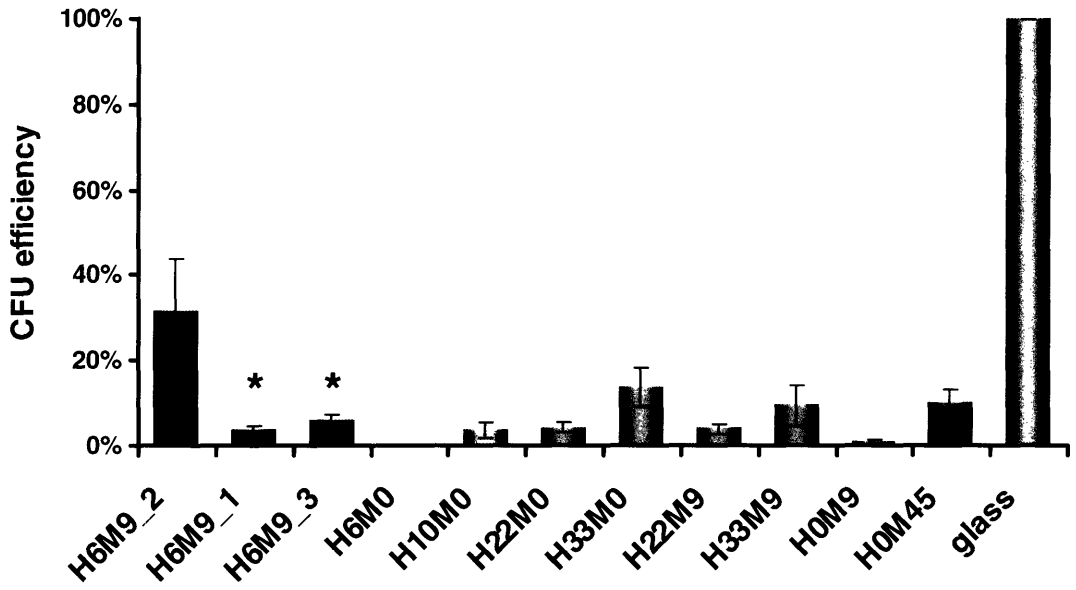

Figure 2.8 CFU efficiency of comb copolymers and glass. CFU efficiency is defined as the ratio of adherent colonies on test surfaces to that on glass, the positive control of the CFU assay. Results are mean ± SE. Statistical significance ($p < 1x10^{-8}$, ANOVA) was observed in the differences in CFU efficiency of comb copolymer and glass. However, other than a $p < 0.001$ vs. glass significance level was observed for all comb copolymers and a * $p < 0.05$ for H6M9_1 and H6M9_3 vs. H6M9_2, the difference in CFU efficiency of the other comb copolymers was not statistically significant. This may be due to the smaller sample size of the non-H6M9 comb copolymers. ($n = 12$ for H6M9's and glass; $n = 3$ for all others).

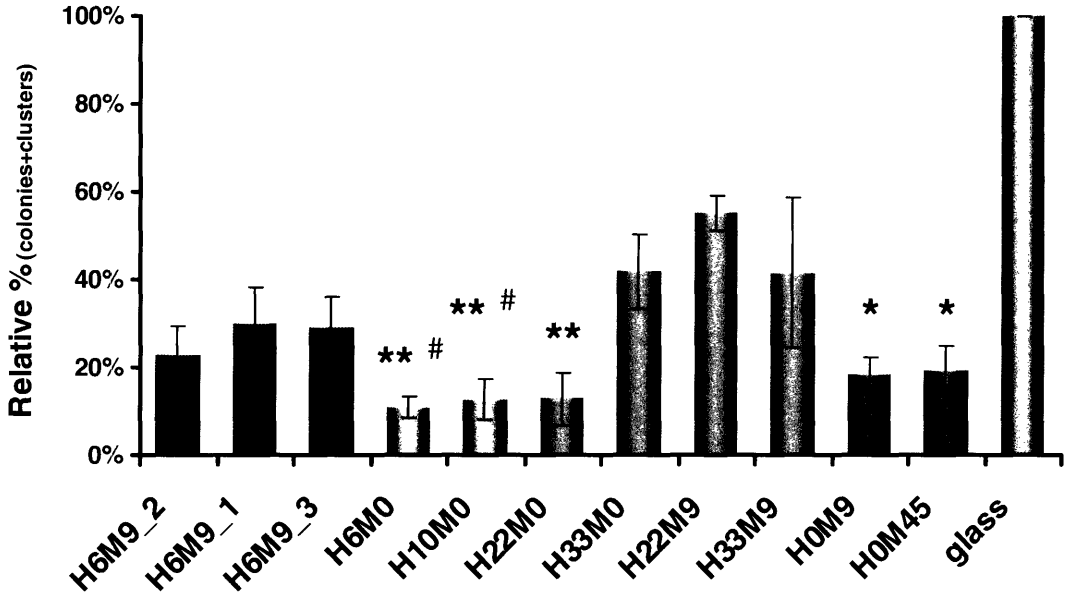

Figure 2.9 Colony and subcolony cluster formation on comb copolymer surfaces. The ratio of the sum of the colonies and clusters on comb copolymer surfaces to the sum on glass control was reported here. Data are mean ± SE. Statistical significance ($p < 0.0009$, ANOVA) was observed in the differences in CFU efficiency of comb copolymer and glass. Relative colony and cluster formation of all comb copolymers were lower than that on glass control ($p < 0.02$, Fisher LSD post hoc). * $p < 0.1$ vs. H22M9, ** $p < 0.05$ vs. H22M9; # $p < 0.1$ vs. H33M0 and H33M9. ($n = 5$)

	Single Cell Adhesion Score
H6M9 1	+/-
H6M9 2	+/+
H6M9 3	+/-
H6M0	+/-
H10M0	+/+
H22M0	+/+
H22M9	+/+
H33M0	+/+
H33M9	+/+
H0M9	+/-
H0M45	+/-
Glass	+/+

Table 2.2 Single marrow cell adhesion on comb copolymers. + is assigned to surfaces with 1 – 10 adherent single cells, ++ to 11-99 cells and +++ to > 100 cells. ($n \geq 5$)

2.4 Discussion

Bovine serum albumin has been widely used in model investigations of non-specific protein adsorption. It is chosen in this study on comb copolymer surfaces because of the high prevalence of albumin in blood. BSA is known to adsorb on a great variety of both hydrophilic and hydrophobic surfaces due to its low conformation stability, and therefore is a favorable model protein for studying adsorption on the amphiphilic comb copolymers. Hence, the first part of the study on bio-inertness of bone graft surface materials consists of a simplified protein-surface system to measure the adsorption of the well-characterized protein BSA on comb copolymers in PBS.

BSA has a molecular weight of 66500 Da and an isoelectric point of 4.7. It has been widely demonstrated in the literature that at neutral pH, BSA takes on its native or "N" form. The "N" form is a heart-shaped molecule with dimensions of 8.0 nm on the sides and a depth of 3.0 nm (Peters, 1985; Giacomelli et al., 1997). Based on these dimensions, the estimated structural area of BSA was calculated to be 27.7 nm^2 and therefore, assuming BSA molecules could be closely-packed into a monolayer, a monolayer would contain 397 ng/cm^2 of BSA. When taking into consideration the electrostatic repulsion between adsorbed BSA molecules, with contribution from the double-layer thickness ($1/\kappa_m$), the effective area of BSA for adsorption, can be estimated by

$$A_{eff} = (\sqrt{(A_{calc})} + \frac{2}{\kappa_m})^2$$

where κ_m is the Debye-Hückel parameter, which because BSA is a soft molecule (Giacomelli et al., 1997), is expressed as

$$\kappa_m = \kappa(1 + (\frac{\rho}{2zen^{\infty}})^2)^{\frac{1}{4}}$$

where ϱ is the charge density of BSA (~ 3.6 x 10^{-20} C/nm^3) at pH ~7-8, e the elementary electrical charge, z_i and n_i the electrolyte solution valence and concentration, respectively and κ, a Debye-Hückel parameter -

$$\kappa = \left(\frac{e^2 \sum n_i z_i^2}{\varepsilon k T} \right)^{1/2}$$

where ε is the dielectric constant. The main composition of PBS was NaCl at 120mM. The Debye-Hückel parameter, κ, is thus, 0.787 nm^{-1} and the double-layer thickness ($1/\kappa_m$) is 0.88nm. Hence the effective area can be estimated to be about 49 nm^2. Based on this effective area of BSA, a monolayer would contain approximately 225 ng/cm^2 of BSA, which is lower than but in the same order of magnitude as that estimated solely from the size of a BSA molecule.

Comparing the results from the BSA adsorption study to these estimates of a BSA monolayer, BSA adsorption on glass surfaces leveled off at an asymptotic value of about 500 ng /cm^2. This value, higher than that of the estimated BSA monolayer, could be an indication that more than a monolayer of BSA was adsorbed on glass surfaces. However, BSA adsorption for all comb copolymer substrates was lower than that of a BSA monolayer. Several comb copolymers performed superbly in resisting non-specific BSA adsorption. Isotherms of H6M0, H10M0, H6M9_03, H6M9_01 all reached an asymptotic adsorption value of less than 30 ng/cm^2, which was about one-tenth of the calculated monolayer. H22M9 and H33M9 also showed less than 30 ng/cm^2 adsorption up to the highest concentration of BSA tested. However, at that concentration, their adsorption isotherms were still increasing and thus these two polymers could show an elevation in BSA adsorption and thus may not be non-fouling at a higher concentration. The amount of adsorbed BSA measured in this study was likely to be higher than in reality. Comb copolymer was cast on glass coverslips by spincoating. This technique created relative smooth films at and near the center of the coverslips, but as the polymer solution was spun off during the process, residues accumulated near the edge and around

dust particles on the surface giving rise to irregularities such as small folds and cracks which increased the surface area and exposed the underlying glass leading to an elevated amount of BSA adsorption. These irregularies, the result of a shortcoming of spincoating, were visible under the microscope even at 5X magnification. However, even with the increased amount of BSA adsorption due to the presence of these surface defects, comb copolymers, H6M0, H10M0, H6M9_03, H6M9_01, H22M9 and H33M9 were still non-fouling at high BSA concentrations, as discussed above.

We compared the performance of these "non-fouling" comb copolymers with other similar BSA adsorption investigations on PEO-grafted polymer or surfaces reported in the literature. One of the most non-fouling surfaces found in the literature was polyethylene and polytetrafluoroethylene surfaces deposited with tetraethylene glycol dimethyl ether (TEGDME) by glow discharge plasma deposition (Lopez et al., 1992). Lopez et al. performed a series of protein adsorption studies on these surfaces with Baboon albumin at 0.2 mg/mL concentration. After two hours of adsorption, the amount of BSA adsorbed on these non-fouling TEGDME surfaces was about 20 ng/cm^2, and our results showed that BSA adsorption on the non-fouling comb copolymers was in the same range. Our results are also in agreement with previous investigations by Hester et al. who showed by x-ray photoelectron spectroscopy and BSA stained with anionic colloidal gold that BSA resistance was imparted by H0M9 comb copolymer segregated on the surface of poly(vinylidene fluoride) (PVDF) membranes (Hester et al., 1999).

The BSA adsorption study only gave a rough estimate of how much protein would be adsorbed onto comb copolymer substrates in an oversimplified scenario, with only one protein in PBS. Nevertheless, it served to provide a first-pass screening of whether a given comb copolymer was non-fouling and allowed us to compare its performance with other model protein adsorption studies in the literature. However, in *in vitro* culture and more so in an *in vivo* grafting site, comb copolymer would be subjected to aqueous environment with various proteins, including those secreted by cells. With proteins of

different size, charge, bulk concentration and surface activity, adsorption to surfaces becomes a lot more complicated as proteins dynamically compete for sites on the surface. The conformation of the adsorbed protein also could not be predicted by this kind of protein adsorption study. However, it is the type of adsorbed proteins and their conformation at the surface that determine whether cells would adhere to the surface through binding their receptors to the adsorbed proteins. Therefore, to investigate which comb copolymer is the most inert in *in vivo* and *in vitro* situations, empirical studies were needed to measure the relative amount of non-specific cell adhesion on various comb copolymers using cells directly relevant to the *in vitro* and *in vivo* situations of interest.

As mentioned before, the wtNR6 fibroblast cell line was used to study the cell resistance of comb copolymers because of its known strong adhesiveness to attach non-specifically to surfaces (Maheshwari et al., 2000) and the prevalence of fibroblasts in the body. Our studies indicated that most comb copolymers tested showed excellent fibroblast resistance. Less than 5% of the amount of cells adhered to TCPS adhered to H6M9_3, H6M0, H10M0, H22M0, H0M9 and H0M45. It needs to be pointed that the amount of adherent cells measured, whether at 48 hrs or on day 7, reflects the number of fibroblasts initially adhered as well as the ones proliferated during the course of the experiments. Results from the study also showed that comb copolymers with methoxy-terminated sidechains were more fibroblast resistant than those with hydroxyl-terminated sidechains, or a mixture of both. However, its marrow resistance was similar to that of the most marrow-resistant HPOEM or H6M9 combs. Previous experimental data from our group also indicated that comb copolymers with methoxy-sidechains were more wtNR6 resistant than hydroxyl ones (Irvine, 2000). Comb copolymers with longer sidechains were in general less resistant to non-specific cell adhesion than those with shorter sidechains. This could be due to the increased average distance between POEM sidechains exposing the PMMA layer to non-specific adsorption of proteins in the media. As a consequence, cells could adhere themselves to the adsorbed proteins. Even though less cell adhesion was observed on H6M9_3 which had 36 wt% total POEM compared

to the 34 wt%-POEM H6M9_1 ((10.46 ± 2.4) % and (2.03 ± 1.24) %), the margin POEM content was too small and the statistical insignificance as analyzed by post hoc comparison test made it impossible to conclude whether a higher POEM content contributed to better cell inertness. Note that in both H6M9_1 and H6M9_3, the ratio of HPOEM to MPOEM was roughly 1:1. The much-higher non-specific cell adhesion observed on H6M9_2, despite its high POEM content (37 wt%), was unexpected. Even the higher HPOEM:MPOEM ratio (2.3:1) compared to the other two H6M9 polymers could not explain its compromised cell resistance as H6M0 had no MPOEM sidechains at all and contained 40 wt% HPOEM. The results of wtNR6 resistance showed no correlation with the BSA adsorption studies. For instance, H0M45 substrates, one of the most cell resistant surfaces, supported the highest amount of BSA adsorption. This showed that despite the fact that BSA is the main constituent of serum, BSA adsorption studies were not a good predictor of the total amount of all proteins that would adsorb onto the surface and/or the amount of non-specific cell adhesion was not only dependent on the amount of protein adsorption.

The marrow aspirate resistance study was the most direct estimate of how comb copolymers would behave in bone marrow grafts or in *in vitro* studies with marrow aspirates. Bone marrow consists of various cell types and in measuring the number of colonies, subcolony-clusters and single adherent cells, the investigation hoped to shed light on how different cells, differentiated by their adhesion and colony-forming characteristics, would behave on comb substrates. Colonies and subcolony clusters on surfaces would most likely be populated by colony forming cells such as the connective tissue progenitors (CTPs). Subcolony clusters indicated the presence of these cells but probably with a slower proliferation rate than those in the colonies. Single cells found on test surfaces could be any adherent cell types in bone marrow, such as fibroblasts, endothelial cells, macrophages or CTPs that have not proliferated to form clusters or colonies. Further details of the colony forming assay will be discussed in Chapter 5. Colony formation requires both the initial adhesion of a colony forming cell to the surface as well as subsequent proliferation of that cell within 6 days to become a colony.

Thus, failure to support colony formation on an inert surface may be by means of resisting the initial adhesion of colony forming cells and/or inhibiting or retarding the proliferation of an adherent colony forming cell. In the case in which proliferation of an adherent colony forming cell was retarded, one would expect to see an increase in $\%_{colonies+clusters}$, the ratio of the sum of colonies and subcolony clusters on test surfaces to that on the glass control and/or the number of single cells on test surfaces. By day 6 in CFU assays, most colonies that were capable of forming would have formed on glass surfaces and our data showed that the number of subcolony clusters on glass was very small compared to the number of colonies. Therefore, increase in $\%_{colonies+clusters}$ signified an increase in the number of subcolony clusters on test surfaces. This increase was very significant in the case of three of the four long sidechain combs, H22M9, H33M0 and H33M9, as well as all of the three-component combs, H6M9. This showed that there were a number of non-specifically adhered colony-forming cells on these comb substrates, but that their proliferation was relatively slow so they did not fully develop into colonies. Our data showed that the number of adherent single cells on all surfaces fell in the narrow range of a score of 1.2 to 2.25, i.e., around 10 – 100 single adherent cells per 2 million marrow cells seeded. The low percentage of cells adhering to the surfaces indicated that comb copolymers were very inert to non-specific cell adhesion in bone marrow aspirates.

From the cell resistance studies done empirically as described above, comb copolymers that were the most resistant to both fibroblasts, a cell type highly present in human tissues, as well as human marrow aspirates, which would be the cell source to be used for bone graft and subsequent studies, were identified. Only comb copolymers with functionalizable sidechains, in this case, the HPOEM sidechains, were chosen here. The hydroxyl end-groups of HPOEM sidechains could be activated a number of ways, such as with tresyl chloride, 4-nitrophenylchloroformate (NPC) and p-maleimidophenylisocyanate (PMPI) for covalent coupling with peptides and small proteins to engender specific cell response in subsequent studies. In light of that, two comb candidates, H6M0 and H10M0 were identified. Both polymers had excellent cell

resistance. Calculations from GPC and NMR results showed that each H6M0 polymer molecule had, on average, 86 HPOEM sidechains, ie, 86 functionalizable sites, while 107 HPOEM sidechains were present on each H10M0 molecule. The higher number of sidechains for the H10M0 polymer was due to the polymer's higher molecular weight and hence more repeating units. The H10M0 comb copolymer was chosen at the end as the comb copolymer to be used for subsequent studies due to its higher number of HPOEM sidechains and longer sidechains which may be preferable due to the higher flexibility of the sidechains. A large-scale batch of H10M0 comb copolymer was synthesized as a result. Its cell resistance was re-verified to be similar to the H10M0 comb copolymer tested previously. Unless otherwise noted, this polymer was used in all subsequent studies.

2.5 References

Giacomelli, C.E., Avena, M.J. and DePauli, C.P. (1997). "Adsorption of bovine serum albumin onto TiO2 particles." Journal of Colloid and Interface Science **188**(2): 387-395.

Hester, J.F. (2000). Surface Modification of Polymer Membrances by Self-Organization. Ph.D. Thesis, Massachusetts Institute of Technology.

Hester, J.F., Banerjee, P. and Mayes, A.M. (1999). "Preparation of protein-resistant surfaces on poly(vinylidene fluoride) membranes via surface segregation." Macromolecules **32**(5): 1643-1650.

Irvine, D.J. (2000). Spatially controlled presentation of biochemical ligands on biomaterial surfaces using comb copolymers. Ph.D. Thesis, Massachusetts Institute of Technology.

Irvine, D.J., Mayes, A.M. and Griffith, L.G. (2001a). "Nanoscale clustering of RGD peptides at surfaces using comb polymers. 1. Synthesis and characterization of comb thin films." Biomacromolecules **2**(1): 85-94.

Irvine, D.J., Ruzette, A.V.G., Mayes, A.M. and Griffith, L.G. (2001b). "Nanoscale clustering of RGD peptides at surfaces using comb polymers. 2. Surface segregation of comb polymers in polylactide." Biomacromolecules **2**(2): 545-556.

Lopez, G.P., Ratner, B.D., Tidwell, C.D., Haycox, C.L., Rapoza, R.J. and Horbett, T.A. (1992). "Glow discharge plasma deposition of tetraethylene glycol dimethyl ether for fouling-resistant biomaterial surfaces." Journal of Biomedical Materials Research **26**: 415-439.

Maheshwari, G., Brown, G., Lauffenburger, D.A., Wells, A. and Griffith, L.G. (2000). "Cell adhesion and motility depend on nanoscale RGD clustering." Journal of Cell Science **113**: 1677-1686.

Muschler, G.F., Nittoa, H., Boehm, C.A. and Easley, K.A. (2001). "Age- and gender-related changes in the cellularity of human bone marrow and the prevalence of osteoblastic progenitors." Journal of Orthopaedic Research **19**(1): 117-125.

Peters, T. (1985). "Serum-Albumin." Advances in Protein Chemistry **37**: 161-245.

Ratner, B.D., Hoffman, A.S., Schoen, F.J. and Lemons, J.E. (2004). Biomaterials Science : An Introduction to Materials in Medicine, Elsevier Academic Press, San Diego, USA.

Walton, D.G. and Mayes, A.M. (1996). "Entropically driven segregation in blends of branched and linear polymers." Physical Review E **54**(3): 2018-2021.

Chapter 3

Functionalization of Comb Polymer, Surface Modification and Characterization

3.1 Introduction

In the previous chapter, we identified the comb copolymer, H10M0, as the choice of biomaterial to be used for the surface design of bone marrow grafts. This polymer, as we have shown, was resistant to protein adsorption and non-specific cell adhesion. To engender specific cell response, the polymer must be functionalized with biomolecules and be presented to surrounding cells. As the primary interest of this thesis is to optimize the interaction of bone marrow aspirate cells with the surface of bone grafts to achieve better efficacy in bone formation, a two-dimensional model to study cell interactions with surfaces is preferred. Therefore, methods for functionalizing comb copolymers were developed with this in mind. The objective of work described in this chapter is to develop methods for coupling small adhesion peptides to the sidechain ends of comb copolymer at the surface. With small modifications, the protocols could be easily adapted to coupling bigger proteins. Small adhesion peptides were focused on due to their robustness and low risks of undesirable immune response compared to proteins of bigger size and complicated tertiary structure. Peptides exhibit higher stability towards pH-variation (Ito et al., 1991), storage (Boxus et al., 1998) and sterilization conditions (Weiss et al., 2001). Such stabilities are highly favorable for the fabrication of peptide surfaces as well as the preparation of them for biological studies. In addition, it has been shown that cell integrins can bind to small adhesion peptides such as the tri- residue sequence RGD (Pierschbacher and Ruoslahti, 1984; Ruoslahti and Pierschbacher, 1987). The reasons for using peptides and the choice of peptides used in these studies are discussed in greater detail in Chapter 4.

Two steps of chemical reactions were involved in the functionalization of comb copolymer. First was the activation of the polymer sidechain ends so that in the second reaction, peptides can be coupled to them. Peptides can be covalently coupled to the hydroxyl sidechain ends of comb copolymer via the amine or carboxylic terminal groups or via the thiol of a cysteine or sidechains of other residues. Here we focus on developing methods to couple peptides via the amine terminus as it is the most readily available in all peptides, compared to, for example, cysteine or other sidechain groups in a particular residue. In activating the comb polymer for peptide coupling via the amine terminus, numerous reports could be found in the literature in activating polyethylene glycol (PEG) chains, for example, by alkylation or acylation, for subsequent peptide or protein conjugation. For instance, hydroxyl-terminated PEG could be activated with tresyl chloride (Delgado et al., 1990; Sperinde et al., 1999) or carboxylated then activated with hydroxysuccinimidyl esters (Shah and Watson, 1993). These protocols, however, could not be transferred directly to activate the comb copolymer. The amphiphilic nature of the comb presented complications both in activating the polymer as well as in purification and processing after the activation. Issues such as solubility could be anticipated. Previous work done in our lab had used N-hydroxylsuccinimide (NHS) to activate comb copolymer after the hydroxyl chain-ends had been first carboxylated (Irvine et al., 2001a). Later in this chapter, this method of comb functionalization and its companion protocol of peptide coupling to NHS-comb in solution will be revisited and compared with the methods developed in this chapter. In the work presented here, as we were primarily interested in cellular interactions with peptides presented by the comb at the surface, peptides are coupled to activated comb copolymer at the surface instead of in solution. Surface coupling allows a much more economical use of peptides compared to solution coupling and purification is much easier due to the amphiphilic nature of the comb polymer and the fact that the addition of peptides could change the solubility of the polymer after coupling. This chapter describes the development of methods for activating and peptide-coupling the comb copolymer, and the

characterization methods that were central to the implementation of the two-dimensional experimental model for subsequent cell studies. An additional advantage of the comb copolymer was the possibility to allow easy tuning of peptide surface density, an essential feature for the experiments directed at determining the effect of peptide density on cell function. The optimization of the coupling reaction and post-reaction purification, as well as the quantification of peptide densities on these surfaces is discussed. At the end of the chapter, peptide-coupled comb surfaces are evaluated on their sturdiness and stability over a 21-day period.

3.2 Materials and Methods

3.2.1 NPC activation of comb copolymer, purification and characterization

Comb copolymer was dissolved in benzene and free-dried azeotropically to remove all the moisture in the polymer. The polymer was then dissolved in dichloromethane and 4.5 times excess of triethylamine (TEA) was added. (Since this procedure was to activate the hydroxyl- terminal of PEO sidechains of comb copolymer, all stated molar excess ratios are relative to the number of moles of hydroxyl end-groups to be activated.) The reaction flask containing the reaction mixture was cooled in an ice bath while the flask was purged with nitrogen. When the mixture was cooled to 4°C, 2.5 times molar excess of 4-nitrophenyl chloroformate (NPC) dissolved in dichloromethane, was injected into the reaction flask. The mixture was allowed to react for 2 hours on ice and overnight at room temperature or 4 hours on ice.

At the end of the reaction, the product was concentrated by rotary evaporation. TEA salts were removed by precipitating the mixture in ethyl acetate followed by centrifugation to separate the salt precipitate from the activated polymer solution. After a second precipitation, the NPC-activated comb polymer was purified by filtering the polymer solution into petroleum ether to form precipitates. The amount of petroleum ether used was more than 8 times the amount of polymer-ethyl acetate solution in order for the comb copolymer to precipitate. The precipitate was re-dissolved in ethyl acetate, filtered and re-precipitated in petroleum ether two more times before the polymer was dried in vacuo. NPC comb polymer was aliquoted and stored at -20°C until use.

NPC-activated comb copolymer was analyzed by gel permeation chromatography with inline light scattering (GPC-LS, Wyatt MiniDawn) and the percentage conversion of sidechain hydroxyl-terminal groups to NPC was determined by NMR (Bruker Avance DPX400 proton NMR running at 400 mHz). ^{1}H NMR spectra were obtained for 1% copolymer solutions in deuterated chloroform.

3.2.2 Peptide-coupling to comb substrates and preparation of surfaces with different peptide densities

To prepare surfaces with various peptide surface densities, a series of comb copolymer solutions were made by mixing NPC-activated comb copolymer with its non-activated counterpart in defined proportion. These comb copolymer solutions with various percentages of NPC-activated comb were then spincoated on glass coverslips, as described in the previous chapter, to give rise to surfaces with various densities of NPC comb sidechains. Hence, when peptides were allow to couple to these surfaces, different peptide surface densities could be obtained.

Peptides were obtained from several sources, the MIT Biopolymers Laboratory, Tufts University Core Facility or synthesized in our own laboratory. All peptides were purified by high performance liquid chromatography and analyzed by MALDI mass spectroscopy. Peptides with free amine terminal groups were dissolved in 0.1 M sodium bicarbonate ($NaHCO_3$) buffer (pH 8.3) at ~ 1mM, unless otherwise specified. Peptide coupling was done by placing spincoated surfaces with NPC-activated comb copolymer in contact with peptide solution for 4 to 5 hours at room temperature. The surfaces were then rinsed twice with sodium bicarbonate buffer before ethanoamine (EtAm) solution (0.025M EtAm in 0.25M $NaHCO_3$ buffer) was added to the surfaces to deactivate the remaining NPC groups that had not been coupled to peptides. The surfaces were allowed to incubate in the EtAm solution at 37°C overnight and then rinsed three times with $NaHCO_3$ buffer and finally with milliQ water to remove residual bicarbonate salts.

3.2.3 Quantification of side product release

The amount of 4-nitrophenol, side product given off by the reaction of NPC groups, could be measured by colorimetry. The peptide solution used for coupling was collected at the end of the experiment. The absorbance of the solution at 400 nm was measured by a spectrophotometer. Correlating the absorbance with a standard curve of

absorbance versus known amount of 4-NP, the amount of 4-NP given off by the reaction of NPC-activated comb was calculated. Note that the amount of 4-NP measured was the collective amount given off by both the hydrolysis and peptide-coupling to NPC groups. Since 4-NP is a small molecule that can easily diffuse, contributions can come from reaction throughout the polymer film, and not just limited to the very top surface.

3.2.4 Quantification of peptide surface density

To quantify peptide surface density, peptides were radiolabelled with iodine-125 using a similar iodobead method as reported by Brown (Brown, 1999) but modified to accomodocate the peptides used here. In brief, 20 μL of peptides (approximately 2mg/mL in PBS) were allowed to react with an iodobead and 5mCi of ^{125}I for 15 minutes. The reaction was then quenched with 80 μL of the reducing agent sodium metabisulfite (12 mg/mL in PBS) followed by cold potassium iodide solution. Peptides were purified with a C18 Sep-Pak Reverse phase cartridge (Waters, MA). ^{125}I - peptide solution was loaded on the cartridge and a series of water-based solutions containing 1% trifluoroacetic acid (TFA) and an increasing amount of methanol (10% to 80%) were run through the cartridge to elute the ^{125}I -bounded peptides and separate them from free ^{125}I. A gamma counter was used to determine the fractions which contained the most ^{125}I - peptides. 2 mg of cold peptides were then added to the ^{125}I - peptide fraction and because of the relatively negligible amount of ^{125}I - peptides in the solution compared to that of the cold peptides added, the final concentration was based only on the amount of added cold peptides. The peptide solution was then titrated to approximately pH 8.3.

To quantify peptide surface density, ^{125}I - peptide solution prepared as described above was diluted to the concentration at which peptide-coupling would usually be done. In essence, the reaction parameters of peptide-coupling were kept the same as that used in preparing regular peptide-coupled comb surfaces of which the peptide density was of interest. After deactivating with ethanoamine and several washes with 0.1M sodium

bicarbonate buffer, gamma activity of the ^{125}I-peptide-coupled coverslips was measured with a Packard Cobra II Gamma Counter. By correlating gamma activity with the standard calibration curve of gamma activity versus number of ^{125}I - peptides, obtained by gamma counting a series of ^{125}I - peptide solutions with known concentrations, overall peptide surface density on a substrate was calculated.

3.2.5 Surface stability studies

Spincoated surfaces with NPC-activated comb and its non-activated counterpart were prepared as described in previous sections. Surfaces were coupled with ^{125}I-peptides and de-activated with EtAm as described above. After washing, substrates were placed in 24 well-plates where cell growth media (DMEM with 10% FBS, 2mM L-glutamine, 1mM sodium pyruvate, 100 i.u./mL penicillin and 200 μg/mL streptomycin) were added. The substrates were incubated in media at 37°C for up to 21 days. During this 21-day period, a triplicate of substrates were taken out on day 0, day 1, 3, 7, 14 and 21 to assess the gamma activity on the substrates and in the media.

3.3 Results

3.3.1 Characterization of NPC-activated polymer

Comb copolymer activated with NPC was characterized by GPC and NMR. Results from GPC did not show any detectable difference in molecular weight and polydispersity index before and after the NPC activation. The conversion of hydroxyl sidechain ends of comb copolymer to NPC was assessed by NMR. The characteristic pair of proton peaks of 4-nitrophenyl carbonate at 7.4 – 8.4 ppm indicated the successful activation by NPC (Figure 3.1). The ratio of the proton peak of the ethylene group attached directly to 4-nitrophenyl carbonate to the proton peak corresponding to the ethylene group attached to a MMA group gave the percentage of POEM sidechains that were activated. Without azeotropic freeze-drying of the comb copolymer before the activation, the percentage of NPC activation, for both the H10M0 and H6M9_3 comb copolymer, was consistently only around 55%. The percentage of NPC activation drastically increased to over 80% with freeze-drying preparation of the polymer.

3.3.2 Peptide-coupling to comb polymer surfaces and quantification of peptide surface density

3.3.2.1 Effect of pH on peptide coupling

In attempt to optimize the peptide-coupling reaction as well as the removal of non-specifically adsorbed peptides on the substrates, parameters of the peptide-coupling reaction and the washing procedures were varied. For all the peptide-coupling reactions, the amount of peptides used was always in excess in order to maximize the amount of coupling. Thus the main parameter to be varied was the pH of the reaction. Two different pH conditions were used for peptide coupling, pH 8.3 and pH 10. The results for coupling the peptide GRGDSPY to the H6M9_3 polymer under these two pH

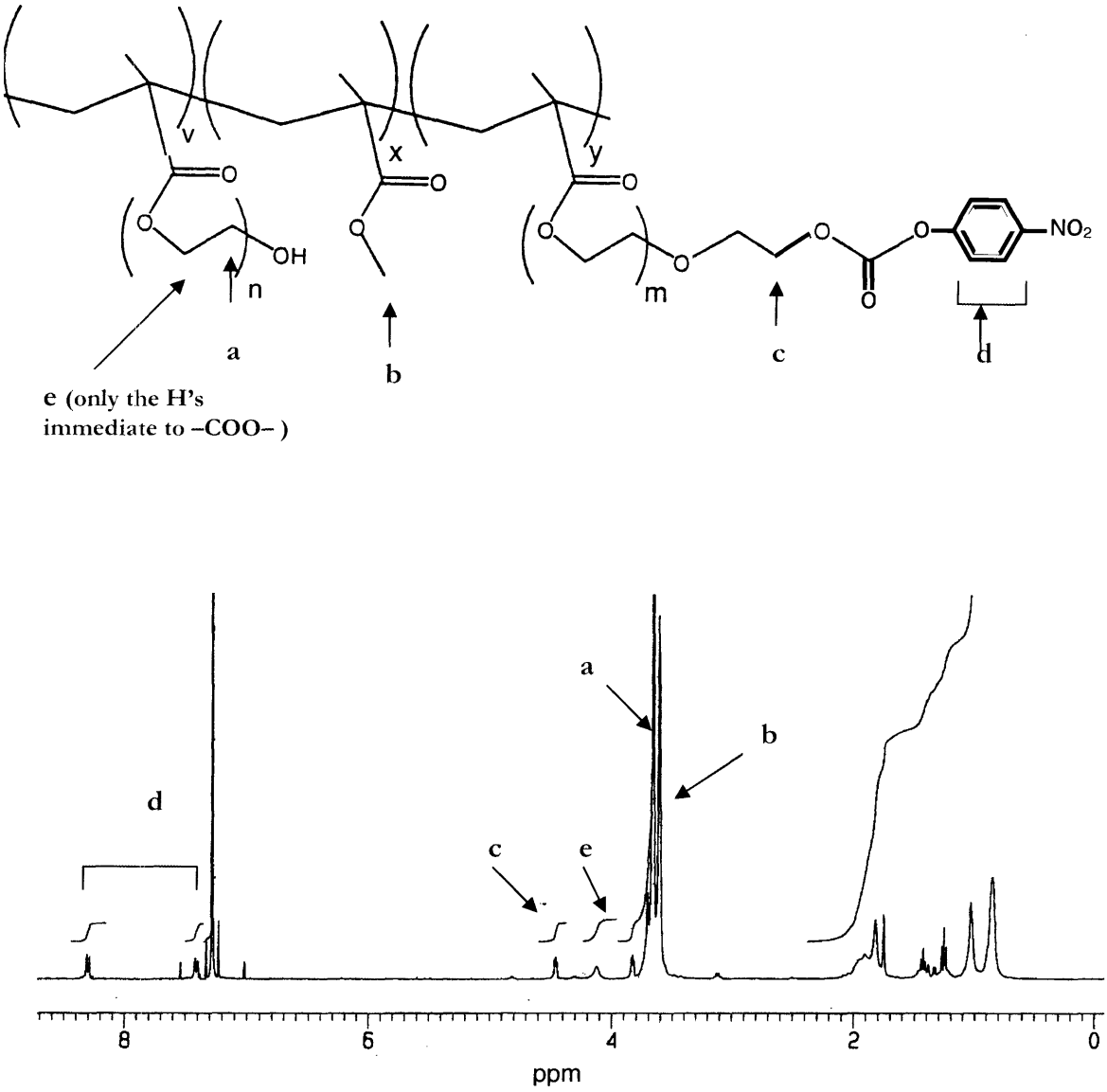

Figure 3.1 ^{1}H NMR spectra of NPC-activated comb copolymer. **e** refers to the two hydrogens immediate to – COO – in all POEM sidechains. The ratio of **c** to **e** gives the percentage of – OH groups to – NPC.

conditions are shown in Figure 3.2. Peptide densities were obtained by using ^{125}I - peptides, as outlined in the Methods and Materials section. The peptide density shown in Figure 3.2 was the per unit area difference in the number of peptides as measured from the gamma activity on a surface and that on a substrate with no NPC-activated comb (ie, the non-activated version of the same comb copolymer). The amount of peptides measured on the non-activated comb surface represented the amount of non-specifically adsorbed peptides. Coupling efficiency was higher at pH 8.3 than pH 10 and the same results were observed for other peptides with the same polymer as well as the 3-component polymer H6M9.

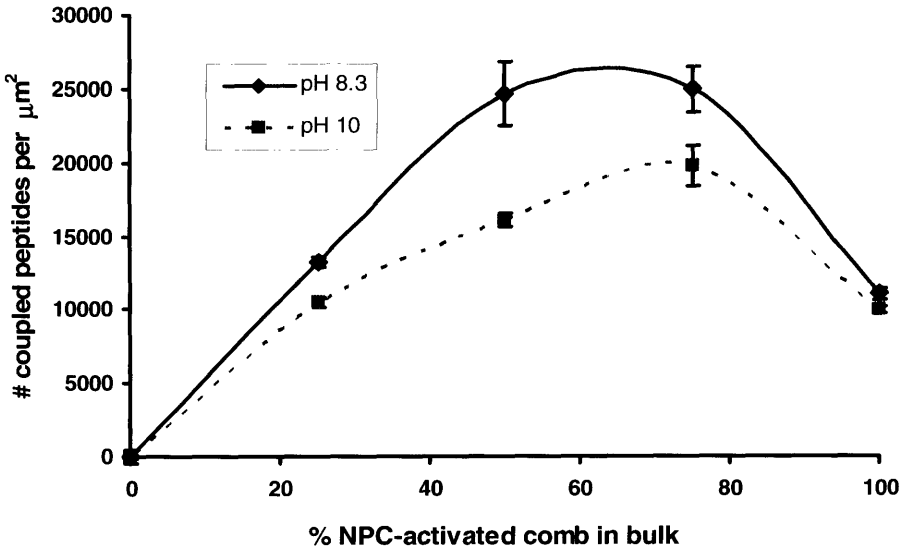

Figure 3.2 Amount of GRGDSPY peptides coupled to surfaces with NPC-activated comb at pH 8.3 and pH 10. Error bars showed standard errors of substrate quadruplicates within a representative experiment. The experiment was repeated twice and similar results were obtained.

3.3.2.2 Quantification of surfaces with various peptide densities

Spincoated surfaces with 0% to 100% NPC-activated comb in the bulk spincoating solution were synthesized. Figure 3.3 and Figure 3.4a showed the two general trends of

peptide densities when ^{125}I - peptides were coupled to surfaces with increasing NPC-comb densities. When the percentage of NPC-activated comb was increased from 0% to about 30%, the increase of surface peptide density was linear ($R^2 > 0.95$ for all peptides), as shown in Figure 3.4b. However, beyond about 30%, the increase in peptide density started to plateau off or even decreased at the highest percentages of NPC-activated comb, as in Figure 3.3.

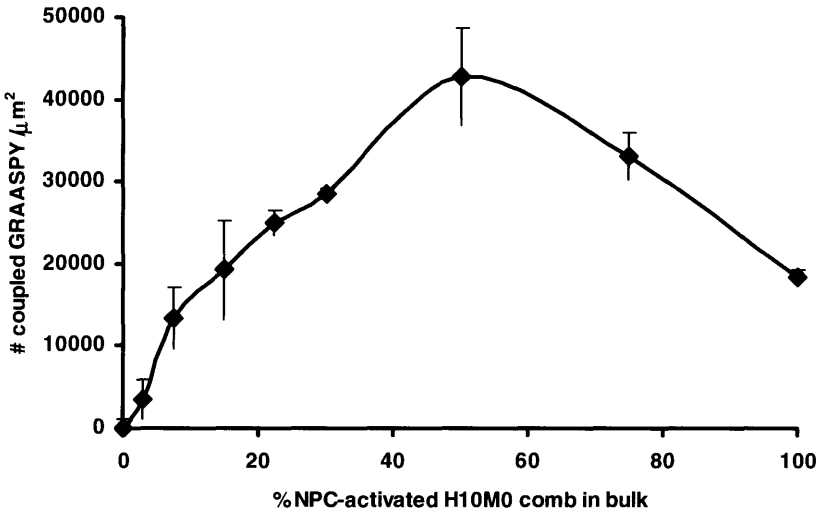

Figure 3.3 The biphasic trend of peptide surface density with increasing % NPC-activated comb on the surface. Peptide surface density decreased at high % of NPC-activated comb on the surface. Figure 3.4 showed another typical trend in peptide quantification in which peptide surface density leveled off beyond ~ 30% NPC-activated comb on the surface. Error bars showed standard error of technical triplicates.

As the expected trend was a monotonic increase in peptide density as the ratio of NPC-comb to non-activated comb on the surface was increased, a number of experiments were carried out to explain the biphasic variation of peptide density with increasing NPC-comb. We hypothesized that the side product released from the reaction of NPC groups may have an effect. A set of experiments was therefore carried out to investigate the effect of the reaction side product, 4-nitrophenol, which was given off by both the

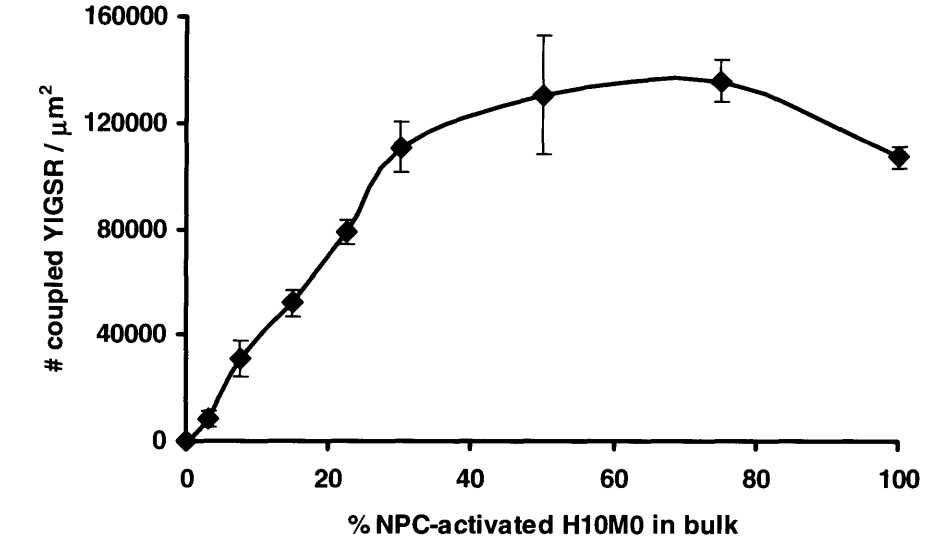

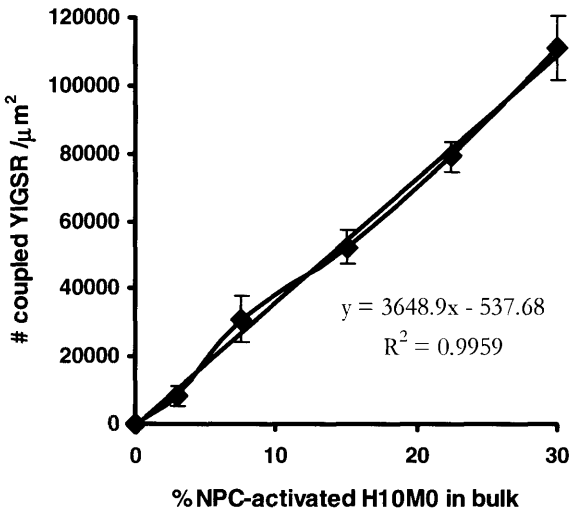

Figure 3.4 **Top (a)** Surface YIGSR peptide density increased with increasing % NPC-activated comb then leveled off beyond 30% NPC-activated comb. **Right (b)** Magnification of linear region of (a). From 0% to 30% of NPC-activated H10M0, the increase of peptide surface density with % NPC-activated comb was linear. Error bars showed standard errors of substrate triplicates of a representative experiment. Three experiments were performed and similar results were obtained

coupling and hydrolysis reactions, on peptide density. The amount of 4-NP given off by NPC-activated comb coverslips were measured by colorimetry. The total amount given off by a 10mm diameter 100% NPC-activated comb surface was 1.0 μg. Assuming this amount was concentrated within the couple hundred microns immediately above the surface before mixing, the concentration of 4-NP near the surface would be approximately 0.23 μmol/mL. Exogenous 4-NP, at this concentration, was added to the peptide coupling buffer to investigate its effect on coupling. Peptide-coupling densities

on these surfaces were compared to that without the exogenous 4-NP and peptide density was lower on coupling with exogenous 4-NP, as shown in Figure 3.5. Peptide surface density was also lower when peptide solution that had been previously used for coupling to NPC-activated comb was used in the coupling reaction (Figure 3.6). Since the amount of peptide in the coupling solution was in excess, the only difference between recycled and new peptide solution was the 4-NP from the previous reaction.

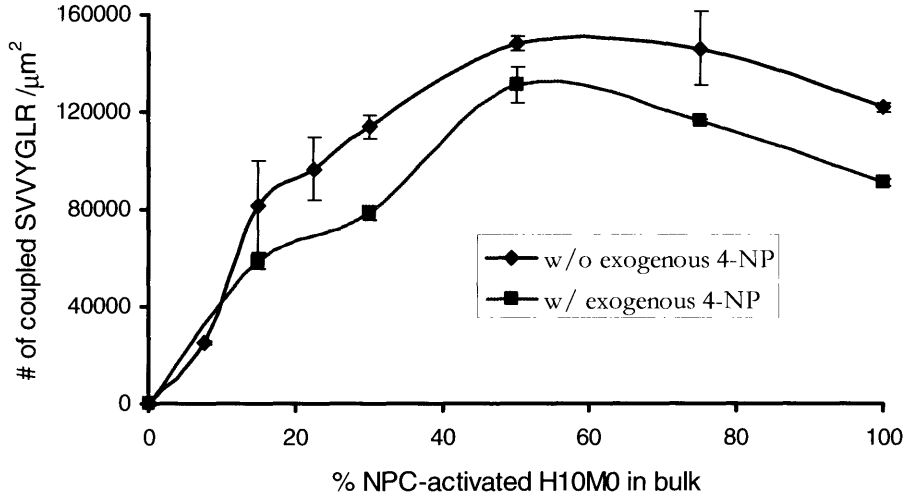

Figure 3.5 Effect of 4-nitrophenol on surface peptide coupling yield. The amount of exogenous 4-NP added was comparable to the amount local at the surface due to the side product released by the reaction of NPC groups. Error bars showed standard errors of substrate triplicates of a representative experiment. Two more experiments were performed (one with the same peptide and the other with GRGESPY) and almost identical trends were obtained.

3.3.3 Surface stability studies

The objective of the surface stability studies was to examine the stability and integrity of the spincoated thin film and the stability of peptides introduced to the surface after prolonged immersion in cell culture media. For incubation in culture media at 37°C for up to 7 days, spincoated thin films remained integral. However, after that, at around day

14, films started to detach from the coverslips. By day 21, slight disturbance to the films would cause the film to delaminate from the coverslip.

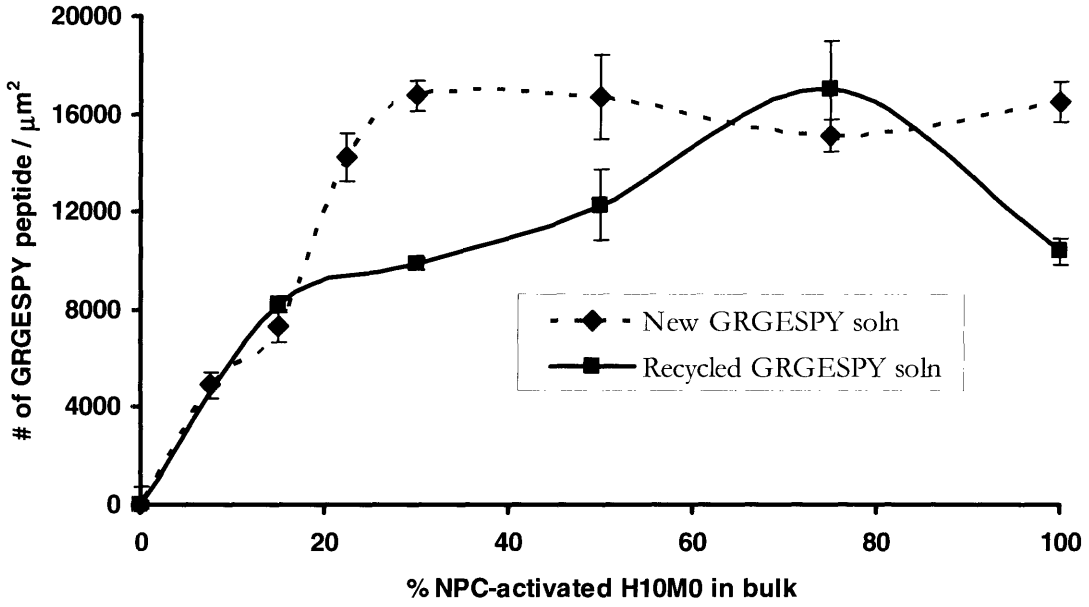

Figure 3.6 Effect of 4-nitrophenol on surface peptide coupling yield. GRGESPY peptide solution that had been used for coupling, and hence contained 4-NP but same peptide concentration, was recycled for another coupling. Surface peptide density obtained was lower than when new peptide solution was used. Error bars showed standard errors of substrate triplicates of a representative experiment. Three experiments were performed and similar results were obtained

An array of surfaces encompassing three peptides and two different comb copolymers was tested for the amount of peptides given off by the surface over the course of 21 days. For each type of comb copolymer, when surfaces with low peptide density (7.5% NPC-comb in bulk) and high peptide density (22.5% - 30% NPC-comb in bulk) were compared with non-activated comb control (0% NPC-comb), it was found that the absolute amount of peptides released for all three types of surfaces were the same, within experimental error. The amount of peptides released was attained after 7 days of immersion in media, and the decline in the amount of peptides remaining on the surfaces

was stabilized after day 7. The amount remained the same, and did not increase between day 7 and 21 (Figure 3.7a and 3.7b).

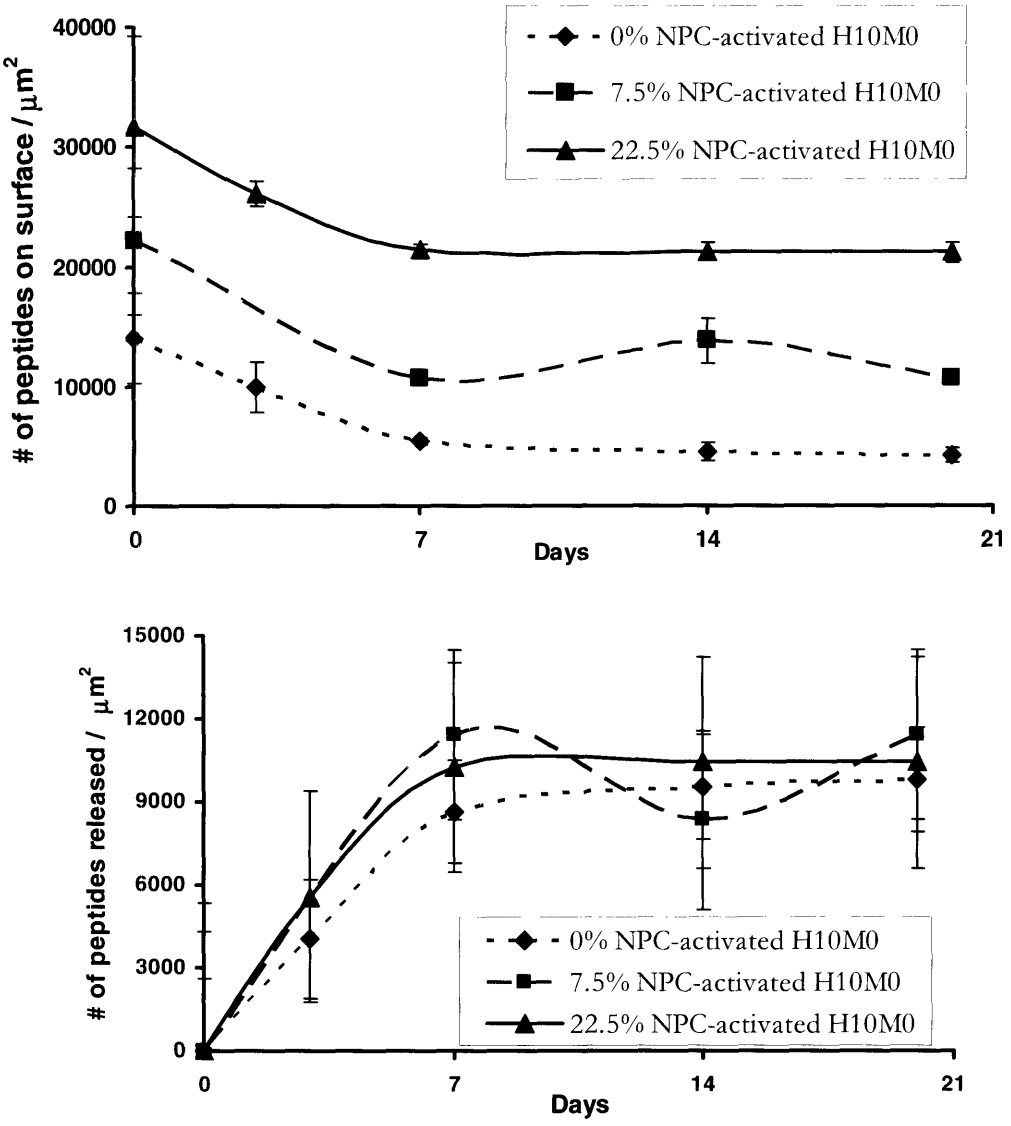

Figure 3.7 Surface stability studies. **(a)** amount of GRAASPY remained on the peptide-coupled comb surfaces after immersion in cell growth media. **(b)** the amount of GRAASPY released by the surfaces under the same conditions. Error bars showed standard errors of 6 substrate replicates of a representative experiment. The experiment was also performed with 2 other peptides and with comb copolymer H6M9. The same trend was obtained for all cases.

3.4 Discussion

3.4.1 NPC activation of comb copolymer

Several methods of activating the comb copolymer for functionalization with peptides or small proteins had been used or developed previously. Irvine et al. had used NHS for activation after carboxylizing the hydroxyl end-groups of POEM side chains (Irvine et al., 2001a). This method had worked with solution coupling with peptides. However, we found that the yield was extremely low due to the extra step needed before NHS activation could be done. Considerable efforts had been put in activating the comb copolymer with tresyl chloride and subsequent coupling with peptides. In addition to the high hydrolysis rate, we found that even after strenuous purification procedures, the amount of tresyl chloride salts from the activation and still associated with the comb copolymer caused a significant amount of non-specific cell adhesion, even after the tresyl-activated chain ends of comb copolymer had been hydrolyzed. Coupling of tresyl-activated comb with peptides in solution and the further purification of the peptide-comb product did not alleviate the problem. However, NPC activation of the comb copolymer was a one step reaction with high yield and as we and others have shown, hydrolysis rate was low at neutral and acidic pH. NPC activation also proved to be a much cleaner method – the TEA salts could be removed easily and when tested for cell resistance, deactivated NPC-comb did not promote the non-specific adhesion of fibroblasts.

NMR spectra of the NPC-activated comb showed a consistent > 80% conversion of hydroxyl chain-ends to NPC, when the polymer was freeze-dried prior to the activation reaction. The NPC-characteristic peaks observed in our NMR spectra of NPC-activated comb was consistent with the NMR spectra of other NPC-activated polymers reported in the literature (Jo et al., 2001). The H10M0 comb copolymer shown here contained 40% hydroxyl-terminated POEM sidechains by weight and had a number average molecular weight of 142,000. Stoichiometric calculations showed that with 81%

conversion, per NPC-activated H10M0 molecule, there were 959 repeating units, among which 852 were MMA, 87.5 were NPC-POEM and 20.5 were unconverted hydroxyl-terminated POEM. Based on the simulation results by Irvine et al., P(MMA-r-POEM) comb molecules configured themselves as quasi-2D non-interpenetrating disks at the top layer of the polymer thin film. The hydrated POEM side chains anchor to the underlying layer of primarily PMMA backbone. Given this prediction of quasi-2D configuration of comb copolymer molecules at the very top layer, the radius of gyration of comb copolymer confined in 2-dimensions, R_g^{2D}, can be estimated by

$$R_g^{2D} \approx aC\sqrt{\frac{N_n}{6\phi_{bb}^s}}$$

where a is the backbone segment length ≈ 6.4 Å, C is a constant with an approximate value of 1.1 – 1.45 based on simulations (the mean value, C≈ 1.27, is used here), N_n is the number of backbone segments in the chain = 960, and $\varphi^s_{bb} \approx 0.67$ is the surface volume fraction of backbone segments estimated from self-consistent field calculations (Irvine et al., 2001a). Hence, with the physical data of our comb copolymer as listed above, R_g^{2D} is found to be ≈ 12.5 nm. Given this dimension, the number of NPC-activated sidechains per unit area is approximately 180 x 10^3 per μm^2. This number is also an estimation of the maximum possible surface density of peptides per unit area.

The above estimation of radius of gyration gave us an approximation of the size of the footprint of a comb molecule. However, it did not capture the polydispersity of the comb copolymer. Recently, Kuhlman et al. in our laboratory was able to observe directly the conformation of comb copolymer molecules using transmission electron microscopy and obtained a direct empirical estimation of the number average radius of gyration, R_g^{2D} = 9.2nm, which is on the order of magnitude as the simulated R_g^{2D} estimated above (Kuhlman et al., 2005). With this more realistic R_g^{2D} , the number of NPC-activated sidechains per unit area is roughly 330 x 10^3 per μm^2. The maximum surface density of all the peptides quantified were in the order of 50,000 to 200,000 per μm^2, except for

YGGFHRRIKA, a highly positively charged peptide at neutral or slightly basic pH. This showed that the values obtained by ^{125}I - peptide quantification was in good agreement with the calculated density of NPC-activated sidechains. The maximum surface density for YGGFHRRIKA was around 600,000 per μm^2 which was higher than, but still within the same order of magnitude as, the maximum possible value as estimated above.

3.4.2 Peptide-coupling to surfaces with NPC-activated comb

In an attempt to optimize the surface coupling of peptides to NPC-activated comb surface, the pH of the coupling buffer has been varied to determine the effect of pH on the coupling yield. When the pH of the coupling buffer is higher than the pK of the peptide's amine terminus, more peptides will exist with deprotonated amine. We assume the pK of terminal amine in peptides is similar to the pK value (~ 9 – 9.5) of terminal amine in most amino acids, even though the value deviates with different sidechains in a peptide. The more of this deprotonated amine form of peptides is desired in maximizing the peptide coupling reaction to NPC-activated comb as it is only the deprotonated form, rather than the protonated one ($-NH_3^+$) reacts with NPC. More peptides exist in their deprotonated form at higher pH but a basic pH favors the hydrolysis of NPC. NPC hydrolysis occurred at a much faster rate at basic pH (pH>10) than at acidic (pH 4) or neutral pH (pH 7) at which hydrolysis occurred very slowly, as measured by the release of 4-NP from spincoated surfaces of NPC-activated comb (data not shown). Studies by Veronese et al. on polyethylene glycol activated with a very similar chemistry also showed a much higher hydrolysis rate at basic pH (Veronese et al., 1985). Therefore, in optimizing the peptide coupling reaction, an intermediate pH has to be found to maximize the number of deprotonated amines in peptides while minimizing hydrolysis of NPC groups. In addition, for peptides with lysine or arginine residues, it is desirable to run the reaction at a pH much lower than the pKa of the side chains to minimize side reactions with the amine and amidine groups when deprotonated. (pKa of lysine and arginine is 12.5 and 10.5 respectively.) In light of all these factors, coupling reactions at two different pH, pH 8.3 and pH 10 were tested. Coupling yield was higher at pH 8.3

for both peptides tested, possibly due to the lower hydrolysis rate of NPC groups at that pH such that more NPC was available for peptide coupling. This finding is consistent with a previous report on coupling the proteins ribonuclease and superoxide-dismutase to NPC-activated polyethylene glycol for which the authors also reported an optimal reaction yield at around pH 8.3 (Veronese et al., 1985).

3.4.3 Removal of non-specifically adsorbed peptides on comb surfaces

A moderate amount of peptides were found to be non-covalently linked but associated with the comb surfaces, even on substrates without any NPC-activated comb. Although later it was proven that the amount of adsorbed peptide had no effect on cell adhesion or function, several approaches had been experimented to remove these non-specifically adsorbed peptides. A surfactant, sodium dodecyl sulfate (SDS) and different salts and at various ionic strengths were empirically tested for the ability to remove non-specifically adsorbed peptides. One possibility that peptides were associated with comb surfaces was preferential hydrogen bonding between peptides and the POEM chains over between water molecules and peptides and between POEM and water. Salt has been shown to modify the interactions between proteins and water and induce the solubility (or insolubility) of proteins. However, the molecular basis for this effect, in particular the anionic or cationic interactions with either backbone or side chain groups on the protein is still speculative. Some researchers showed that the ability of salts to induce or reduce protein-water interactions follow the lyotropic or Hofmeister series (Kumosinski and Unruh, 1994; Curtis et al., 2000). The Hofmeister series is given by $SO_4^{2-} > CH_3COO^- > HCO_3^- > Cl^- > NO_3^- > SCN^-$ (Hofmeister, 1888) where salts high in the Hofmeister series interact strongly with water and thus tend to induce proteins to associate with themselves and vice versa. The molecular mechanism of this effect is not known and there exists reports where salt-protein interactions follow a trend opposite to that predicted by the Hofmeister series (Curtis et al., 2000). Therefore, in this work, an empirical approach was taken. Three different salts, sodium sulfate Na_2SO_4, sodium bicarbonate $NaHCO_3$, and sodium nitrate $NaNO_3$, high, in the middle of, and low in the

Hofmeister series, respectively were tested for their ability to remove peptides by the hypothesis of inducing peptide-water interactions, hence dissociating peptides from the polymer surface. At the end of coupling, these buffers with the same ionic strength (0.3M $NaHCO_3$, 0.1 M Na_2SO_4 and 0.3M $NaNO_3$) were used to make up the 0.025M ethanoamine solution to deactivate the remaining surface NPC groups. During the overnight period of NPC deactivation, the salts in the buffer were allowed to act on the adsorbed peptides. Buffers with the same ionic strength were used here so the effect would solely be due to the action of the different anions. No major difference in the effect of different salt type on non-specific adsorbed peptide removal was observed, as shown in Figure 3.8a. Sodium bicarbonate solutions of 0.05M, 0.25M and 0.5M were then used to investigate the effect of ionic strength on adsorbed peptide removal. Again, no noted effect of ionic strength on peptide removal was observed (Figure 3.8b). The effect of ionic strength and salt type may not be effective for the salt concentration tested. However for the comb copolymer, the salt concentration was limited to below 0.75M. When a higher salt concentration was used, the polymer layer disintegrated within a very short period of time. It was also possible that salt did not have much effect on inducing peptides to dissociate with the comb copolymer.

Surfactant was used with reservation to remove non-specifically adsorbed peptides due to the difficulty in removing it at the end of the process and could interfere with cells that were subsequently seeded onto the surfaces. Therefore, only a 1% SDS solution was used in attempt to remove non-specifically adsorbed peptides and at this concentration, no major effect was seen.

The major concern for these non-specifically adsorbed peptides on the surface is if a significant amount is released from the surface, they may compete with peptides covalently linked to the surface for binding with cell adhesion receptors and thus may cause the cells to de-adhere. Fortunately, our long-term cell adhesion experiments substantiated that the adsorbed peptides had no effect on cell adhesion. This will be discussed in Section 3.4.5.

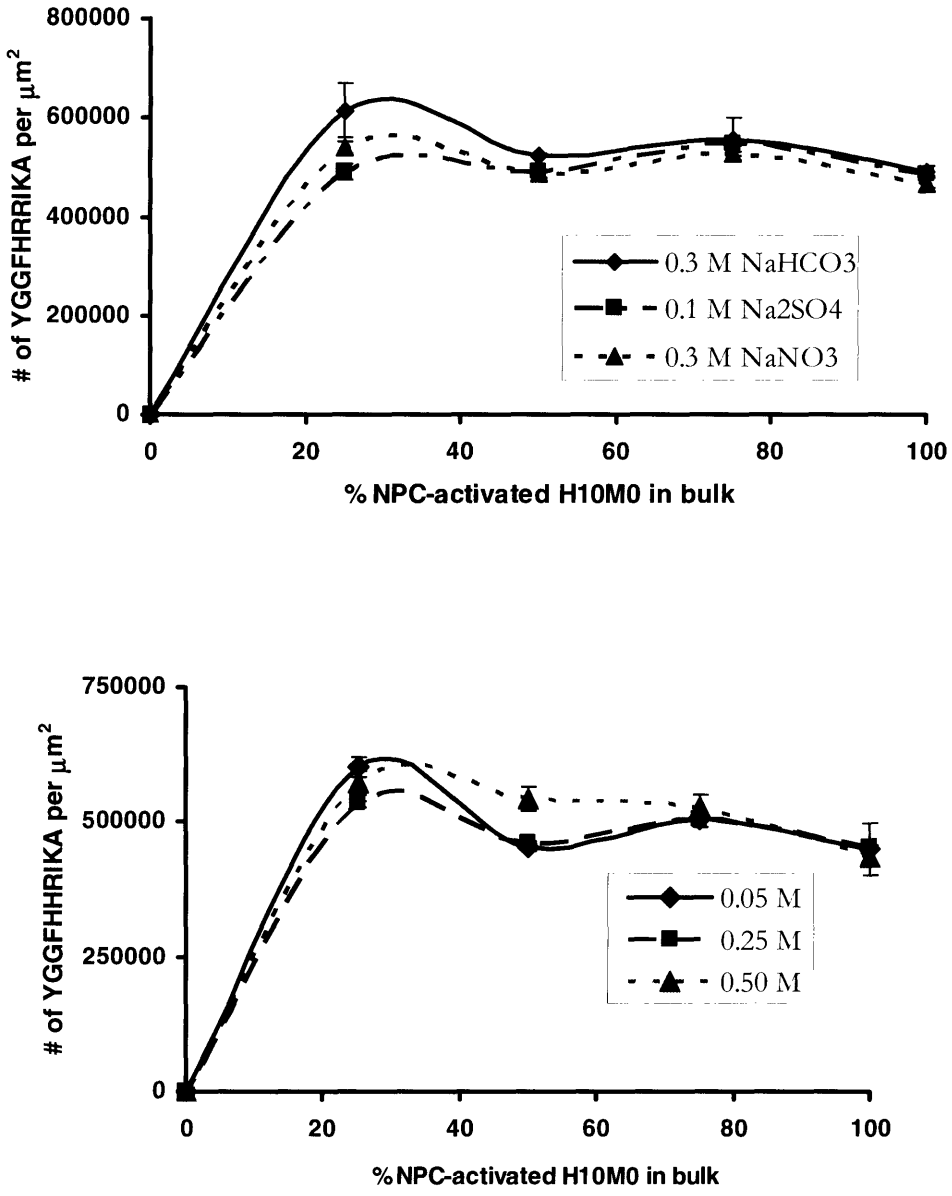

Figure 3.8 Effect of salt types and ionic strength on the removal of non-specifically adsorbed peptides. **(a)** Different salt types were used but had no distinguishable effect on non-specific peptide removal **(b)** Various ionic strength of $NaHCO_3$ solutions were used but no effect on the removal of non-specifically adsorbed peptides. Error bars showed standard errors of substrate triplicates of the experiment.

3.4.4 Side-product inhibition in surface peptide-coupling reaction

The most puzzling results in the quantification of peptide surface density were the biphasic variation of peptide surface density with increasing NPC-activated comb content on the surface. One would expect the peptide surface density to increase monotonically with increasing NPC-activated comb at the surface, or at least increase monotonically till a certain density of NPC-activated comb and level off due to saturation. The decrease in peptide surface density as observed in our experiments could only be explained by the inhibition of the coupling reaction by the side product, 4-nitrophenol that was accumulated at the surface. As NPC-activated POEM side chains were reacted at the surface, due to peptide-coupling and hydrolysis, 4-NP was given off as the only side product. As there was no flow during the entire time the reaction occurred and the reaction was confined to the surface, 4-NP could only be carried away from the surface by diffusion, a slow process, 4-NP was thus built up at the surface. By simple Le Chatelier's principle, a significant amount of the side product 4-NP could possibly shift the equilibrium of the reaction to favor the reactants. In fact, when 0.23 μmol/mL of exogenous 4-NP, an amount equivalent to that given off by 100% NPC-activated comb during the time of reaction, was added to the peptide coupling buffer, the amount of peptide coupling to comb surfaces decreased (Figure 3.5). In addition, when peptide solution recycled from previous peptide coupling was used to couple to comb surfaces, the coupling yield was lower (Figure 3.6). Since the amount of peptide in the coupling solution was in excess, the first coupling reaction would only consume an insignificant amount of peptides, so the peptide concentration remained essentially unchanged. The pH of the solution was readjusted when necessary. Thus, the only difference between the new and recycled peptide solution was the presence of 4-NP. Note that the concentration of 4-NP in the recycled peptide solution, which has been mixed with the rest of the solution in bulk, was much lower than that originally confined at the surface and yet a difference in coupling yield could be observed with this diluted amount of 4-NP. It is not surprising that for surfaces with a high NPC-activated comb content, the peptide coupling yield could be quite drastically inhibited by the significant

amount of 4-NP given off. If the decrease in peptide density at higher NPC-comb surfaces was indeed due to side product inhibition, the quantification of peptide surface coupling to comb polymer using a chemistry that did not yield any side product but water should show a monotonic increase in peptide density with percentage of activated comb on the surface. Very recently, Ufret et al. in our laboratory quantified the amount of peptides coupled to surfaces with various densities of comb copolymer activated with N-(p-Maleimidophenyl)isocyanate (PMPI). Cysteine- containing peptides react with PMPI-activated comb to form a covalent bond with the PMPI- POEM side chains of the polymer with water as the only side product. For this reaction, peptide surface density indeed increased monotonically with increasing PMPI-activated comb on the surface (Ufret, 2005). Although the results from PMPI coupling were not direct evidence to the side product inhibition theory, it substantiated that the presence of a side product could inhibit peptide coupling with NPC-activated comb.

Despite this unexpected side product inhibition that decreased peptide coupling yield at surfaces with high percentage of NPC-activated comb, the peptide surface density increased linearly with the percentage of NPC-activated comb from 0% up to 30% of NPC comb at the surface. The R-squared coefficients for linear regression for that range were all greater than 0.93 (Figure 3.4b). This span gave us a sufficiently wide range of peptide density to control cell integrin binding as we will show in Chapter 4.

3.4.5 Surface stability studies

In the surface stability studies in which peptide-coupled comb coverslips were submerged in cell growth media for up to 21 days, it was found that by day 7 almost all the peptides that would dissociate from the surface had dissociated by then. The amount released (in μg / μm^2) was the same within experimental error for surfaces with high and low peptide densities, as well as for plain non-activated comb control that has been in contact with the peptide solutions under the same condition as coupling. This led us to believe that the peptides released were ones that were non-specifically adsorbed to the

polymer surface, rather than those that were covalently bound but being cleaved by proteases in cell growth media. We compared the results of our surface stability studies to that performed by Irvine, in which RGD-comb on surfaces were labeled with 30 nm-diameter fluorescent polystyrene nanospheres and total fluorescence from surfaces was assessed as a measure of the loss of ligands from the thin film (Irvine, 1999). The results from their studies showed that only about 10% of ligands on the surface were lost after immersion in PBS for 21 days. The difference between the amounts of peptides released between the two studies could be due to a number of reasons: the way the surfaces were prepared and the way the peptide release was assayed. In the study by Irvine, fluorescent nanospheres much bigger than the peptides were used for labeling. The size of the nanospheres used was about the size of the comb copolymer footprint on the surface and therefore, a nanosphere could bind to multiple peptides within a cluster. So, even when a peptide that was bound to the nanosphere was released from the surface, the nanosphere would still be immobilized by other peptides. Thus the amount of peptide loss as measured by this method was expected to be lower than that measured by coupling ^{125}I - peptides to comb copolymer surfaces. In fact, the amount of peptides associated with the comb copolymer but not covalently linked was also expected to be lower in the degradation studies by Irvine. RGD-comb was prepared by solution coupling and purified by dialysis in solution for days. Hence it is not surprising that the amount of peptides non-specifically associated with the polymer was lower than that from coupling peptides to comb copolymer at the surface.

The major concern for the presence of the non-specifically adsorbed peptides was how they might affect cell function, especially cell adhesion when the peptides were released over the time course of the first 7 days in media and could compete with the peptides still covalently bound to the surface. To elucidate any effect these peptides might have on cell adhesion, wtNR6 fibroblasts were seeded on comb surfaces coupled with GRGDSPY and GRGESPY (as negative control) for 8 days and were monitored daily for any difference in cell adhesion. No detachment was observed on GRGDSPY surfaces. Fibroblasts that adhered initially continued to spread and proliferate over the

time course of the experiment, suggesting the non-specifically adsorbed peptides did not interfere with the adhesion of the cells. On the other hand, nearly no cells adhered to GRGESPY surfaces, even at the end of the 8-day experiment. This indicated that cell adhesion on GRGDSPY surfaces was engendered by the peptides and not due to proteins that adsorbed onto the surfaces over the time-course of the experiment.

By closely examining the system of peptide-coupling to NPC-activated comb surfaces through all these studies, we came to know the strengths and limitations of this 2-dimensional model in presenting peptides for interactions with cells. This knowledge is invaluable in the design of our subsequent cell experiments. Given the constraints of the stability of the spincoated polymer thin film, long term experiments that extended beyond 10 days of surfaces in culture would not be reliable. However, the stability and robustness of surfaces for a week in culture, the characterized peptide surface densities and the ability to tune the density through varying the ratio of NPC-activated and non-activated comb and other features of the system opened up numerous opportunities to study the interactions of cells with surface-bound peptides in a mimicked extracellular environment. In addition, with modifications of the coupling and quantification protocols developed, we have also implemented the method of co-coupling two peptides to the same comb copolymer surface and the methods of tuning the overall peptide density as well as the relative ratio of the surface density of the two peptides. This was done by varying the percentage of NPC-activated comb at the surface and the relative amount of the two peptides in the coupling solution. By using one radiolabeled-peptide at a time in the coupling and quantification process, peptide surface density for each peptide was quantified. In Chapter 4, this co-coupling method was utilized to develop a 2-D model to study the effect of clustered vs. unclustered peptides on fibroblast spreading. Furthermore, in the next few chapters, we will look at how different cells interacted with the various peptides presented by this 2-dimensional model and how we utilize the model to develop a 6-day colony forming assay in which enrichment of connective tissue progenitors from bone marrow and their ability to form colonies on these peptides surfaces are investigated.

3.5 References

Boxus, T., Touillaux, R., Dive, G. and Marchand-Brynaert, J. (1998). "Synthesis and evaluation of RGD peptidomimetics aimed at surface bioderivation of polymer substrates." Bioorganic and Medicinal Chemistry **6**: 1577 - 1595.

Brown, G.L. (1999). Spatial control of ligand presentation on biomaterial surfaces. Ph.D. Thesis, Massachusetts Institute of Technology.

Curtis, R.A., Prausnitz, J.M. and Blanch, H.W. (2000). "Protein-protein and protein-salt interactions in aqueous protein solutions containing concentrated electrolytes." Biotechnology and Bioengineering **57**(1): 11-21.

Delgado, C., Patel, J.N., Francis, G.E. and Fisher, G. (1990). "Coupling of poly(ethylene glycol) to albumin under very mild conditions by activation with tresyl chloride: characterization of the conjugate by partitioning in aqueous two-phase systems." Biotechnol Appl Biochem **12**: 119-128.

Hofmeister, F. (1888). "Zue lehre von der wirkung der salze." Arch. Expt. Pathol. Pharmakol. **24**: 247-260.

Irvine, D.J. (1999). Spatially controlled presentation of biochemical ligands on biomaterial surfaces using comb polymers. Ph.D. Thesis, Massachusetts Institute of Technology.

Irvine, D.J., Mayes, A.M. and Griffith, L.G. (2001a). "Nanoscale clustering of RGD peptides at surfaces using comb polymers. 1. Synthesis and characterization of comb thin films." Biomacromolecules **2**(1): 85-94.

Ito, Y., Kajihara, M. and Imanishi, Y. (1991). "Materials for enhancing cell adhesion by immobilization of cell-adhesive peptides." Journal of Biomedical Materials Research **25**: 1325 - 1337.

Jo, S., Shin, H. and Mikos, A.G. (2001). "Modification of oligo(poly(ethylene glycol) fumarate) macromer with a GRGD peptide for the preparation of functionalized polymer networks." Biomacromolecules **2**(1): 255-261.

Kuhlman, W., Olivetti, E., Mayes, A.M. and Griffith, L.G. (2005). "Conformations of Polymer Chains Confined to Two Dimensions Through Surface Segregation." (in preparation).

Kumosinski, T.F. and Unruh, J.J. (1994). "Molecular-dynamics of salt interactions with peptides, fibrous proteins, and casein." Molecular modeling ACS symposium series **576**: 420-445.

Pierschbacher, M.D. and Ruoslahti, E. (1984). "Cell attachment activity of fibronectin can be duplicated by small synthetic fragments of the molecule." Nature **309**: 30-33.

Ruoslahti, E. and Pierschbacher, M.D. (1987). "New Perspectives in cell adhesion: RGD and integrins." Science **238**: 491-497.

Shah, B. and Watson, E. (1993). "Determination of N-hydroxylsuccinimidyl-activated polyethylene-glycol esters by gel-permeation chromatography with postcolumn alkaine hydrolysis." Journal of Chromatography **629**(2): 398-400.

Sperinde, J.J., Marteins, B.D. and Griffith, L.G. (1999). "Tresyl mediated synthesis: kinetics of competing coupling and hydrolysis reaction as a function of pH, temperature and steric factors." Bioconjudate Chem **10**: 213-220.

Ufret, M.L. (2005). Personal communications.

Veronese, F.M., Largajolli, R., Boccu, E., Benassi, C.A. and Schiavon, O. (1985). "Surface modification of proteins- Activation of monomethoxy-polyethylene glycols by phenylchloroformates and modification of ribonuclease and superoxide-dismutase." Applied Biochemistry and Biotechnology **11**(2): 141-152.

Weiss, N., Klee, D. and Hoecker, H. (2001). "Konzept zur bioaktiven Ausruestung von Metallimplantatoberfaechen." Biomaterialien **2**: 81-86.

Chapter 4

Biophysical and Biochemical Design of Substrates for Enriching Connective Tissue Progenitors from Bone Marrow

4.1 Introduction

In Chapter 2, through protein and cell resistance studies and comparison of peptide-functionalizable sites, the comb copolymer H10M0 was identified as the best base graft surface material due both to its excellent cell resistance and the high number of functionalizable sites in the molecule. In Chapter 3, we developed methodologies for utilizing this comb copolymer as a vehicle to present small adhesion peptides. Methods for activating hydroxyl chain ends of the comb copolymer with NPC and the subsequent peptide-coupling were developed. With this foundation, we now explore how the biophysical and biochemical properties of this system can be used for the selective adhesion and proliferation of connective tissue progenitors (CTPs) from bone marrow aspirates.

Small adhesion peptides were chosen to be presented by comb copolymer surfaces for mediating the selective adhesion and proliferation of CTPs from bone marrow aspirates. Peptides are relatively chemically robust and non-immunogenic compared to large proteins. In addition, in Chapter 3, and also later in this chapter, we showed that a high peptide surface density can be achieved on peptide-immobilized comb surfaces. Previous studies had shown that integrins bind to extracellular matrix molecules by recognizing short amino acid motifs in the molecule. The tri-residue RGD sequence recognized by various integrins is perhaps the most well-known example (Ruoslahti and Pierschbacher, 1987; Pfaff, 1997). In the next section, through an extensive literature

search, a short list of peptides was identified for their potential of enhancing the selective adhesion and proliferation of connective tissue progenitors.

In addition to the biochemical design criterion, the biophysical presentation of peptides is considered. As mentioned in Chapter 1, previous studies in our lab showed that peptides presented in a clustered manner was more effective in promoting cell adhesion and migration. In particular, Koo et al. showed a higher adhesion force by fibroblasts on comb copolymer surfaces with clustered RGD peptides, compared to unclustered peptide surfaces of the same density (Koo et al., 2002). These works showed that the biophysical presentation of peptides is important in elucidating full cellular responses. In the discussion section of this chapter, various biophysical parameters associated with the peptide-comb surfaces were evaluated based on experimental results and critically compared with the dimensions and densities of cell integrins.

The experimental aspect of this chapter focused on validating the biophysical and biochemical effects on cell adhesion and proliferation with cell lines and primary pig mesenchymal stem cells (pMSCs). Firstly, surfaces with peptide candidates identified in Section 4.2 were prepared and the bioactivity of these surfaces was validated with various cell lines and pMSCs. These cells were chosen because they had been previously characterized and some were selected as they express certain integrins that would bind to the peptides on the surfaces to be tested. Through these studies, the bioactivity of peptides that were immobilized on comb surfaces were validated before the substrates were set in experiments with human bone marrow. Secondly, the effect of clustered and unclustered presentation of peptides on cell adhesion was studied by measuring fibroblast spreading on GRGDSPY surfaces with various degrees of nanoscale clustering. These cell studies served to validate the biochemical and biophysical design of peptide-comb substrates so that the finest substrates could be identified and used in experiments with human marrow aspirates.

4.2 Biochemical design – strategically identifying peptide candidates for the selective adhesion and proliferation of CTPs

Although a few methods have been developed to isolate enriched populations of human CTPs from bone marrow, the ECM receptor profile of these cells immediately following isolation has not been described. Indeed, illuminating the adhesion behavior of CTP is one of the goals of this work. Two complementary sources of literature information were used to compile a short list of candidate peptides. First, receptors mediating adhesion of some cell types closely related to primary human CTPs, such as immature osteoblasts from rat calvariae, have been described. Peptide sequences that target these receptors were then identified based on their affinity and potential. Second, by reviewing reports of adhesion assay of CTP or related cells to ECM proteins and their specific fragments, domains that mediated the selective adhesion, proliferation and differentiation of CTP related cells were identified. A search for active sequences in those domains was then conducted to identify possible recognition sites by CTPs. These two approaches allowed us to combine complementary information in the literature to develop a short set of peptide candidates, and were especially useful given the relatively scarce information available in this area and the large number of potential sequences within a fragment of matrix molecule identified.

ECM molecules that mediate the binding of bone cells to bone extracellular matrix include collagen I, the major constituent of bone protein, bone sialoprotein, the largest bone matrix component after collagen, fibronectin, laminin, vitronectin, thrombospondin, osteopontin as well as hyaluronan and proteoglycans (Horton, 1995; Robey, 1996; Schaffner and Dard, 2003). Fibronectin, collagens, laminin as well as proteoglycans have been shown to be expressed by marrow-derived mesenchymal progenitors (Chichester et al., 1993; Minguell et al., 2001). In addition, using primary fetal rat calvariae, Roche and co-workers showed that laminin-1 inhibited the adhesion of non-osteoprogenitor cells but enriched the cell population in osteoprogenitor cells by

about 5 folds. Tenascin also promoted the enrichment of osteoprogenitor cells but to a lesser extent while fibronectin, bone sialoprotein, and type I collagen only increased attachment of all cells (Roche et al., 1999a).

Therefore, laminin-1 is a ECM molecule of particular interest in osteoprogenitor enrichment. It contains heterotrimeric proteins composed of α_1, β_1 and γ_1 chains. Cellular receptors for laminins include eight different integrins, mostly from the β_1 group. Laminin can induce proliferation of osteoblasts and accelerate differentiation up to the formation of nodules (Panayotou et al., 1989). It contains EGF-like repeats, like other matrix proteins, such as fibronectin and thrombospondin, and can exhibit growth factor activity on cells which express an EGF receptor (Scutt et al., 1992). According to the studies by Roche et al. (Roche et al., 1999a), laminin-1 selects osteoprogenitors by favoring their attachment to the matrix while being anti-adhesive for other rat-calvariae-derived cells. Laminin-1 also efficiently promoted osteoprogenitor adhesion from early, undifferentiated calveriae cell populations. When calvariae cells were plated on increasing amounts of coated laminin-1, overall cell attachment decreased dose-dependently. However, the number of nodules formed increased concomitantly with the decrease of overall cell attachment. The increase in the ratio of bone nodules to total number of cells was a cell attachment effect, as laminin-1 did not significantly stimulate differentiation and thus bone nodule formation in the studies (Roche et al., 1999a). More importantly, the E1 fragment of laminin displayed a similar preferential promotion of osteoprogenitor adhesion as the whole molecule while the E1+ fragment, which encompasses the entire segment of E1 as well as the N-terminal short arms, enhanced the preferential recruitment of osteoprogenitors to an even greater extent than complete laminin (Roche et al., 1999b). In addition, the N-truncated laminin variant, laminin-5, did not show any specific affinity for osteoprogenitors. In light of the results of these studies, laminin became an ECM molecule of particular interest. Later in this section, we identified active sequences in this molecule that may have the potential in promoting CTP adhesion and colony formation.

The very few reports of integrin expression profile of CTPs in the literature are often contradicting to each other due to the possible reasons outlined in Chapter 1. Integrins $\alpha_1\beta_1$, $\alpha_2\beta_1$, $\alpha_5\beta_1$, $\alpha_6\beta_1$, $\alpha_v\beta_3$, and $\alpha_v\beta_5$ have been reported to be expressed on human bone marrow derived STRO-1+ CFU-F cells although other published data give different accounts on integrin expression on osteoprogenitor cells, but most reported the presence of α_4, α_5, $\alpha_v\beta_3$, $\alpha_v\beta_5$, and β_1 (Soligo et al., 1990; Conget and Minguell, 1999; Franceschi, 1999; Gronthos et al., 2001). Osteoprogenitor cells from bone marrow aspirates seem to share a similar integrin expression pattern with mature bone cell populations (Soligo et al., 1990; Clover et al., 1992; Hughes et al., 1993; Conget and Minguell, 1999; Gronthos et al., 2001). Stromal derived osteoprogenitor cells express $\alpha_4\beta_1$ transiently and a subpopulation of differentiated bone cells also express this integrin (Grzesik and Robey, 1994). Based on these reports, we identified $\alpha_4\beta_1$, $\alpha_5\beta_1$, $\alpha_v\beta_3$, to be the integrins of greatest interest. However, adhesion receptors other than integrins may also be key players in mediating CTP adhesion and proliferation. Blocking of the β_1 integrin subunit by incubating rat calvariae cells with anti- β_1 antibodies did not reduce the osteoprogenitor recruitment ability of laminin-1, an implication that adhesion may not be mediated by β_1 integrins (Roche et al., 1999b). Therefore, in search of peptides that would mediate the selective adhesion of CTPs, peptides that target proteglycans were also considered as some studies demonstrated that adhesion was at least partially mediated by a non-integrin, such as syndecan (Imai et al., 1998; Rezania and Healy, 1999; Gronthos et al., 2001).

Most of the active motifs from ECM molecules described in the literature were identified by either site-directed mutagenesis of protein fragments or systematic screening of overlapping peptides covering the protein chain of interest. The affinity of these peptides to integrins or cells was usually assayed by examining their ability to block binding of cells to the complete molecule from which the peptide was derived. Very few studies actually tested whether these peptides alone, when immobilized on a surface, could support the adhesion and function of the target cells. For some peptides, even though they can inhibit the adhesion of cells by blocking their target integrins, their

affinity may not be high enough such that solely the immobilized form of the peptide itself can support cell adhesion. Moreover, some integrin binding requires the presence of a synergy site or only with the binding to both the primary and synergy sites elicit full cell response (Garcia et al., 2002). Blocking of the primary site can reverse binding but the presence of the primary sequence alone may support very little or even no adhesion at all. Therefore, in identifying peptide candidates for supporting cell adhesion via a particular integrin or on a particular ECM protein of interest, peptides that had been shown in the literature to support adhesion via the particular integrin were first considered. As very few peptides had been tested for their ability to support adhesion, active motif sequences that could block cell adhesion were considered next, although the success in supporting adhesion was not guaranteed. However, their affinity may be improved by the appropriate biophysical presentation.

RGD Peptides

Since the identification of the RGD sequence in 1986 as a critical determinant of integrin-mediated cell adhesion (Ruoslahti and Pierschbacher, 1987), RGD-containing peptides have been widely studied for both promotion and inhibition of cell adhesion (Maheshwari et al., 2000; Koo et al., 2002). The RGD sequence is found in the fibronectin 10 domain and is conserved in vitronectin, laminin, collagen, bone sialoprotein and many other ECM molecules (Yamada and Kleinman, 1992; Hubbell, 1995; Stubbs et al., 1997). RGD was chosen as the first peptide to be screened as it is the most well-characterized adhesion peptide. In addition, colony forming cells derived from human marrow have been shown to co-express $\alpha_5\beta_1$ and $\alpha_v\beta_3$. with STRO-1 (Gronthos et al., 2001). Both $\alpha_5\beta_1$, $\alpha_v\beta_3$ are primary receptors for RGD but other integrins, $\alpha_3\beta_1$, $\alpha_8\beta_1$, $\alpha_{IIb}\beta_3$, $\alpha_v\beta_1$, $\alpha_v\beta_5$, $\alpha_v\beta_6$, $\alpha_v\beta_6$, $\alpha_v\beta_8$, and to a small extent under particular condition, $\alpha_2\beta_1$ and $\alpha_4\beta_1$, have also been shown to bind to ECM molecules in a RGD dependent manner (Pfaff, 1997). RGD was chosen also because of its interactions

with osteoblastic cells. Rezania and Healy also showed that the amino acid sequence CGGNGEP**RGD**TYRAY enables adhesion and focal contact formation mediated by $\alpha_2\beta_1$ and $\alpha_v\beta_3$ integrins of osteoblastic cells derived from primary adult human tissue (Rezania and Healy, 1999). Fibronectin, which contains the RGD motifs, mediates osteoprogenitor adhesion (Gronthos et al., 2001). The sequence GRGDSPY is chosen for our studies instead of the minimal RGD sequence due to its higher affinity. It has been shown that cells could adhere to surface-immobilized GRGDSP via $\alpha_v\beta_3$ (Massia and Hubbell, 1991) and $\alpha_5\beta_1$ (Dillow et al., 2001; Massia and Stark, 2001). A tyrosine residue was added to the sequence for ^{125}I-labelling for peptide quantification purpose. GRGESPY and GRAASPY, inactive analogs for GRGDSPY, were used as negative control peptides. Two inactive negative controls were chosen as there were a few reports that showed cell response to RGE and RAD control (Olbrich et al., 1996; Bearinger et al., 1998; Massia and Stark, 2001) and there was no explanation for this phenomenon. Interaction might occur due to residual peptide affinity or changed surface properties during the processing in which peptides were immobilized in those reports.

Bone sialoprotein peptide FHRRIKA

The peptide FHRRIKA was derived from the heparin-binding domain of bone sialoprotein (BSP). Some studies reported in the literature suggested that human bone cells may have an attachment mechanism for the heparin-binding region of ECM proteins. Attachment to this region is probably mediated by cell surface proteoglycans (Dalton et al., 1995). BSP is the major non-collagenous ECM molecule found in bone matrix and it has been shown to be primarily localized in newly synthesized bone matrix (Rezania and Healy, 1998). In addition, BSP, which has been shown to be osteoinductive (Wang et al., 1998), exhibits to a certain extent specificity in osteoblast-like cell attachment. Moreover, endogenous protease degraded BSP fragments have been shown to mediate attachment of primary human osteoblast-like cells (Bianco et al., 1991; Mintz

et al., 1993). Even though most of the studies reported here were between osteoblasts and BSP, some recent reports suggested the role of proteoglycans in regulating cell functions in bone marrow mesenchymal stem cells (Zou et al., 2004). Therefore, a peptide derived from the heparin-binding domain of BSP was of high interest to be tested for its ability to mediate CTP adhesion and function. In identifying such an active sequence from BSP, the fact that attachment to heparin-binding domains of ECM proteins is largely electrostatic-based was considered. The positively-charged basic amino acids of the heparin-binding domain interact with the negatively-charged carboxylate and sulfate groups found in the glycosaminoglycans associated with the proteoglycans found in the cell membrane (Massia and Hubbell, 1992a). Cardin et al. identified the consensus amino acid sequences such as [-X-B-B-X-B-X] (X = hydrophobic residue, B = positively charged basic residue) in heparin-binding domains of adhesive proteins and showed that the sequence is involved in heparin binding (Cardin and Weintraub, 1989; Bober-Barkalow and Schwarzbauer, 1991). The BSP peptide FHRRIKA chosen is a motif that follows this consensus amino acid sequence.

$\alpha_4\beta_1$ peptides

Sequences that are recognized by $\alpha_4\beta_1$ were selected for screening because a subpopulation of STRO-1^+ human bone marrow derived cells, as well as expanded human marrow mesenchymal stromal cells, have been shown to express $\alpha_4\beta_1$ (Conget and Minguell, 1999; Gronthos et al., 2001). In Chapter 6, our own FACS results showed a significant level of $\alpha_4\beta_1$ expression in CD45$^-$CD105$^+$ marrow aspirate cells, at a level higher than the rest of the population. In addition, $\alpha_4\beta_1$ has been detected in osteoblasts obtained from rat calvariae (Rezania et al., 1997). There are a number of motif sequences derived from ECM molecules that are recognized by the $\alpha_4\beta_1$ integrin. However, other than REDV (Massia and Hubbell, 1992b), none of these peptides have been shown to have the ability to mediate adhesion when immobilized on the surface. The other

peptide sequences, such as ILDV from the CS-1 region of fibronectin, IDS from VCAM-1, had only been shown to block cell adhesion to ECM proteins via $\alpha_4\beta_1$ (Clements et al., 1994; Hodde et al., 2002). Therefore, multiple peptides that target $\alpha_4\beta_1$ were chosen to be set in cell experiments. In addition to the two peptides that contain key sequence identified from ECM molecules, namely ILDV and REDV, a 59-mer $\alpha_4\beta_1$ peptide identified from bacterial display with two binding domains, EHSDV and LDSAS, fanned by a sequence of 45 amino acids (Ashkar, 2001), was also chosen as a potential peptide candidate.

Collagen I peptide DGEA

The motif DGEA from type I collagen (Staatz et al., 1991) was chosen as it has been shown to be specific for the $\alpha_2\beta_1$ integrin on osteoblasts-like cells, including the MC3T3-E1 rat calvarial cell lines (Xiao et al., 1998; Gilbert et al., 2003). Human bone marrow STRO-1^+ cells have been shown to express $\alpha_2\beta_1$ as discussed above.

$\alpha_9\beta_1$ EIDGIEL peptide

Tenascin-C is one of the few known ligands for the integrin $\alpha_9\beta_1$. It also binds integrins $\alpha_5\beta_1$, $\alpha_v\beta_3$, $\alpha_v\beta_6$, and $\alpha_8\beta_1$, all via the fibronectin type III repeat (Yokosaki et al., 1996; Mackie and Tucker, 1999; Jones and Jones, 2000). The integrin, $\alpha_9\beta_1$, binds to the minimal sequence EIDGIEL in that region (Schneider et al., 1998; Yokosaki et al., 1998). Tenascin-C, a multimeric ECM glycoprotein, has been shown to enrich the osteoprogenitor population of fetal rat calvaria cells (Roche et al., 1999a). Its upregulation is also observed in many physiological situations including wound healing, cancer and embryonic development (Machie, 1997; Shrestha et al., 1997). The peptide sequence chosen here contains a motif, IDG, homologous to other known $\alpha_4\beta_1$ binding motifs, such as the vascular cell adhesion molecule-1 (VCAM-1) $\alpha_4\beta_1$ binding motif IDS

(Clements et al., 1994) and the fibronectin LDV active site (Komoriya et al., 1991), underscoring the similarities in structure, function and specificity of $\alpha_4\beta_1$ and $\alpha_9\beta_1$. We therefore selected the sequence PLAEIDGIELTY in the peptide-screening list.

Laminin peptides

Two laminin peptides were chosen to be screened, YIGSR and C16. Laminin peptides were of special interest because of the role of laminin in mediating the preferential adhesion of fetal rat calvarial cells and supporting the enrichment of bone marrow-derived colony forming cells (Roche et al., 1999b; Gronthos et al., 2001). Laminin is also a major component in the bone marrow environment with which bone marrow mesenchymal cells, including the CTPs, would interact directly. Therefore, it is reasonable to believe that these cells express receptors that mediate adhesion to laminin. C16 is an active sequence in the globular domain of the γ1 chain in laminin-1. Its activity was identified by the systematic screening of synthetic peptides covering the entire γ1 chain (Nozimu et al., 1997). The globular domains are of particular interest as they are part of the E1+ fragment of laminin-1 but not E1. As mentioned earlier, the E1+ but to a much lesser extent the E1 fragment enhanced the selective adhesion of osteoprogenitor cells from fetal rat calvariae. Therefore, the affinity to osteoprogenitor cells can be attributed to motifs found in the globular domains. C16 was chosen because of its highest potency among the few active sequences in the globular domains of the γ1 chain. Cell attachment has been demonstrated on C16-conjugated sepharose beads. Adhesion could only be partially inhibited by ethylenediaminetetraacetic acid (EDTA) and even though $\alpha_5\beta_1$ and $\alpha_v\beta_3$ were identified as receptors for C16, a cyclic-RGD peptide did not block C16 adhesion, suggesting that adhesion could be $\alpha_5\beta_1$ or non-integrin mediated (Ponce et al., 1999; Ponce et al., 2001; Ponce and Kleinman, 2003). C16 was thus chosen as a peptide candidate for its potency as a laminin E1+ peptide, a $\alpha_v\beta_3$ and $\alpha_5\beta_1$ peptide and its probable non-integrin binding activity.

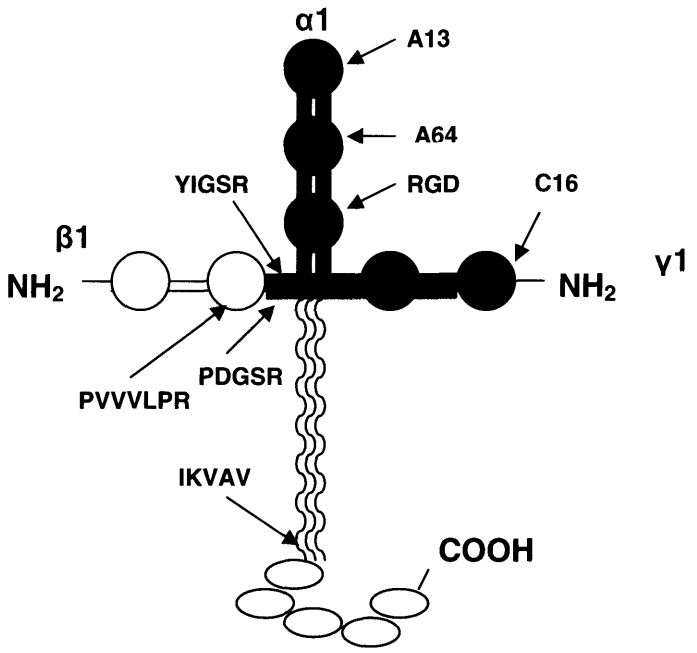

Figure 4.1 Diagram of laminin-1 molecule showing its different domains and approximate position of various known active binding motifs. The E1 fragment encompasses all the green regions in the diagram and the red regions depict E1+ fragment. (The red-and-green global domains and parallel red and green lines showed regions common to both E1 and E1+ fragments.)

YIGSR is another active peptide sequence found in the E1/E1+ fragment of laminin. It is a sequence in the β1 chain, known for its ability to promote neurite growth and migration. Adhesion has been shown to be mediated by the 67kD laminin receptor and possibly other receptors. Although YIGSR is not a peptide candidate as compelling as the other peptides discussed above, the mediation of laminin on osteoclast differentiation was inhibited by YIGSR (Kukita et al., 1998). This peptide also inhibited the attachment of osteosarcoma cells on laminin (Yudoh et al., 1996).

Based on the above findings, the peptide candidates chosen to be screened for their ability to mediate the selective adhesive and function of CTPs are listed in Table 4.1. GRGESPY and GRAASPY were used as inactive controls.

Peptide	Source	Sequence
RGD	FN and other ECM molecules	G**RGD**SPY
BSP-H	BSP heparin-binding domain	YGG**FHRRIKA**
CS-1	FN CS-1 region	YLHPGE**ILDV**PST
REDV	FN CS-5 region	G**REDV**Y
59-mer $\alpha_4\beta_1$	Bacterial Display	EH**SDV**IDSQELSKVSREFHSHEFHS HEDMLVVDPKSKEEDKHLKFRISH E**LDSAS**SEVN
C16	LN γ1 globular domain	YGGAFDIT**YVRL**K
DGEA	Collagen I	YP**DGEA**
EIDGIEL	Tenascin-C FN III repeat	PLA**EIDGIEL**TY
YIGSR	LN β1 E1/E1+	**YIGSR**

Table 4.1 List of peptide candidates chosen for screening for their ability to promote selective adhesion and proliferation of CTPs. Residues in bold are key residues of the sequence. (abbreviations used: FN, fibronectin; BSP, bone sialoprotein, LN, laminin)

4.3 Materials and Methods

4.3.1 Cell line and primary cell isolation and culture

Several cell lines were used to assess the ability of peptide-comb surfaces to support integrin-mediated adhesion. The WT NR6 fibroblast cell line was generated and maintained as described in Chapter 2. All cell lines were obtained from the American Type Culture Collection (ATCC) unless otherwise indicated. The human osteosarcoma (HOS) cell line was routinely cultured in minimum essential medium-α (MEMα) supplemented with 10% FBS, 200 i.u./mL penicillin, 400 μg/mL streptomycin, 2mM L-glutamine, 1mM non-essential amino acids and 1mM sodium pyruvate. The rat calvarial osteoblast cell line (MC3T3-E1) was also routinely cultured in MEMα supplemented with 10% FBS but with 100 i.u./mL penicillin, 200 μg/mL streptomycin and 1mM sodium pyruvate. MEMα with ascorbic acid was used in cases where osteoblastic phenotype of the cells was desired. The parental Chinese hamster ovary (CHO-K1) cell line was routinely cultured in medium of composition similar to that of WT NR6, but with Dulbecco's Modified Eagle medium (DMEM). All cell lines were maintained at 37°C in 5% CO_2.

Pig mesenchymal stem cells (pMSCs) were harvested and isolated by the Vacanti laboratory in the Massachusetts General Hospital. The procedure is outlined by Abukawa et al. (Abukawa et al., 2004). In brief, 6-month old female Yucatan minipigs were used for bone marrow aspiration. The procedure was performed in accordance with the regulations and approval of the Institutional Animal Care and Use Committee of the Massachusets General Hospital and conformed to the standards of the Associated for Assessment and Accreditation of Laboratory Animal Care. Bone marrow was aspirated from the ilium crest using an 11-gauge bone marrow aspiration needle while the minipig was under general anesthesia. 10 mL of bone marrow aspirates was collected into a syringe containing 6000 units of heparin. After the aspirate has been washed with high-glucose DMEM (Gibco, NY), it is centrifuged at 900 × g. Cell pellets were

resuspended in DMEM and loaded on 70% Percoll (Sigma-Aldrich, St. Louis, MO) gradient. These gradients were centrifuged at 1100 × g for 30 minutes and the pMSC-enriched density fraction was collected. Cells were then cultured by resuspending in culture media (DMEM with 10% FBS) and seeding into 75 mm^2 cell culture flasks (Corning, Corning, NY) at a density of 1.6×10^6 cells per cm^2. The media were changed every 3 days and the non-adherent cells containing mostly the hematopoietic cells were removed at each media change. The cells in culture usually became near-confluent in around 10 days, at which point the cells are detached by 1X trypsin solution (Sigma-Alrich, St. Louis, MO) and split into new flasks. Cells up to the third passage were used in our studies.

Rat hepatocytes were isolated from 150g – 230g male Fischer rats by a collagenase perfusion procedure, as described in Hwa et al. (Hwa et al., 2005). In brief, the liver was perfused with calcium-free HEPES buffer and digestive enzyme mix. The liver was then removed, submerged in DMEM supplemented with 1% FBS and Penicillin-streptomycin at 4°C, and the capsule membrane was removed with surgical forceps. Cells were released by agitating the liver in the buffer. The cell solution was filtered and purified by multiple centrifugation and suspensions.

4.3.2 Preparation of peptide-comb surfaces

Peptides were obtained and purified according to the procedures described in Chapter 3, except for the 59-mer $\alpha_4\beta_1$ peptide which was a generous gift from Dr. Samy Ashkar. All peptides, except for C16 and the 59-mer $\alpha_4\beta_1$ peptide, were coupled to comb copolymer surfaces and characterized as outlined in Chapter 3. The peptide C16, due to its insolubility in sodium bicarbonate buffer, was dissolved in milliQ water with pH adjusted to 8.3 with triethylamine. For the 59-mer $\alpha_4\beta_1$ peptide, a peptide solution of 0.4 mg/mL in 0.1M sodium bicarbonate buffer was used for coupling. The surface peptide density of each type of peptide surfaces used was quantified with ^{125}I-labelled peptides using the methodology described in the previous chapter.

RGD surfaces with different degrees of RGD clustering were prepared by mixing various ratios of NPC-activated comb and its non-activated counterpart. Further, the average overall ligand density was stoichiometrically varied by mixing the active peptide GRGDSPY with the inactive peptide GRGESPY. RGD surfaces with a maximal degree of clustering were prepared by spincoating on glass surfaces polymer solutions of 0/100, 5/95, 15/85 and 25/75 of NPC-activated comb / non-activated comb and subsequently reacted with 1mM GRGDSPY solution to yield surfaces with peptide surface densities of (0 ± 500) peptides / μm^2, (4150 ± 450) peptides / μm^2, (9300 ± 900) peptides / μm^2, and (14000 ± 450) peptides / μm^2 respectively. The average number of peptides in each cluster was the same while the cluster spacing increased as peptide density decreased (Kuhlman et al., 2005). RGD surfaces with comparable average RGD densities but a lower degree of clustering were prepared by coupling peptide solutions of 0/100, 20/80, 60/40, 100/0 GRGDSPY/GRGESPY to substrates spincoated with 25% NPC-activated comb solution. GRGDSPY and GRGESPY have almost identical reactivity towards NPC-comb surfaces, as shown by quantification studies with ^{125}I-labelled peptides, using the method outlined in the previous chapter on co-coupling two peptides. This yielded surfaces with peptide densities comparable to that of the RGD surfaces with maximal degree of clustering listed above, but the number of peptides in a cluster was less on surfaces with lower overall peptide densities and visa versa. Note that at the highest overall peptide surface density, the "less-clustered" RGD surfaces became the same as the maximally-clustered RGD surfaces. Refer to Figure 4.10 for a graphical explanation.

4.3.3 Cell adhesion experiments

GRGDSPY, GRGESPY and GRAASPY surfaces of peptide surface densities up to ~20,000 peptides / μm^2 were tested for their ability to support cell adhesion and proliferation with wtNR6 fibroblasts, MC3T3-E1 rat calvarial osteoblasts and primary pig mesenchymal stem cells. Peptide-coupled substrates were placed in 24-well plates and fixed in place with rings cut out from protein-resistant, biocompatible medical

silicone tubing (Nalgene). 10,000 cells per cm^2 were seeded on these peptide surfaces, in the presence of serum-containing media free of phenol red, and incubated for 16 – 18 hours. Microscopy and MTT (3-(4,5-dimethylthiazol-2-yl)-2,5-diphenyltetrozolium bromide) assay were then performed on these surfaces to quantify the amount of cell adhesion and to examine cell morphology. MTT assays were performed using the Vybrant MTT cell proliferation assay kit (Molecular Probes, Eugene, OR). After culture, surfaces were gently washed twice with media before MTT solution (12mM) was added and incubated with the cells for 4 hours. The solution was then removed and dimethyl sulfoxide (DMSO) was added for 10 minutes to solubilize the formazan crystals formed. Solutions were taken out for absorbance reading at 540 nm. The amount of cells on each surface relative to tissue culture polystyrene (TCPS) control was calculated by the ratio of absorbance of the two surfaces. Results from MTT assay were correlated with that from microscopy, the method of which was outlined in Chapter 2. Three experiments were carried out for each cell type, and for each experiment, triplicates of each type of surface were used. The same methodology was used to quantify the number of adherent cells (MC3T3-E1 or primary pMSCs) on surfaces with various densities of the peptide FHRRIKA.

Substrates presenting the $\alpha_2\beta_1$ peptide YPDGEA were tested for their ability to support cell adhesion using MC3T3-E1 osteoblasts, which express $\alpha_2\beta_1$ (Gilbert et al., 2003). The $\alpha_4\beta_1$ peptides, CS-1 and the 59-mer $\alpha_4\beta_1$ peptide from bacterial display were tested with HOS osteosarcoma cells and pMSCs. In antibody-blocking experiments where adhesion of pMSCs was tested on surfaces with the 59-mer $\alpha_4\beta_1$ peptide identified from bacterial display, cells were pre-blocked with the anti-$\alpha_4\beta_1$ blocking antibody P4G9 (Chemicon, Temecula, CA) prior to seeding on the peptide-coupled surfaces. GREDVY was validated with human umbilical vein endothelial cell line (HUVEC) by graduate researcher David Yin but only little adhesion was observed (Yin, 2004). CHO-K1 and wtNR6 were used to test surfaces with the peptide C16, as well as GRGDSPY and its inactive analogs GRGESPY and GRAASPY.

Adhesion experiments on clustered and unclustered GRGDSPY surfaces were performed by seeding wtNR6 fibroblasts at 10,000 cells / cm^2 on surfaces for 16 – 18 hours. Three to five microscopy images were taken for each surface, avoiding the edges or irregularities of the substrates. Cell counting, tracing and calculation of cell spreading area were performed using the NIH image software. Student t-tests were employed to determine whether the difference in cell spreading area between clustered and unclustered surfaces were significant. 99% confidence levels were reported.

4.4 Results

4.4.1 Cell adhesion on substrates with various peptide surface densities

When wtNR6 fibroblasts were seeded on GRGDSPY, GRGESPY, and GRAASPY of density range up to ~20,000 peptides / μm^2, an increase in the number of adherent cells was observed on GRGDSPY surfaces with increasing peptide density but the number of adherent cells remained minimal for surfaces with GRGESPY and GRAASPY for the entire peptide density range tested (Figure 4.2). When primary pig mesenchymal stem cells were seeded on the same surfaces, the same trend was observed (Figure 4.3a). In addition to cell adhesion, colony formation was also seen on the GRGDSPY surfaces (Figure 4.3b).

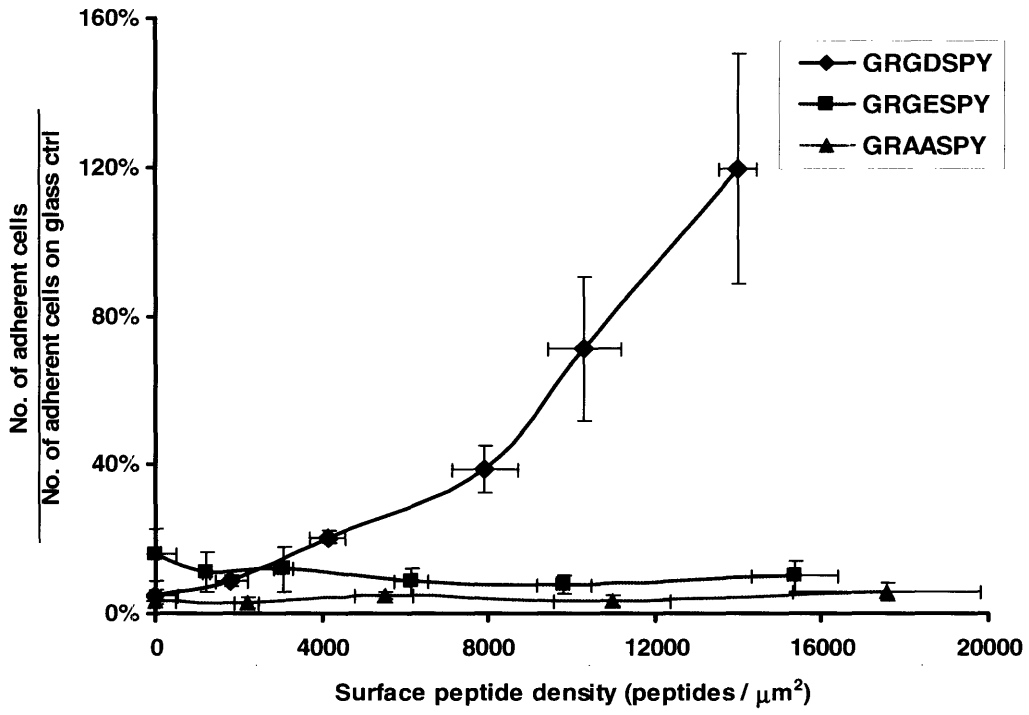

Figure 4.2 wtNR6 adhesion on GRGDSPY, GRGESPY and GRAASPY surfaces with various peptide surface densities. After 16-18 hours of seeding, surfaces were rinsed before MTT assay was performed. Relative adhesion on peptide surfaces to glass control was reported. Error bars show standard errors associated with 3 technical triplicates of 3 separate experiments.

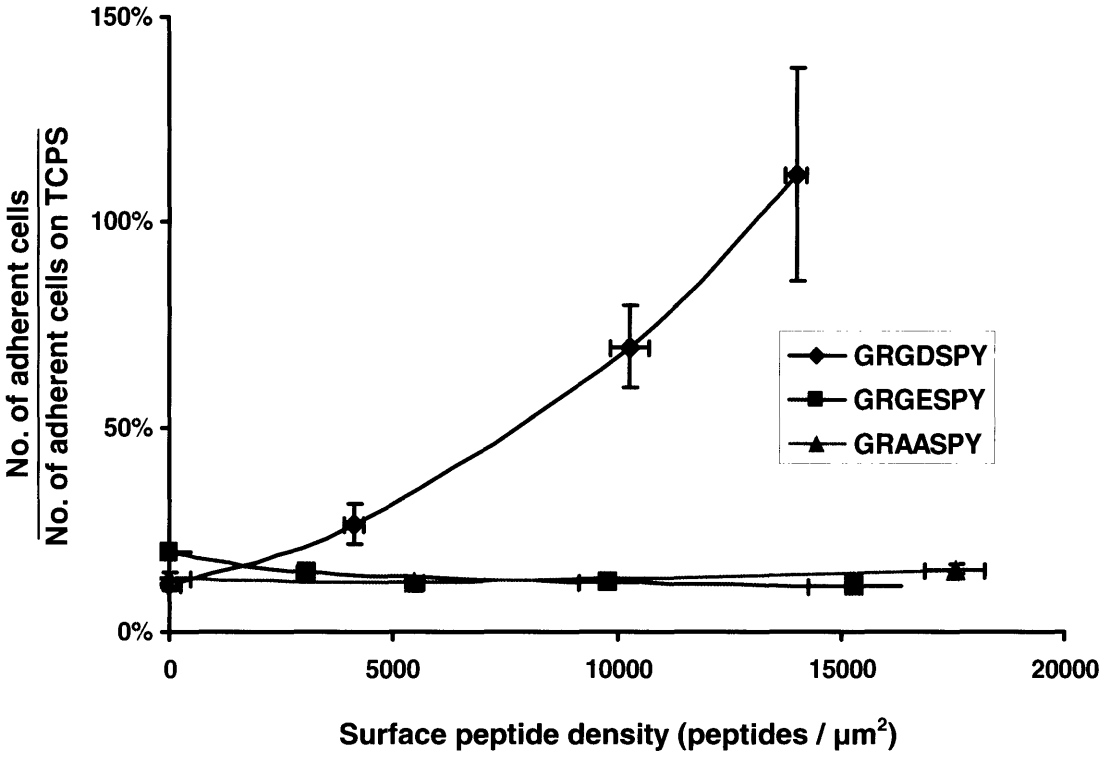

Figure 4.3a Adhesion of primary pMSCs on GRGDSPY, GRGESPY and GRAASPY surfaces with various peptide surface densities. After 16-18 hours of seeding, surfaces were rinsed before MTT assay was performed. Relative adhesion on peptide surfaces to TCPS control was reported. Error bars show standard errors associated with 3 technical triplicates of 3 separate experiments.

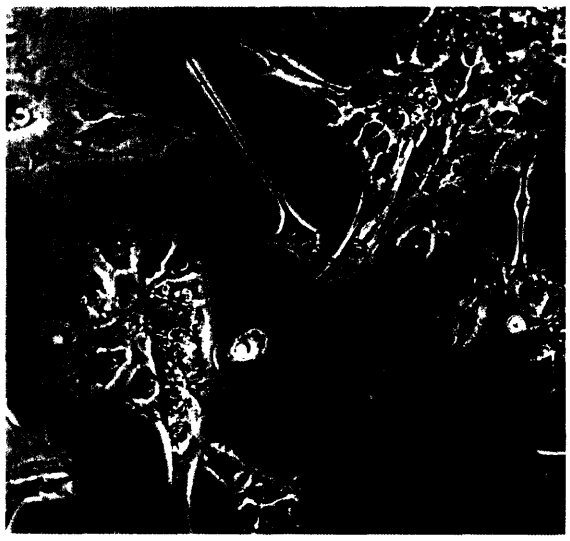

Figure 4.3b Primary pMSCs on GRGDSPY-coupled comb substrate of average surface density 14000 peptides / μm^2. In addition to cell adhesion, colony formation was also seen on GRGDSPY surfaces. Almost no adhesion was observed on GRGESPY and GRAASPY surfaces.

MC3T3-E1 rat calvarial osteoblasts and primary pMSCs were seeded on surfaces with various surface densities of the bone sialoprotein peptide FHRRIKA. An increase in cell adhesion was observed for MC3T3-E1 on surfaces with higher surface FHRRIKA density. However, very little pMSC adhesion was seen even on surfaces with the highest FHRRIKA density tested (Figure 4.4).

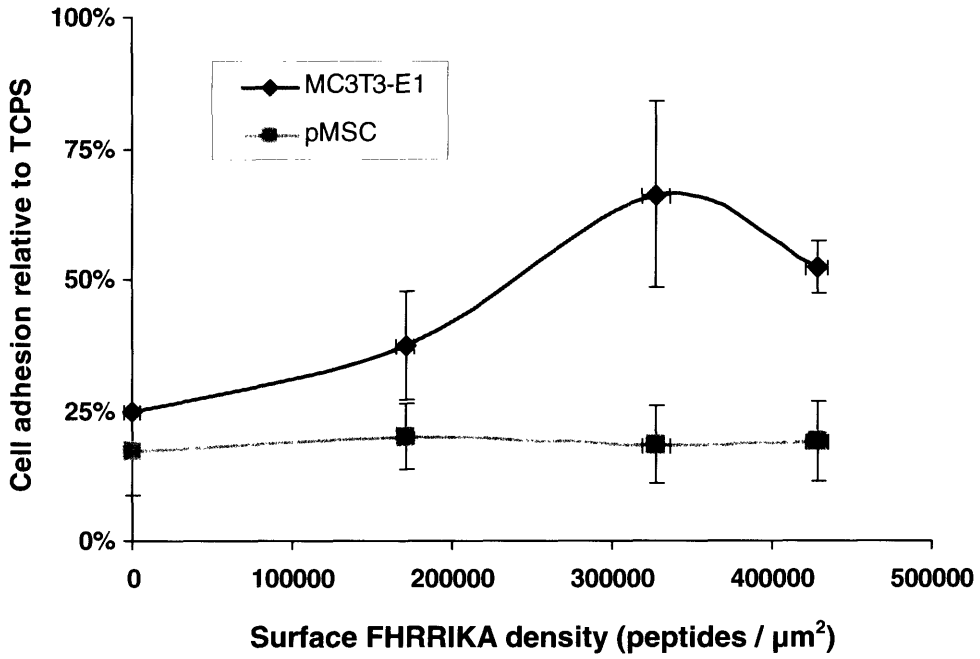

Figure 4.4 MC3T3-E1 rat calvarial osteoblasts and primary pMSC adhesion on surfaces with various peptide surface densities of the BSP peptide FHRRIKA. The ratio of number of adherent cells on FHRRIKA surfaces to that on TCPS surfaces was reported. MC3T3-E1 adhesion increased with increasing peptide density up to (327 ± 9) x 10^3 peptides / μm^2 while little pMSC adhesion was observed even at the highest peptide density. Error bars show standard deviations associated with 3 technical triplicates of a representative experiment. 3 experiments were carried out and similar results were obtained.

4.4.2 Validation of various peptide-comb substrates

The bioactivity of the $\alpha_4\beta_1$ peptides, CS-1 and the 59-mer from bacterial display, was validated using HOS cells and primary pMSCs. Excellent cell adhesion was observed on surfaces with the 59-mer $\alpha_4\beta_1$ peptides for both cell types. pMSC adhesion on this

peptide surface is shown in Figure 4.5a. Adhesion to surfaces with the 59-mer $\alpha_4\beta_1$ peptides was significantly reduced by pre-incubating the cells with anti- $\alpha_4\beta_1$ antibodies before seeding (Figure 4.5b). HOS which expresses $\alpha_4\beta_1$ integrins (Tiisala et al., 1993) also showed excellent adhesion on 59-mer $\alpha_4\beta_1$ surfaces and inhibition of adhesion when cells were pre-incubated with $\alpha_4\beta_1$ antibodies. On the other hand, CS-1 supported only a moderate level of HOS adhesion, as shown in Figure 4.6.

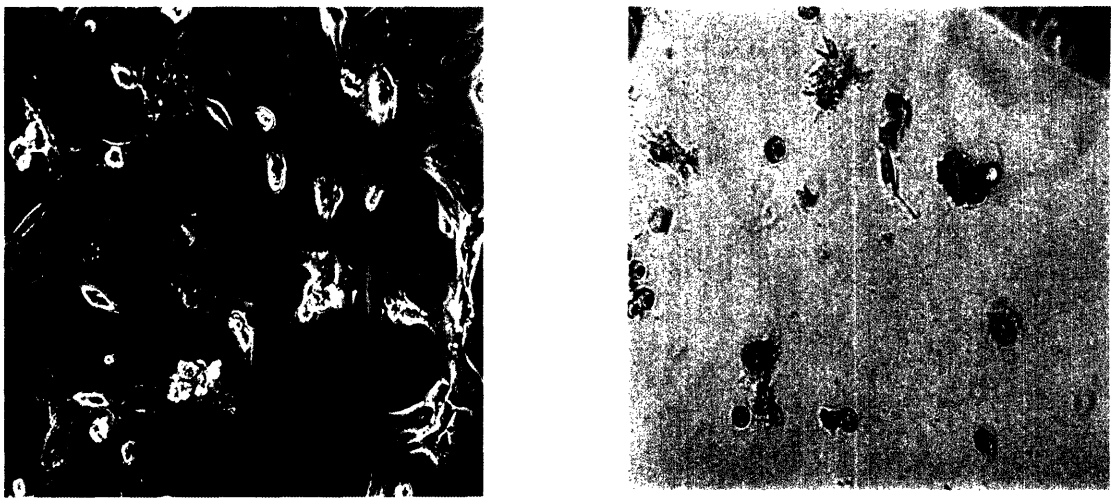

Figure 4.5 Primary pMSC adhesion on surfaces coupled with 59-mer $\alpha_4\beta_1$ peptides identified from bacterial display. **Left (a)** pMSC adhesion. **Right (b)** Adhesion of pMSCs pre-incubated with $\alpha_4\beta_1$ monoclonal antibodies before seeding on peptide-surfaces.

Figure 4.6 HOS adhesion on CS-1 peptide surface. (Average peptide density of the surface shown here was (36.6 ± 3.9) x 10^3 peptides / μm^2.

Surfaces with laminin peptides C16 supported the adhesion of both wtNR6 fibroblasts and CHO-K1 cells, as shown in Figure 4.7a and b. Freshly isolated rat hepatocytes were used to validate the $\alpha_9\beta_1$ EIDGIEL substrates. However, only little adhesion was observed (Figure 4.8).

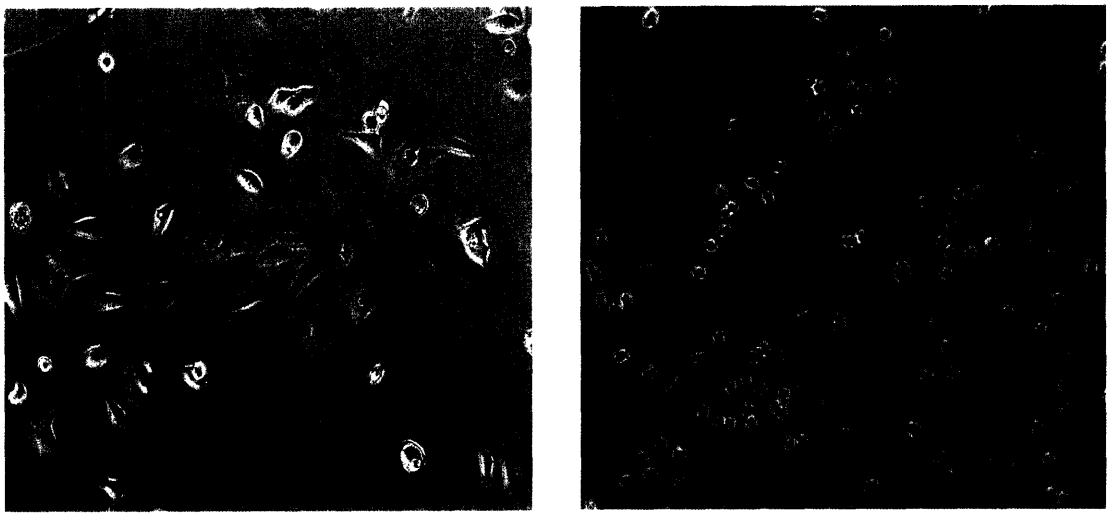

Figure 4.7 **Left (a)** wtNR6 adhesion on C16 surfaces. **Right (b)** CHO-K1 adhesion on C16 surfaces. Peptide density of the surfaces tested here was (260 ± 15) x 10^3 peptides / μm^2.

Figure 4.8 Primary rat hepatocytes, which were believed to express $\alpha_9\beta_1$, did not adhere well on EIDGIEL surfaces.

When MC3T3-E1 were seeded on surfaces with the collagen I peptide DGEA, no adhesion was seen even at a peptide surface density up to (141 ± 22) x 10^3 peptides/μm^2 even after 24 hours of incubation.

4.4.3 Cell adhesion on peptide surfaces with different degrees of clustering

A noted difference in cell spreading was observed between wtNR6 fibroblast adhesion on RGD surfaces with different degrees of clustering (Figure 4.9). Fibroblasts were more spread on RGD surfaces with a higher degree of clustering than the less clustered ones of the same overall RGD surface density and the difference was more pronounced at higher overall surface peptide density. For both types of clustered surfaces, as expected, the ratio of adherent cells to that on TCPS increased with increasing peptide density. Figure 4.10 showed the difference between the two types of clustered surfaces.

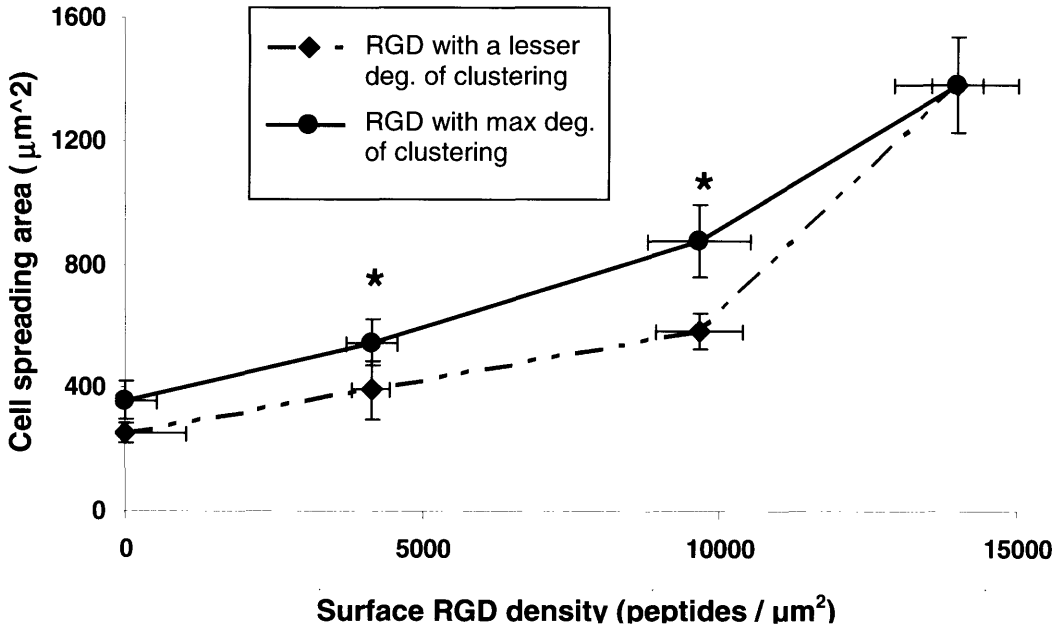

Figure 4.9 wtNR6 fibroblast spreading on RGD surfaces with different degree of clustering. Cell spreading area was quantified by cell-area tracing of microscopy images. See Figure 4.10 for the number of peptides per cluster for both surfaces at each peptide density. * $p < 0.001$ between cell spreading area on RGD surfaces of different degree of clustering of that particular overall peptide density

4.5 Discussion

4.5.1 Biophysical considerations of peptide-comb substrates

The comb copolymer was chosen as the base graft surface material for its ability to present peptides in a clustered manner, as shown previously by our lab. Since peptides were presented as clusters on the surface, there were two associated surface densities – the overall average peptide surface density and the local peptide surface density within a cluster. The peptide densities measured from ^{125}I-peptide quantification yielded the overall average peptide density of a surface. Assuming that there was no preferential segregation between NPC-activated sidechains and its non-activated counterpart at the surface, given peptides were coupled to only NPC-activated comb, the local peptide density within a cluster can be calculated by the ratio of the average surface peptide density to the percentage of NPC-activated comb used in the bulk solution in surface preparation. Taking the example of GRGDSPY-coupling to substrates spincoated with a polymer solution of 16% NPC-activated comb (i.e., 84% non-activated), the average surface density determined from ^{125}I-peptide quantification was (10,300 ± 900) peptides / μm^2. Therefore, within a cluster, the local peptide surface density was (64,400 ± 7100) peptides / μm^2. In Section 3.4.1, we mentioned that recent work in our lab has obtained an empirical estimation of the radius of gyration of the H10M0 polymer, which was ~ 9.2nm (Kuhlman et al., 2005). The size of the cluster was thus ~ 266 nm^2. Based on this dimension and the local peptide density, the spacing between peptides within a cluster was ~4 nm. Comparing this inter-ligand spacing to integrin size, which is about 6 – 9 nm, the spacing of peptides presented by comb copolymer at the surface is estimated to be appropriate for integrin binding. The number of peptides on these peptide-comb copolymer surfaces was also more than sufficient for integrin binding. For a typical cell with an area of about 200 μm^2, there would be ~ 2 x 10^6 peptides under that area available for binding, which is in excess compared to the number of integrins possessed by the cells (on the order of 10^5 per cell). The peptide surface density of these substrates was approximately 20 times higher than the highest concentration of fibronectin used in

most cell studies (10μg/mL fibronectin coating solution, equivalent to a density of 3700 absorbed fibronectin molecules per μm^2 (Asthagiri et al., 1999)) Due to the low affinity of GRGDSPY, 10- to 100-fold less active than that of fibronectin in competition assays (Pierschbacher and Ruoslahti, 1984; Akiyama and Yamada, 1985), a higher RGD density was needed to compensate this difference in affinity. Therefore, a local peptide density of (64,400 ± 7100) peptides / μm^2, which was about 20 times that of the fibronectin density used in most adhesion studies, was a reasonable density to be used.

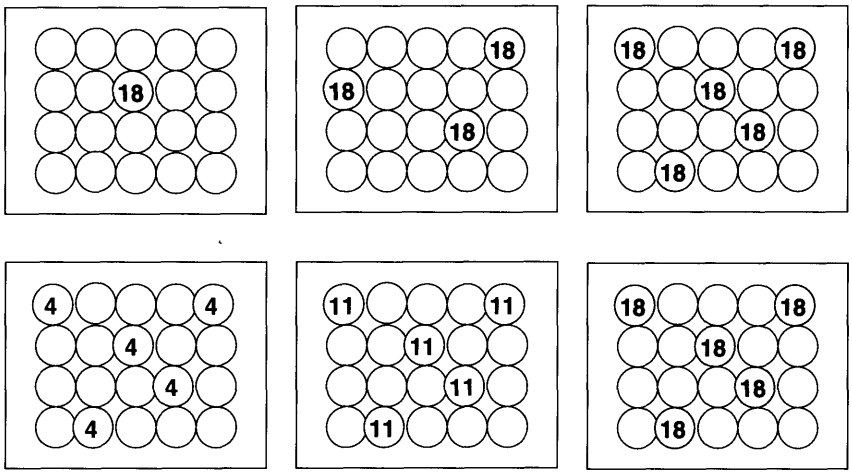

Average peptide density (peptide / μm^2)		4140 ± 430	9660 ± 880	14000 ± 440
# of peptide in cluster	Maximal degree of clustering	18.0	18.0	18.0
	Lower degree of clustering	3.5	10.6	15.0

Figure 4.10 Schematics to illustrate peptide densities and clustering on surfaces with maximal degree and lower degree of peptide clustering. Each circle represents a peptide cluster and the number inside the circle indicates the estimated number of peptides per cluster. These surfaces were used to determine the effect of clustering on fibroblast spreading, as shown in Figure 4.9.

The number of peptides per cluster on these peptide-comb surfaces was sufficient to enhance cell adhesion. With the $R_g^{2D} \approx 9.2$ nm which yielded an average comb molecule footprint area of 266 nm^2 with ~ 18.0 peptides per cluster for RGD surfaces with maximal degree of clustering, regardless of the overall average peptide density. For the case of low-clustering peptide surfaces, at an overall average peptide density of (4140 ± 310) peptides / μm^2 and (9660 ± 720) peptides / μm^2, the number of peptides per cluster was 3.5 and 10.6 respectively. Our results with wtNR6 fibroblasts showed that cell spreading was enhanced on surfaces with higher degree of clustering even at the same overall peptide density. The difference was more pronounced on surfaces with higher average peptide density ((9660 ± 720) peptides / μm^2) even though the difference in the degree of clustering was larger on the lower average peptide density one. (18.0 vs. 10.6 peptides per cluster for overall peptide density of (9660 ± 720) peptides / μm^2 and 18.0 vs. 3.5 peptides per cluster for overall density of (4140 ± 310) peptides / μm^2.) This is in agreement with a previous report from our lab, in which a more pronounced effect on the increase in fibroblast adhesion strength with increasing degree of peptide clustering (1.7, 3.6 and 5.4 peptides per cluster) was observed on surfaces with higher overall peptide density (Koo et al., 2002). In this study, we have confirmed that the biophysical presentation of ligands played an important role in cell adhesion, and consistent with previous studies, cell adhesion can be enhanced by nanoclustering of peptides. The biophysical enhancement through nanoclustering is important to engender adhesion response from peptides with relatively low affinity. As discussed above, some of the peptides selected for screening may have affinity sufficient to reverse adhesion on that parent protein counterpart by competition but its affinity may not be high enough to support cell adhesion on its own when immobilized. As in the case of the peptide YGRGD, to support cell adhesion when immobilized on a surface, RGD sequences required at least one extra amino acid after the aspartic acid residue. However, Maheshwari and co-workers demonstrated cell adhesion on YGRGD surfaces by clustering peptides using star-PEO molecules (Maheshwari et al., 2000).

4.5.2 Cell behavior mediated by various peptide surfaces

When pMSCs were seeded on surfaces with increasing GRGDSPY surface density, not only an increase in cell adhesion but also colony formation was observed. Colony formation was an indication that GRGDSPY surfaces supported not only cell adhesion, but also subsequent proliferation over a period of days, such that the colonies were formed. As very little adhesion was observed on the inactive analog GRGESPY and GRAASPY surfaces over the period of the experiments, it showed that adhesion and proliferation on GRGDSPY surfaces were solely mediated by the peptides and not by proteins non-specifically adsorbed to the protein- and cell-resistant comb substrates. It also confirmed that the coupling of peptides to comb surfaces did not engender addition protein adsorption sufficient to lead to non-specific cell adhesion.

MC3T3-E1 rat calvarial osteoblasts showed an increase in adhesion on surfaces with a higher density of the bone sialoprotein peptide FHRRIKA. Even though MC3T3 adhered and spreaded well on these FHRRIKA substrates, primary pMSCs showed very little cell adhesion. Since adhesion receptors are highly conserved among species, the difference in adhesion behavior was probably not due to the difference of cell species. In addition, Rezania and Healy have previously shown human osteoblasts-like cell adhesion to surfaces with FHRRIKA. Thus, the only other explanation was the receptors for this BSP protein were only expressed by mature osteoblasts but not mesenchymal stem cells that had not been differentiated. The peptide FHRRIKA is quite highly charged. The two arginine and the lysine residues all carry a positive charge and histidine is also slightly charged at neutral pH. (The calculated isoelectric point was 11.0.) The fact that pMSCs did not adhere to the surfaces even at the highest peptide density implied that the adhesion of MC3T3-E1 was specific and not due to the electric attraction between the positive charged surface and the slightly-negative charged cell membrane.

Surfaces with the 59-mer $\alpha_4\beta_1$ peptides identified from bacterial display performed very well in supporting cell adhesion via $\alpha_4\beta_1$ integrins, as shown by our studies with pMSCs

and HOS. Intrigued by the stellar performance, we investigated whether both the binding domains, EHSDV and LDSAS were required to support cell adhesion. Comb copolymer substrates were coupled with only YEHSDV, only YLDSASSE and at 25:75, 50:50, 75:25 YEHSDV:YLDSASSE, using a method similar to that described in Section 4.3.2. No adhesion was observed when pMSCs and HOS were seeded on these surfaces, suggesting that both domains were required for integrin binding or the domains need to be a certain distance apart or in a particular spatial configuration, as given by the 59-mer, for integrin binding. We also noted the homology between the second binding domain and other known active $\alpha_4\beta_1$ sequences, such as IDS on VCAM-1 and LDV on fibronectin. The LDS in the second binding domain and the known $\alpha_4\beta_1$ sequences all contained aspartic acid as the second residue and a hydrophobic amino acid as the first. This may explain why the other $\alpha_4\beta_1$ peptide, CS-1, containing only a single motif LDV in the sequence, supported only a moderate amount of cell adhesion.

Since CHO-K1, which expressed primarily $\alpha_5\beta_1$ but not $\alpha_v\beta_3$, adhered to both the C16 and GRGDSPY surfaces fairly well, it showed, but not exclusively, $\alpha_5\beta_1$ integrins, mediated cell adhesion on these surfaces. No adhesion to collagen I peptide DGEA surfaces was observed when MC3T3 osteoblasts, which expressed $\alpha_2\beta_1$ integrins, were seeded. It is unclear whether the little adhesion was because a particular spatial configuration or mechanical requisite of DGEA was required for $\alpha_2\beta_1$ to bind to, or the affinity of the peptide was not high enough to support cell adhesion. It is unclear which was the case in our studies as the only report in the literature that showed binding of MC3T3-E1 cells to an immobilized form of DGEA was with a DGEA peptide linked to the hydroxyapatite-binding domain of statherin which bind to hydroapatite surfaces on which MC3T3-E1 cells were seeded (Gilbert et al., 2003). Even though these DGEA peptides clearly played a role in cell adhesion, it is unclear whether these peptides alone could support adhesion since the background, hydroxyapatite, was not an inert surface. The addition of the statherin fragment might have given the peptide a particular configuration favorable for $\alpha_2\beta_1$ binding.

Order of screening	Sequence	Notes
RGD	G**RGD**SPY	$\alpha_5\beta_1$ & $\alpha_v\beta_3$ peptide; also as active control
BSP-H	YGG**FHRRIKA**	possibly proteoglycan binding
59-mer $\alpha_4\beta_1$	EH**SDV**IDSQELSKVSREFHSH EFHSHEDMLVVDPKSKEED KHLKFRISH E**LDSAS**SEVN	$\alpha_4\beta_1$ peptide from bacterial display. High affinity as shown by validation experiments.
C16	YGGAFDIT**YVRL**K	LN peptide; binds to $\alpha_5\beta_1$, $\alpha_v\beta_3$ & non-integrins
CS-1	YLHPGE**ILDV**PST	$\alpha_4\beta_1$ peptide from FN CS-1
Peptides of only secondary importance to be screened:		
DGEA	YP**DGEA**	$\alpha_2\beta_1$ peptide (but no activity with MC3T3-E1 in validation expts)
YIGSR	**YIGSR**	LN β1 E1/E1+
EIDGIEL	PLA**EIDGIEL**TY	$\alpha_9\beta_1$ peptide. Low affinity?
REDV	G**REDV**Y	$\alpha_4\beta_1$ peptide from FN CS-5. Low potency?

Table 4.2 Order of peptide candidates to be screened with human marrow aspirates for their ability to promote selective adhesion and proliferation of CTPs. GRGESPY and GRAASPY are used as negative control peptides in screening.

Very little hepatocyte adhesion was observed EIDGIEL surfaces. EIDGIEL is an $\alpha_9\beta_1$ peptide and is one of the integrins expressed by primary hepatocytes. However, there were no published reports on the level of $\alpha_9\beta_1$ expression by hepatocytes. Therefore, it is difficult to conclude whether the little hepatocyte adhesion was due to the small number of $\alpha_9\beta_1$ expressed by the cells, or the low affinity of the peptide. In addition, the low degree of adhesion observed may be due to the de-adhesive effect of $\alpha_9\beta_1$. The integrin has been shown to disrupt focal adhesion (Murphy-Ullrich et al., 1991). Nevertheless, in this chapter, we have validated the bioactivity of other peptide surfaces and confirmed that cell adhesion and function can be mediated biochemically by the choice of peptide presented by comb copolymer on the surface. We have also confirmed that adhesion can be enhanced biophysically, by nanoclustering the peptides. These knowledge and the identified and validated peptide surface candidates allowed us to screen these peptide

candidates with human bone marrow aspirates for their ability to engender the selective adhesion, proliferation and differentiation of CTPs. In light of the results from this chapter, peptide candidates are screened in the following order with marrow aspirates in the next chapter (Table 4.2).

4.6 References

Abukawa, H., Shin, M., Williams, W.B., Vacanti, J.P., Kaban, L.B. and Troulis, M.J. (2004). "Reconstruction of mandibular defects with autologous tissue-engineered bone." Journal of Oral Maxillofacial Surgery **62**: 601-606.

Akiyama, S.K. and Yamada, K.M. (1985). "Synthetic peptides competitively inhibit both direct binding to fibroblasts and functional biological assays for the purified cell-binding domain of fibronectin." Journal of Biological Chemistry **260**: 402-405.

Ashkar, S. (2001). Personal Communications.

Asthagiri, A.R., Nelson, C.M., Horwitz, A.F. and Lauffenburger, D.A. (1999). "Quantitative Relationship among Integrin-Ligand Binding, Adhesion, and Signaling via Focal Adhesion Kinase and Extracellular Signal-regulated Kinase 2." Journal of Biological Chemistry **274**(38): 27119-27127.

Bearinger, J.P., Castner, D.G. and Healy, K.E. (1998). "Biomolecular modification of p(AAm-co-EG/AA) IPNs supports osteoblast adhesion and phenotypic expression." Journal of Biomaterials Science - Polymer Edition **9**: 629-652.

Bianco, P., Fisher, L.W., Young, M.F., Termine, J.D. and Robey, P.G. (1991). "Expression of bone sialprotein (BSP) in developing human tissue." Calcif Tissue Int **49**: 421-426.

Bober-Barkalow, F.J. and Schwarzbauer, J.E. (1991). "Localization of the major heparin-binding site in fibronectin." Journal of Biological Chemistry **266**: 7812-7818.

Cardin, A.D. and Weintraub, H.J.R. (1989). "Molecular modeling of protein-glycosaminoglycan interactions." Arteriosclerosis **9**: 21-32.

Chichester, C.O., Fernandez, M. and Minguell, J.J. (1993). "Extracellular-matrix gene-expression by human bone-marrow stroma and by marrow fibroblasts." Cell Adhesion and Communication **2**: 93-99.

Clements, J.M., Newham, P., Shepherd, M., Gilbert, R., Dudgeon, T.J., Needham, L.A., Edwards, R.M., Berry, L., Brass, A. and Humphries, M.J. (1994). "Identification of a key integrin-binding sequence in VCAM-1 homologous to the LDV active site in fibronectin." Jounral of Cell Science **107**: 2127-2135.

Clover, J., Dodds, R.A. and Gowen, M. (1992). "Integrin subunit expression by human osteoblasts and osteoclasts in situ and in culture." Journal of Cell Science **103**: 267-271.

Conget, P.A. and Minguell, J.J. (1999). "Phenotypical and functional properties of human bone marrow mesenchymal progenitor cells." Journal of Cell Physiology **181**: 67-73.

Dalton, B.A., McFarland, C.D., Underwood, P.A. and Steele, J.G. (1995). "Role of the heparin binding domain of fibronectin in attachment and spreading of human bone-derived cells." Journal of Cell Science **108**(5): 2083-2092.

Dillow, A.K., Ochsenhirt, S.E., McCarthy, J.B., Fields, G.B. and Tirrell, M. (2001). "Adhesion of alpha(5)beta(1) receptors to biomimetic substrates constructed from peptide amphiphiles." Biomaterials **22**(12): 1493-1505.

Franceschi, R.T. (1999). "The developmental control of osteoblast-specific gene expression: Role of specific transcription factors and the extracellular matrix environment." Critical Reviews in Oral Biology and Medicine **10**(1): 40-57.

Garcia, A.J., Schwarzbauer, J.E. and Boettiger, D. (2002). "Distinct activation states of alpha 5 beta 1 integrin show differential binding to RGD and synergy domains of fibronectin." Biochemistry **41**(29): 9063-9069.

Gilbert, M., Giachelli, C.M. and Stayton, P.S. (2003). "Biomimetic peptides that engage specific integrindependent signaling pathways and bind to calcium phosphate surfaces." Journal of Biomedical Materials Research Part A **67A**(1): 69-77.

Gronthos, S., Simmons, P.J., Graves, S.E. and Robey, P.G. (2001). "Integrin-mediated Interactions Between Human Bone Marrow Stromal Precursor Cells and the Extracellular Matrix." Bone **26**(2): 174-181.

Grzesik, W.J. and Robey, P.G. (1994). "Bone matrix RGD glycoproteins: Immunolocalization and interaction with human primary osteoblastic bone cells in vitro." Journal of Bone and Mineral Research **9**: 487-496.

Hodde, J., Record, R., Tullius, R. and Badylak, S. (2002). "Fibronectin peptides mediate HMEC adhesion to porcine-derived extracellular matrix." Biomaterials **23**(8): 1841-1848.

Horton, M.A. (1995). "Interactions of connective tissue cells with the extracellular matrix." Bone **17**: 51S-53S.

Hubbell, J.A. (1995). "Biomaterials in tissue engineering." BioTechnology **13**: 565-576.

Hughes, D.E., Salter, D.M., Dedhar, S. and Simpson, R. (1993). "Integrin expression in human bone." Journal of Bone and Mineral Research **8**: 527-533.

Hwa, A., Fry, R., So, P.T., Stolz, D.B. and Griffith, L.G. (2005). "In vitro co-culture of hepatocytes and liver endothelial cells foster vascular formation." (In Preparation).

Imai, S., Kaksonen, M., Raulo, E., Kinnunen, T., Fages, C., Meng, X.J., Lakso, M. and Rauvala, H. (1998). "Osteoblast recruitment and bone formation enhanced by cell matrix-associated heparin-binding growth-associated molecule (HB-GAM)." Journal of Cell Biology **143**(4): 1113-1128.

Jones, P.L. and Jones, F.S. (2000). "Tenascin-C in development and disease: gene regulation and cell function." Matrix Biology **19**(7): 581-596.

Komoriya, A., Green, L.J., Mervic, M., Yamada, S.S., Yamada, K.M. and Humphries, M.J. (1991). "The minimal essential sequence for a major cell type-specific adhesion site (CS1) within the alternatively spliced type-III connecting segment domain of fibronectin is leucine-aspartic acid-valine." Journal of Biological Chemistry **266**(23): 15075-15079.

Koo, L.Y., Irvine, D.J., Mayes, A.M., Lauffenburger, D.A. and Griffith, L.G. (2002). "Co-regulation of cell adhesion by nanoscale RGD organization and mechanical stimulus." Journal of Cell Science **115**(7): 1423-1433.

Kuhlman, W., Olivetti, E., Mayes, A.M. and Griffith, L.G. (2005). "Conformations of Polymer Chains Confined to Two Dimensions Through Surface Segregation." (in preparation).

Kukita, T., Hata, K., Kukita, A. and Iijima, T. (1998). "A Major Basement Membrane Component of the Blood Vessel, as a Negative Regulator of Osteoclastogenesis." Calcif Tissue Int **63**(2): 140-142.

Machie, E.J. (1997). "Molecules in focus: tenascin-C." Int. J. Biochem. Cell Biol. **29**: 1133-1137.

Mackie, E.J. and Tucker, R.P. (1999). "The tenascin-C knockout revisited." Journal of Cell Science **112**: 3847-3853.

Maheshwari, G., Brown, G., Lauffenburger, D.A., Wells, A. and Griffith, L.G. (2000). "Cell adhesion and motility depend on nanoscale RGD clustering." Journal of Cell Science **113**: 1677-1686.

Massia, S.P. and Hubbell, J.A. (1991). "An RGD spacing of 440 nm is sufficient for integrin $\alpha v\beta 3$-mediated fibroblast spreading and 140 nm for focal contact fiber formation." Journal of Cell Biology **114**: 1089-1100.

Massia, S.P. and Hubbell, J.A. (1992a). "Immobilized amines and basic amino acis as mimetic heparin-binding domains for cell surface proteoglycan-mediated adhesion." Journal of Biological Chemistry **267**: 10133-10141.

Massia, S.P. and Hubbell, J.A. (1992b). "Vascular endothelial-cell adhesion and spreading promoted by the peptide REDV of the IIICS region of plasma fibronectin is mediated by integrin alpha-4-beta-1." Journal of Biological Chemistry **267**(20): 14019-14026.

Massia, S.P. and Stark, J. (2001). "Immobilized RGD peptides on surface-grafted dextran promote biospecific cell attachment." Journal of Biomedical Materials Research **56**(3): 390-399.

Minguell, J.J., Erices, A. and Conget, P. (2001). "Mesenchymal stem cells." Experimental Biology and Medicine **226**(6): 507-520.

Mintz, K.P., Grzesik, W.J., Midura, R.J., Robey, P.G., Termine, J.D. and Fisher, L.W. (1993). "Purification and fragmentation of nondenatured bone sialprotein: evidence for a cryptic RGD-resistant cell attachment domain." Journal of Bone and Mineral Research **8**: 985-995.

Murphy-Ullrich, J.E., Lightner, V.A., Aukhil, I., Yan, Y.Z. and Erickson, H.P. (1991). "Focal adhesion integrity is downregulated by the alternatively spliced domain of human tenascin." Journal of Cell Biology **115**: 1127-1136.

Nozimu, M., Kuratomi, Y., Song, S.-Y., Ponce, M.L., Hoffman, M.P., Powell, S.K., Miyoshi, K., Otaka, A., Kleinman, H.K. and Yamada, Y. (1997). "Identification of cell binding sequences in mouse laminin γ1 chain by systematic peptide screening." Journal of Biological Chemistry **272**(51): 32198-32205.

Olbrich, K.C., Andersen, T.T. and Bizio, R. (1996). "Surfaces modified with covalently immobilized adhesive peptides affect fibroblast population motility." Biomaterials **17**: 759-764.

Panayotou, G., End, P., Aumailley, M., Timpl, R. and Engel, J. (1989). "Domains of laminin with growth-factor activity." Cell **56**: 93-101.

Pfaff, M. (1997). Recognition sites of RGD-dependent integrins. Integrin-Ligand Interaction. J. A. Eble. Heidelberg, Springer-Verlag**:** 101-121.

Pierschbacher, M.D. and Ruoslahti, E. (1984). "Cell attachment activity of fibronectin can be duplicated by small synthetic fragments of the molecule." Nature **309**: 30-33.

Ponce, M.L. and Kleinman, H.K. (2003). "Identification of Redundant Angiogenic Sites in Laminin α1 and γ1 Chains." Experimental Cell Research **285**: 189-195.

Ponce, M.L., Nomizu, M., Delgado, M.C., Kuratomi, Y., Hoffman, M.P., Powell, S., Yamada, Y., Kleinman, H.K. and Malinda, K.M. (1999). "Identification of Endothelial Cell Binding Sites on the Laminin γ1 Chain." Circulation Research **84**(688-694).

Ponce, M.L., Nomizu, M. and Kleinman, H.K. (2001). "An Angiogenic Laminin Site and its Antagonist Bind through the αvß3 and α5ß1 Integrins." FASEB Journal **15**: 1389-1397.

Rezania, A. and Healy, K.E. (1998). "Biomimetic Peptide Surfaces That Regulate Adhesion, Spreading, Cytoskeletal Organization, and Mineralization of the Matrix Deposited by Osteoblast-like Cells." Biotechnol Prog **15**(1): 19-32.

Rezania, A. and Healy, K.E. (1999). "Integrin subunits responsible for adhesion of human osteoblast-like cells to biomimetic peptide surfaces." Journal of Orthopaedic Research **17**(4): 615-623.

Rezania, A., Thomas, C.H., Branger, A.B., Waters, C.M. and Healy, K.E. (1997). "The detachment strength and morphology of bone cells contacting materials modified with a peptide sequence found within bone sialoprotein." Journal of Biomedical Materials Research **37**: 9-19.

Robey, P.G. (1996). "Vertebrae mineralized matrix proteins: structure and function." Connect. Tissue Res. **35**: 131-136.

Roche, P., Goldberg, H.A., Delmas, P.D. and Malaval, L. (1999a). "Selective attachment of osteoprogenitors to laminin." Bone **24**(4): 329-336.

Roche, P., Rousselle, P., Lissitzky, J., Delmas, P.D. and Malaval, L. (1999b). "Isoform-specific attachment of osteoprogenitors to laminins: mapping to the short arms of laminin-1." Experimental Cell Research **250**: 465-474.

Ruoslahti, E. and Pierschbacher, M.D. (1987). "New Perspectives in cell adhesion: RGD and integrins." Science **238**: 491-497.

Schaffner, P. and Dard, M.M. (2003). "Structure and function of RGD peptides involved in bone biology." Cellular and Molecular Life Sciences **60**: 119-132.

Schneider, H., Harbottle, R.P., Yokosaki, Y., Kunde, J., Sheppard, D. and Coutelle, C. (1998). "A novel peptide, PLAEIDGIELTY, for the targeting of alpha9/beta1-integrins." FEBS letters **429**: 269-273.

Scutt, A., Mayer, H. and Wingender, E. (1992). "New perspectives in the differentiation of bone-forming cells." Biofactors **4**(1): 1-13.

Shrestha, P., Takai, Y. and Mori, M. (1997). "Tenascin: A modulator of development and tumorigenesis in human salivary glands." Cancer Journal **10**(4): 197-201.

Soligo, D., Schiro, R., Luksch, R., Manara, G. and Quirici, N. (1990). "Expression of integrains in human bone marrow." British Journal of Haematology **76**: 323-332.

Staatz, D.W., Fok, K.F., Zutter, M.M., Adams, S.P., Rodriguez, B.A. and Santoro, S.A. (1991). "Identification of a tetrapeptide recognition sequence for the alpha 2 beta 1 integrin in collagen." Journal of Biological Chemistry **266**: 7363.

Stubbs, J.T., Mintz, K.P., Eanes, E.D., Torchia, D.A. and Fisher, L.W. (1997). "Characterization of native and recombinant bone sialoprotein: Delineation of the mineral-binding and cell adhesion domains and structural analysis of the RGD domain." Journal of Bone and Mineral Research **12**(8): 1210-1222.

Tiisala, S., Hakkarainen, M., Majuri, M.L., Mattila, P.S., Mattila, P. and Renkonen, R. (1993). "Down-regulation of monocytic VLA-4 leads to a decreased adhesion to VCAM-1." FEBS letters **1-2**: 19-23.

Wang, J., Kennedy, J.G., Kasser, J.R., Glimcher, M.J. and Salih, E. (1998). "Novel bioactive property of purified native bone sialoprotein in bone repair of a calvarial defect." Transactions of the 44th Annual Orthopaedic Research Society Meeting **23**(2): 1007.

Xiao, G., Wang, D., Benson, M.D., Karsenty, G. and Franceschi, R.T. (1998). "Role of the alpha2-integrin in osteoblast-specific gene expression and activation of the Osf2 transcription factor." Journal of Biological Chemistry **273**: 32988-32994.

Yamada, Y. and Kleinman, H.K. (1992). "Functional domains of cell adhesion molecules." Current Opinion in Cell Biology **4**: 819-823.

Yin, D. (2004). The applications of comb polymer to the study of liver cell adhesion and signaling. M.Eng. Thesis, Massachusetts Institute of Technology.

Yokosaki, Y., Matsuura, N., Higashiyama, S., Murakami, I., Obara, M., Yamakida, M. and Shigeto, N. (1998). "Identification of the ligand binding site for the integrin alpha9/beta1 in the third fibronectin type III repeat of tenascin-C." Journal of Biological Chemistry **273**: 11423-11428.

Yokosaki, Y., Moris, H., Chen, J. and Sheppard, D. (1996). "Differential effects of the integrins alpha 9 beta 1, alpha v beta 3, and alpha v beta 6 on cell proliferative responses to tenascin. Roles of the beta subunit extracellular and cytoplasmic domains." Journal of Biological Chemistry **271**: 24144-24150.

Yudoh, K., Matsui, H., Kanamori, M., Ohmori, K., Yasuda, T. and Tsuji, H. (1996). "Characteristics of High and Low Laminin-Adherent Dunn Osteosarcoma Cells Selected by Adhesiveness to Laminin - Correlation between Invasiveness through the Extracellular Matrix and Pulmonary Metastatic Potential." Tumor Biology **17**(6): 332-340.

Zou, X.N., Li, H.S., Chen, L., Baatrup, A., Bunger, C. and Lind, M. (2004). "Stimulation of porcine bone marrow stromal cells by hyaluronan, dexamethasone and rhBMP-2." Biomaterials **25**(23): 5375-5385.

Chapter 5

Adhesion and Colony Formation of Connective Tissue Progenitors from Bone Marrow Aspirates

5.1 Introduction

In the previous chapter, a priority list of peptide candidates with the potential to mediate the selective adhesion and proliferation of connective tissue progenitors from bone marrow aspirates was critically chosen from the literature. These peptides were immobilized on the otherwise inert comb-copolymer substrates and the bioactivity of these peptide-surfaces was validated with various cell lines or primary cells that expressed integrins or receptors that recognize the peptides to be tested. In this chapter, these validated peptide surfaces were set in experiments with human marrow aspirates to screen for their potential to promote the adhesion and proliferation of CTPs, as well as the differentiation of CTPs to cells of osteoblastic lineage. A critical evaluation of the CTP assay was also performed.

To evaluate the potential of each peptide in targeting CTPs, the colony forming unit (CFU) assay was developed to measure colony formation of CTPs in a two-dimensional model. This functional assay was needed to evaluate empirically the adhesion and colony formation of CTPs on these peptide surfaces in order to correlate with any molecular profile of marrow cells, as shown in Chapter 6. With the integrin expression profile alone, it is impossible to tell whether an expressed receptor actually mediates the process of CTP adhesion and proliferation. Moreover, to date, markers that target only CTPs have not been identified. Thus, one can at best assay the adhesion receptor profile of an enriched but not pure population of CTPs. It is also impossible to analyze the adhesion receptor profile of a marrow cell while assaying its ability to form colonies. Once a

marrow cell adheres to a surface *in vitro*, its molecular profile will likely have been changed. On the other hand, assaying CTP colony formation directly on peptide substrates allowed us to explore peptides that have the potential of enhancing CTP adhesion and proliferation but the adhesion receptors which the cells utilized to mediate the process were not known. Therefore, CTP adhesion measurements were first performed in this chapter before we examined the integrin expression profile of marrow aspirate cells in Chapter 6. The CFU assay was developed based on the one reported by Muschler et al. (Muschler et al., 2001) but modified to assay colony formation on peptide-comb substrates. Previous studies by Muschler et al., showed that the mean prevalence of CTPs in bone marrow was about 1 in 23,000. However, the number varied greatly with patients' age, gender, disease states and other factors (Majors et al., 1997; Muschler et al., 2001). It has been established that CTPs from bone marrow, when given the right condition, formed colonies when cultured. Colony expression of alkaline phosphatase (AP), an early marker for osteoblastic differentiation (Turksen and Aubin, 1991; Bianco et al., 1993; Lee et al., 1993), is an indication that they are progenitors of osteoblasts. Therefore, the formation of colony (also denoted as CFU from here on) and the expression of AP by these colonies gives a lumped measure of how well peptide substrates supported the initial adhesion of CTPs, the subsequent proliferation so a colony of cells was formed, as well as the differentiation of these progenitors into osteoblastic lineage. Failure to support any one of the above three aspects would not lead to the formation of osteoblastic colonies.

In this chapter, in addition to examining the ability of the peptide candidates identified in the previous chapter for their ability to promote CTP colony formation using the CFU assay, a statistical model that captured the unique characteristics of the CFU assay was developed to analyze the findings of the experiments. Lastly, we evaluated glass on its performance as the "gold standard control" of the CFU assay and from the studies, revealed the extent of patient-to-patient variability.

5.2 Materials and methods

5.2.1 Surface preparation for Colony forming unit assay

Peptide-coupled comb copolymer substrates were prepared using a protocol similar to that developed in Chapter 3, with slight modifications. Instead of round coverslips, comb copolymer was spincoated on silanized 18 x 18 cm^2 square glass coverslips (VWR International) such that they could fit well in 2-well Lab-tek chambers for CFU assays. The same glass coverslips, non-silanized but treated by sonicating in 200 proof ethanol, was used as glass control surfaces in the CFU assay. Plain non-activated comb substrates were prepared to be used as the negative control of the CFU assay. All surfaces were stored at room temperature after preparation and drying *in vacuo*. Substrates were used within a month of preparation. For marrow experiments, surfaces were placed in 2-well 4-cm^2 Lab-tek glass chamber slides (Labtech, Nagle Nunc International, Naperville, IL, USA) and sterilized by UV light for 30 minutes prior to marrow experiments.

5.2.2 Colony forming unit (CFU) Assay

Bone marrow was aspirated from human subjects as described in Chapter 2. Marrow aspirates were heparinized and suspended in complete media (MEM-α with 10% fetal bovine serum (BioWhittaker, Walkersville, MD, USA), 200 i.u./mL penicillin, 400 μg/mL streptomycin (Gibco)). After the number of nucleated cells in the marrow sample was counted, a density of 2×10^6 nucleated cells, unless otherwise noted, was seeded in each of the two 4-cm^2 wells on a glass Lab-tek chamber containing either peptide-comb substrates or glass coverslip control. Quadruplicates of peptide-comb substrates or glass coverslips were plated for each patient sample. Cultures were maintained at 37°C in a humidified atmosphere of 5% CO_2 in air. Medium was first changed after 48 hours of plating at which point the non-adherent cells from each chamber were removed and replated on Lab-tek slides. After the media change and the non-adherent cells removed, the substrates were continued to be cultured for another 4 days before harvest. The

surfaces were then washed and fixed and the number of colonies formed on these substrates were counted. These colonies were defined as "early adherent colonies" for they originated from cells that adhered to the test surfaces within 48 hours of plating. Subcolony clusters and single adherent cells were also counted. The non-adherent cells replated on Lab-tek slides were cultured for 6 days after the replate. Colonies formed on Lab-tek from the replate were defined as "late adherent colonies" for they were formed from cells that did not adhere to the first test surfaces within 48 hours of plating but adhered and formed colonies after they were replated. Figure 5.1 shows the schematic of CFU assay.

Cells and colonies on substrates were stained for alkaline phosphataste (AP) expression by first rinsing the substrates with Hanks balanced salt solution and then incubating the with 120 mM Tris buffer, pH 8.4, containing 0.9 mM Naphtol AS-MX Phosphate and 1.8 mM Fast Red TR. Naphtol AS-MX Phosphate was solubilized with N,N-dimethylformamide (Curtis Matheson Scientific, Houston, TX, USA) prior to dilution with the Tris buffer. After 30 min at 37°C, the cultures were washed with deionized water. Any CFU that was AP-positive was denoted as CFU-AP.

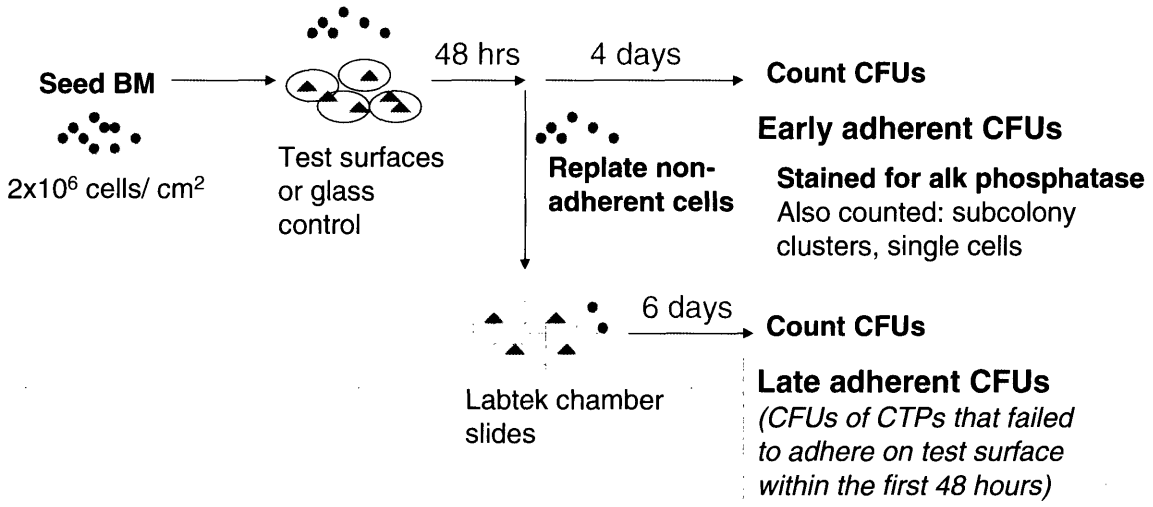

Figure 5.1 Schematic showing the flow of marrow aspirate CFU assay.

5.3 Statistical model for colony formation

In presenting and comparing biological data, statistical analysis techniques such as those utilizing the Gaussian distribution, student t-test and fisher test were often employed. Often the mean and standard deviation of data based on the Gaussian distribution worked sufficiently well in capturing the expected value and variance of data due to the central limit theorem when the sample size is large even though in reality the data do not follow a Gaussian distribution due to characteristics inherent to the experiment. However, the assumption that experimental data follow the Gaussian distribution became problematic when the sample size is small and when some of the assumptions behind the Gaussian distribution were clearly flawed for the particular experiments. The statistics are often skewed by outlying data points and fail to capture the real physical situation. When dealing with such clinical data, researchers often end up presenting the data from each patient or sample separately, or use various rank tests to compare only the trend from each patient. These approaches avoid the misleading presentation of the data but can at best compare only trends but not the magnitude of the difference within the trend. There were a number of aspects in the CFU assay and the process of colony formation itself that were inconsistent with the assumptions behind the Gaussian distribution. The discrete process of colony formation as discussed below, the small number of patient marrow samples we could test on each peptide substrates and the small number of colonies formed on surfaces also made the use of Gaussian distribution unsuitable for analyzing CFU data. In light of that, a statistical model that captures key characteristics of CFU formation was developed.

Distinctive characteristics of the process of colony formation in the CFU assay were first identified in order to build a model that captures this distinctiveness. As we defined a colony as a cluster of more than 8 cells, the number of colonies on a surface was by definition a natural discrete number. In addition, it was valid to assume that the formation of a colony on a surface was independent of, and not determined by whether another colony formed on the same peptide surface or another peptide surface. The

discreteness of the number of colonies, the independence of colony formation, and the process of cell adhesion and colony formation itself can be best described by the poisson process, a discrete distribution for which one of the requirements, in statistical terms, is the number of changes in nonoverlapping intervals is independent for all intervals. On the other hand, since the number of CTPs in a patient sample was reflected by the number of colonies formed on glass positive control, the number of colonies formed on a peptide surface was correlated with how many colonies were formed on glass. In statistical terms, the observed likelihood of colony formation on a peptide surface, i.e., the likelihood that was measured in the assay, was the probability of a colony formed on the peptide-surface given a colony formed on glass. For peptide substrate *i* assayed with marrow aspirate from patient *j*, this probability can be denoted by $P(M_{ij} \mid N_j)$ where M_{ij} is the number of CFUs formed on substrate *i* for patient *j* and N_j is the number of CFUs formed on glass control with patient *j* sample. Given the poisson process, the probability of obtaining exactly M_{ij} CFUs with N_j total available CTPs (as reflected by the number of CFUs formed on glass) is given by the limit of a binomial distribution:

$$P(M_{ij} \mid N_j) = \frac{N_j!}{(N_j - M_{ij})!M_{ij}!} P_i^{Mij}(1-P_i)^{N_j - M_{ij}}$$

where $P(M_{ij} \mid N_j)$, as defined above, is a discrete probability distribution and P_i is the probability of a colony forming on substrate *i*. Considering all *n* patient samples that had been tested for substrate *i*, the overall probability of the model is the product of the probabilities of colony formation given a colony formed on glass:

$$\prod_{j=1}^{n} P(M_{ij} \mid N_j) = \prod_{j=1}^{n} \left(\frac{N_j!}{(N_j - M_{ij})!M_{ij}!} P_i^{Mij}(1-P_i)^{N_j - M_{ij}} \right)$$

where P_i, the probability of colony formation on substrate *i*, is independent of the number of colonies formed on glass. The P_i that maximizes the overall probability of the model, $P_{i,max}$, is the probability of interest. $P_{i,max}$ is a true measure of probability of colony formation on substrate *i*, independent of colony formation on glass. Therefore, despite

large variability of colony formation on glass due to the use of different patient samples, the model takes a fair contribution from each patient data. Owing to this independence, unlike rank tests in which only patient sample sets tested with all peptide substrates can be used, this model allows us to consider data in which different patient samples were used to test different substrates.

The statistical model was programmed and probabilities were calculated and maximized using Microsoft Excel. Each peptide substrate composition considered in the model was assayed with three to eight different patient marrow samples. Standard deviation (66% confidence interval) and 90% confidence level were also determined for each probability by building the probability distribution curve and calculating the P_i interval around $P_{i,max}$ for which the area under the probability curve is 66% and 90% to that of the total area. Increment of 0.0025 of P_i was used in this calculation. The results of the model were presented in Whiskers diagrams. This statistical model was applied to analyze both the CFU and CFU-AP data of peptide-comb substrates.

5.4 Results

5.4.1 Colony formation in CFU assay and statistical analysis

Seven marrow samples were plated on GRGDSPY, GRGESPY and GRAASPY substrates of a range of peptide surface densities to see if there is a peptide dose-response behavior on CFU formation, similar to that on cell adhesion seen in the previous chapter. For these experiments, only 5 x 10^5 nucleated marrow cells, instead of 2 x 10^6, were plated in each of the two 4-cm^2 wells on a glass Lab-tek chamber. Data from one set of marrow samples had to be discarded due to the extremely low CFU formation even on glass. (Only 5 early adherent colonies were formed on glass for that individual sample.) Results are shown in Figure 5.2. Despite the apparent increase in CFU efficiency (ratio of the number of early adherent CFUs on test surface to that on glass) with increasing GRGDSPY density, the difference in CFU efficiency between GRGDSPY and GRGESPY surfaces was not statistically different (p=0.1) due to the failure of colony formation on GRGDSPY surfaces with samples that had very few CTPs, as reflected by the low number of CFUs on glass control. Hence a large variance was associated with the mean CFU efficiency.

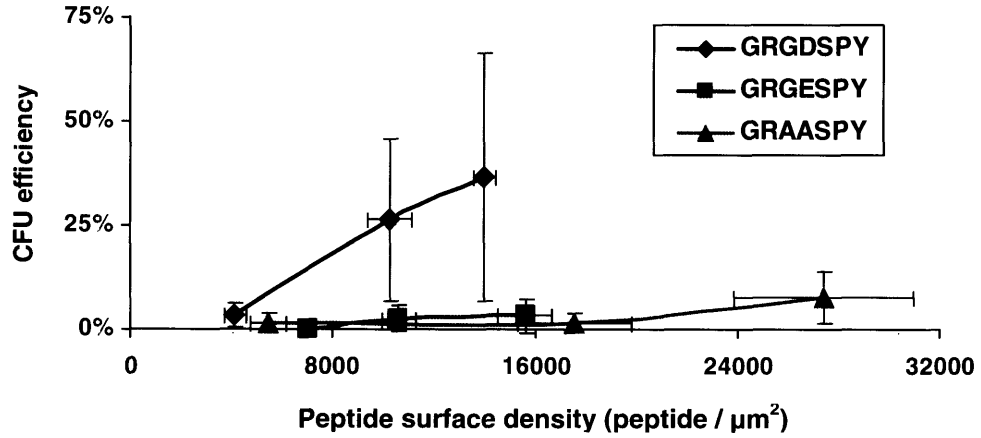

Figure 5.2 CFU efficiency on GRGDSPY and inactive peptide analog surfaces. (data from 6 patients) Student t-test was used to compare the difference in CFU efficiency of GRGDSPY and GRGESPY for the medium and high peptide densities (p=0.087 and 0.1 respectively). The differences were statistically insignificant.

In light of the large variations which made the study of dose-response inconclusive, only surfaces with the highest peptide density was assayed and compared subsequently. GRGDSPY, GRGESPY and GRAASPY substrates were prepared by coupling these peptides to surfaces spincoated with 25% NPC-activated comb, yielding substrates with surface densities of (14000 ± 440) / μm^2, (15330 ± 1040) / μm^2, and (27440 ± 3540) / μm^2 respectively. Figure 5.3a and b show the results when marrow aspirate samples from seven individuals (different from the ones used in the dose-response studies above and at a seeding density of 2×10^6 nucleated cells in each of the two 4-cm^2 wells of Lab-tek chamber slides) were plated on these substrates. For five out of the seven samples tested, CFU formation was enhanced on GRGDSPY surfaces compared to its inactive peptide analog and non-activated comb control. This is reflected by the higher CFU efficiency, defined as the ratio of the number of CFUs on test surface to that on glass control. Almost no subcolony clusters were found on the peptide surfaces and less than 100 single adherent cells were observed. In many cases, less than 10 single cells were found on the substrates. The only exception was the patient sample *CL* where more than 100 single cells were adherent on all the "early adherent" substrates respectively. All CFUs on GRGDSPY, GRGESPY and GRAASPY substrates and comb surfaces were stained positive for AP, except for 30% of the CFUs on GRGESPY surfaces with patient sample *RW*. Even though GRGDSPY enhanced the formation of CFU-AP (ratio of the number of AP+ CFU on test surface to that on glass) in five out of seven marrow samples screened, the degree of enhancement varied widely among patients. In addition, the number of colonies formed on the same peptide or control surface by different patient samples varied greatly. This is due to the variation observed on glass control surfaces. The number of early adherent CFUs formed on glass from the 7 patients' marrow aspirate ranged from 10 to 70 and the total number of CFUs (sum of the number of adherent CFU and non-adherent CFU) also showed a 4-fold variation among the 7 patients. However, the ratio of CFU-AP to all CFU on glass control showed a much smaller variation ((91.3 ± 4.8) %).

Bone sialoprotein peptide FHRRIKA and the 59-mer $\alpha_4\beta_1$ peptide showed a significantly higher CFU efficiency in comparison with the negative control GRAASPY and comb control (Figure 5.4). For the peptide FHRRIAK, CFU efficiency was consistently between 22% and 30% for four out of five marrow samples tested. The fifth sample, *CL*, which did not support any colony formation on FHRRIKA surfaces, was the same sample that showed little colony formation even on GRGDSPY surfaces. The 59-mer $\alpha_4\beta_1$ peptide was highly potent in promoting colony formation. CFU efficiency was over 30% for all three marrow samples tested.

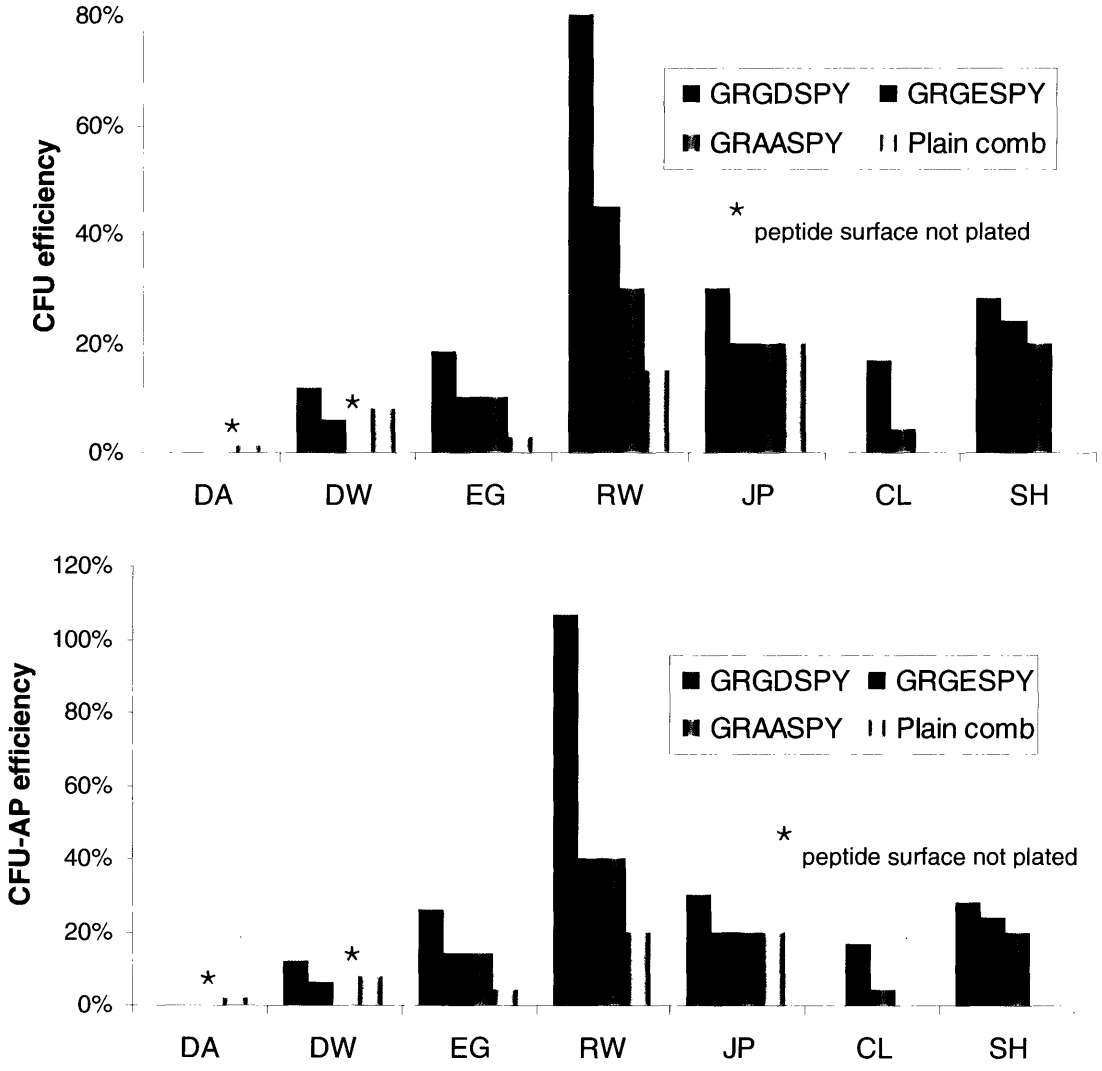

Figure 5.3 **Top (a)** CFU efficiency of GRGDSPY, inactive analog peptide and non-activated comb surfaces. **Bottom (b)** CFU-AP efficiency. Marrow aspirates from 7 individuals were used in the experiment. Patient classifiers were denoted on the x axes.

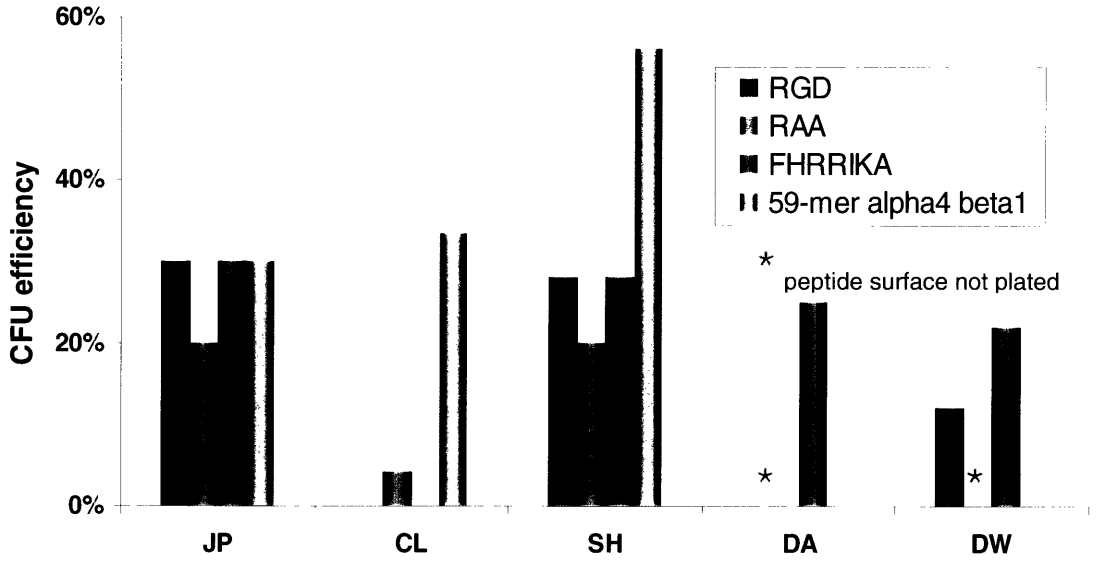

Figure 5.4 CFU efficiency of FHRRIKA and 59-mer $\alpha_4\beta_1$ substrates. 5 marrow aspirate samples were used to assay colony formation on FHRRIKA surfaces and 3 were used on 59-mer $\alpha_4\beta_1$ substrates. Patient classifiers were denoted on the x axes.

The CFU assay statistical model was used to analyze all the colony formation data from screening peptide substrates using the CFU assay. Figure 5.5 shows the Whiskers diagram of the probability of CFU formation on all the candidate peptide substrates. Peptide candidates that are potent in enhancing colony formation were defined as those with a probability of CFU formation higher than that of the negative control peptides RGE (0.129 ± 0.19) and RAA (0.140, +0.275/-0.225). (Standard deviation was reported as the variance here.) The peptides RGD, CS-1, FHRRIKA and 59-mer $\alpha_4\beta_1$ supported colony formation to various extents. The probability of colony formation on 59-mer $\alpha_4\beta_1$ substrates was 0.424, higher than RGE and RAA with 95% confidence interval. The probability of CFU formation for CS-1, another $\alpha_4\beta_1$ peptide, FHRRIKA, and RGD was 0.24, 0.23, and 0.185 respectively, all higher than that of RGE and RAA by at least one standard deviation. The probability of colony formation on all peptide surfaces, except for YIGSR, was higher than that on plain comb copolymer substrates (0.064, +0.0135/-0.0115) by at least one standard deviation.

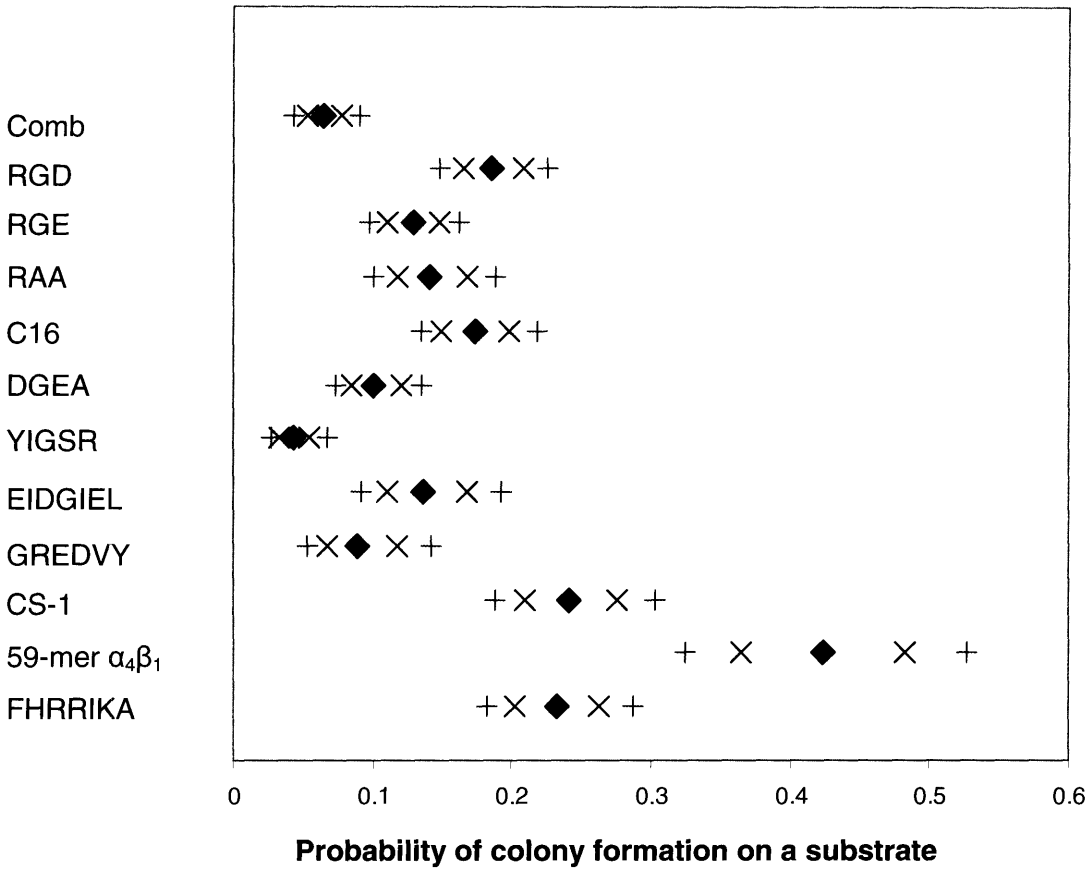

Figure 5.5 Whiskers diagram showing the probability of CFU formation on various substrates with × 1 standard deviation (66% confidence interval) and + 90% confidence interval. The probability reported here is the $P_{i,max}$ in the statistical model developed in Section 5.3.

When the CFU assay statistical model was used to analyze CFU-AP data from CFU assays, a similar trend was observed (Figure 5.6). The 59-mer peptide remained to be the surface with the highest probability of AP^+ colony formation (probability = 0.42 ± 0.06), followed by FHRRIKA and CS-1 (probability = 0.25 ± 0.03 and 0.23 +0.04/-0.03 respectively). Substrates with these two peptides, as well as RGD, showed a significantly higher probability of supporting CFU-AP than the negative control peptide RGE with 90% confidence interval. C16 peptide showed a probability of CFU-AP formation of (0.197, +0.028/-0.025), one standard deviation interval higher than RGE. All other peptides showed no significant probability of CFU-AP formation. As a negative control,

the probability of CFU-AP formation on RAA surfaces was slightly high, the reason for which is unknown.

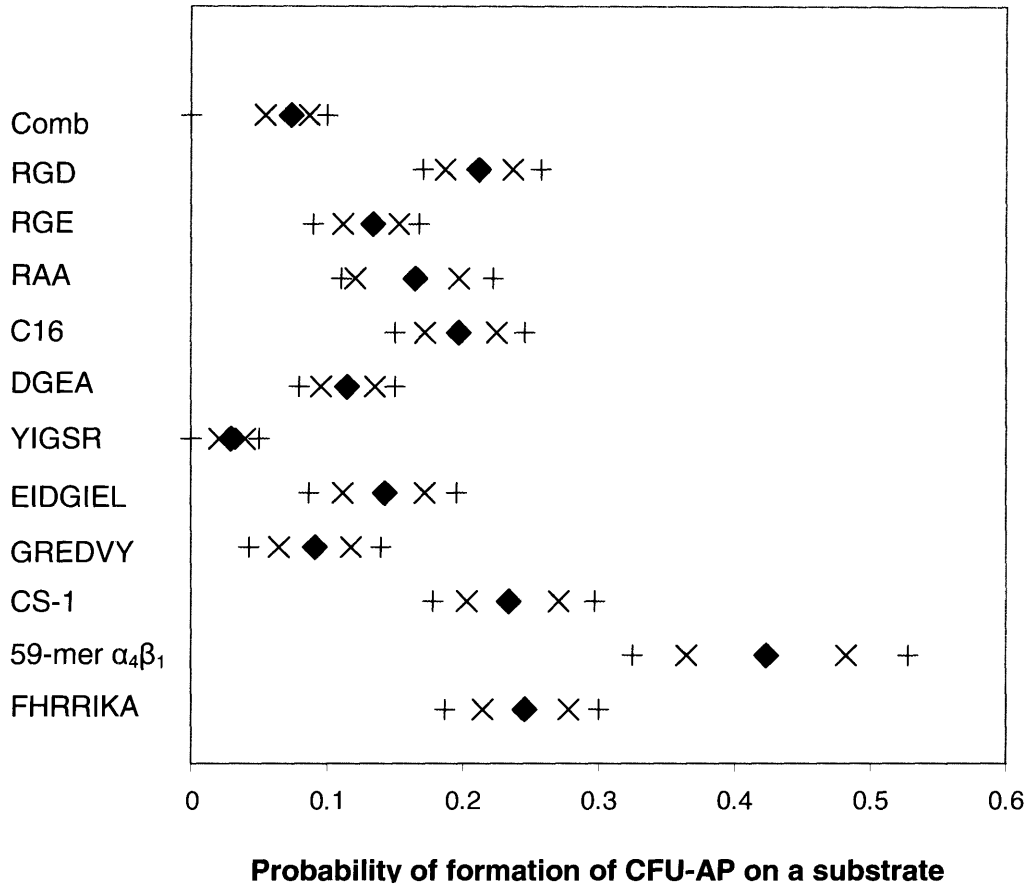

Figure 5.6 Whiskers diagram showing the probability of CFU-AP formation on various substrates with × 1 standard deviation (66% confidence level) and + 90% confidence interval. The probability reported is the $P_{i,max}$ in the statistical model developed in Section 5.3

5.4.2 Evaluation of glass as the gold standard control

As mentioned briefly in the previous section, a large patient variability in colony formation was observed in CFU assay, even on glass controls. To understand more of this phenomenon, marrow aspirates were seeded on glass coverslip control and Lab-tek chamber glass slides at a density of 2×10^6 nucleated cells in each of the two 4-cm^2 wells

on a glass Lab-tek chamber (i.e., at $5x10^5$ cells / cm^2 seeding density). The performance of these two surfaces in supporting colony formation is compared in Figure 5.7. Huge variations in the total number of CFUs (the sum of early and late adherent CFUs) and in CFU efficiency (the ratio of the number of early adherent to total CFU) were observed. The median total number of CFUs formed on glass and Lab-tek was only (36.0 ± 8.9) and (34.7 ± 5.5) respectively. The median CFU efficiency was also low, (44.4 ± 6.3)% and (47.8 ± 4.3)% for glass and Lab-tek respectively. The percentage of CFUs that were CFU-APs at this seeding density was (90.7 ± 5.3)%.

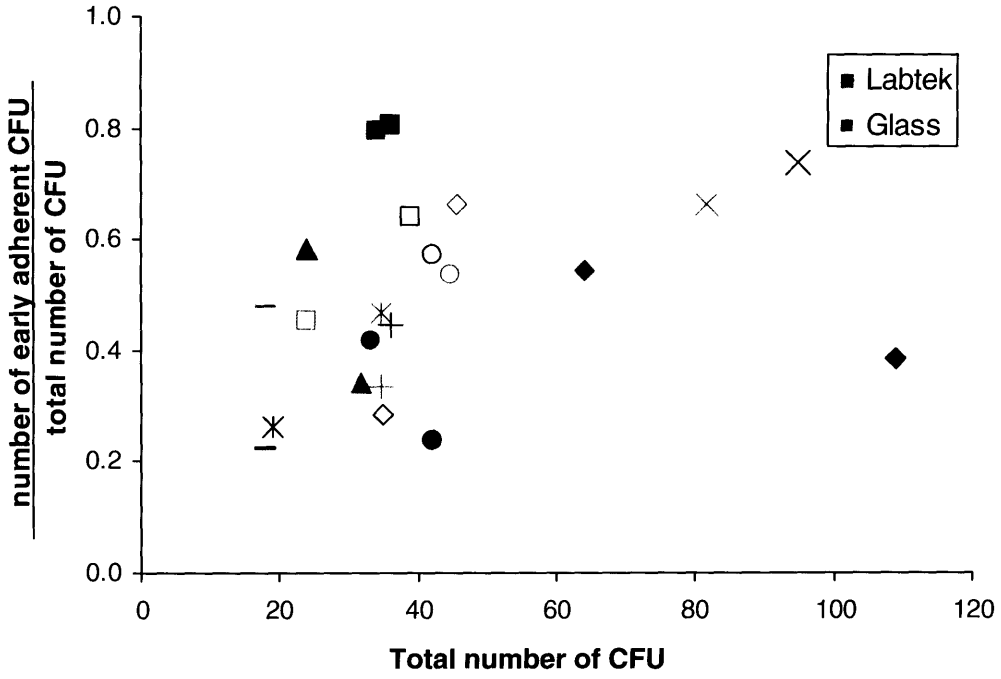

Figure 5.7 CFU formation on glass coverslips and Lab-tek glass chamber slides at $5x10^5$ cells / cm^2 seeding density. For each point, a total of 8 $x10^6$ cells were seeded. Large patient variability was observed. The number of CFUs on glass and Lab-tek was normalized to the area of the respective surface. The same symbols (different colors) in the graph denote substrates plated with marrow sample from the same individual.

At a quarter of the original marrow seeding density, $1.25x10^5$ cells / cm^2, significant patient variability in the performance of glass coverslip and Lab-tek in supporting CFU was also observed (Figure 5.8). However, to our surprise, even though only one quarter of the original seeding density was used, the median total number of CFUs on both glass and Lab-tek, (34.0 ± 7.2) and (34.3 ± 5.8) respectively, remained approximately the same as when four times more marrow cells were seeded. The median ratio of early adherent CFUs to the total number of CFUs on glass coverslips increased by about 30% to (56.6 ± 4.5)% as the seeding density decreased. The median ratio increased drastically from (47.8 ± 4.3)% to (79.1 ± 4.8)% for Lab-tek as the seeding density was decreased to one quarter of the original.

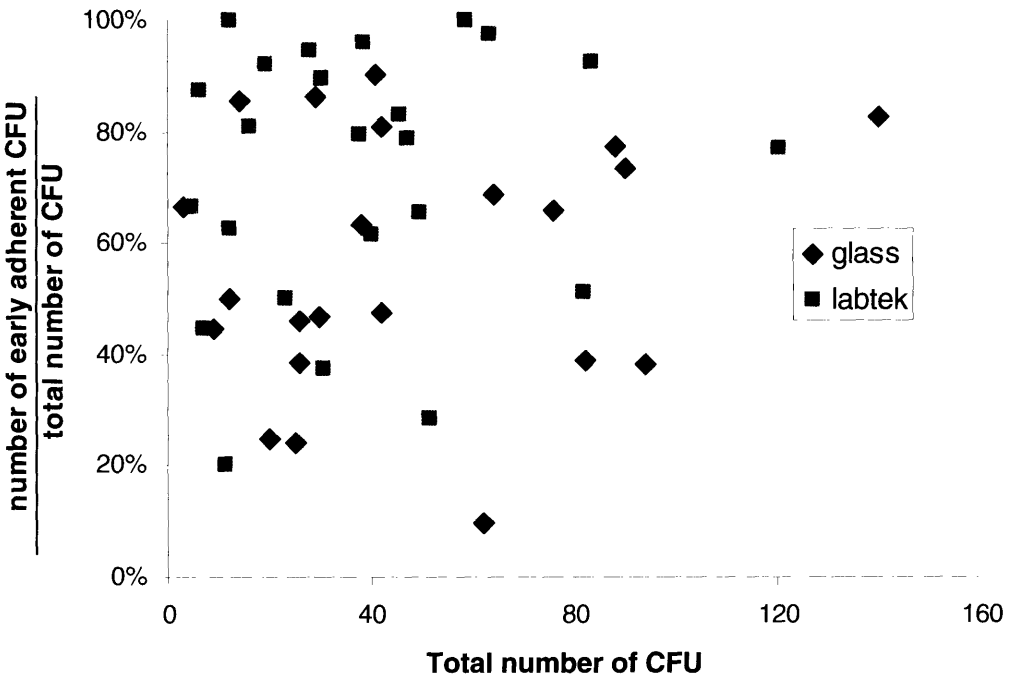

Figure 5.8 CFU formation by each marrow sample on glass coverslips and Lab-tek glass chamber slides at $1.25x10^5$ cells / cm^2 seeding density. Large patient variability was observed. However, the median total number of CFU on both glass and Lab-tek remained approximately the same as when the 4-times higher seeding density was used (i.e., 4X higher total cells seeded). In addition, the median ratio of the number of early adherent to total CFU increased significantly at this lower seeding density.

5.5 Discussion

5.5.1 CFU formation and statistical analysis

Patient variability is a major issue in analyzing data obtained from CFU assay in which fresh human marrow aspirates were used. The variation observed on peptide substrates was not unusual, as such variation was seen even on glass, the "gold standard control" of the CFU assay. Traditionally, glass has been established to be the gold standard control for its exceptional ability to promote colony formation from CTPs in marrow aspirates. However, at the seeding density (5×10^5 nucleated marrow cells / cm^2) that was used, a 6-fold variation in the total number of CFUs and a 4-fold variation in the ratio of early adherent CFUs to the total number of CFUs was observed over all the patients. The latter observation suggests a variation in the adhesion receptor profile of CTPs. Therefore, it was not surprising to see a large fluctuation of CFU efficiency for even the same type of peptide substrates but tested with different marrow samples. This inherent patient variability created difficulties in comparing CFU data collected with different patient marrow samples. The CFU assay statistical model was implemented to alleviate some of the contribution by this patient variability by considering each entry of colony formation measured on peptide substrate as the likelihood of a colony forming on the substrate given a colony formed on glass using the same patient sample. With the model, the overall probability of colony formation on a given substrate was computed as a parameter independent of whether colony formation is high or sparse on glass control for the marrow samples tested. Based on the analysis on CFU data using this statistical model, the 59-mer $\alpha_4\beta_1$ peptide has the highest ability in promoting CFU formation and CFU-AP formation, indicating that the peptide has exceptional ability in supporting the adhesion, proliferation and differentiation of CTPs into osteoblastic lineage. Interestingly, the other $\alpha_4\beta_1$ peptide CS-1 was among the second highest in supporting both CFU and CFU-AP formation. Thus, $\alpha_4\beta_1$ may be one of the integrins utilized by CTPs to mediate adhesion and proliferation. Previous reports in the literature showed that a portion of osteoblastic progenitor cells expressed $\alpha_4\beta_1$ and that $\alpha_4\beta_1$ was expressed

transiently by stromal-derived osteoprogenitors (Grzesik and Robey, 1994; Gronthos et al., 2001). Therefore, the $\alpha_4\beta_1$ substrates might be capturing a subpopulation of CTPs that were of osteoblastic lineage and was at a certain differentiating state in which $\alpha_4\beta_1$ was expressed. We could rule out the possibility that the colonies on the substrates were macrophages even though hematopoietic cells in marrow aspirates, such as most lymphocytes (except neutrophils) and granulocytes, are known to express $\alpha_4\beta_1$ (VLA-4) since almost all the CFUs captured on these $\alpha_4\beta_1$ substrates were AP^+. The third $\alpha_4\beta_1$ peptide, REDV, did not promote colony formation probably because the peptide itself might not be potent enough to support significant cell adhesion. As pointed out in Chapter 4, surfaces with REDV peptides only supported little adhesion of HUVEC.

The bone sialoprotein peptide FHRRIKA also promoted the formation of CFU-AP, with a similar efficiency to that of the CS-1 peptide. In Chapter 4, we showed that FHRRIKA supported the adhesion of MC3T3-E1 osteoblasts but not primary pMSCs, leading us to hypothesize that the more differentiated osteoblastic cells and MSCs expressed different adhesion receptors and hence the different adhesion behavior on FHRRIKA. If this hypothesis were correct, and bearing in mind that CTP is a term that collectively refers to all progenitors that have the potential to differentiate into connective tissue lineage, from the pluripotent mesenchymal stem cells to preosteoblasts, then the CTP colonies captured on FHRRIKA surfaces could be derived from CTPs that were more differentiated than the truly mesenchymal stem cells. This could be possible as the CFUs formed on FHRRIKA surfaces were all AP^+, indicative that their differentiation states were somewhere along the osteoblastic lineage. However, more experiments were needed to reveal how differentiated these CFUs were in relation to CFUs on other peptide surfaces or glass.

The likelihood of colony formation and AP^+ colony formation on RGD surfaces were higher than that on RGE as expected, with 90% confidence interval. The laminin C16 peptide, which has been shown to bind to $\alpha_5\beta_1$, $\alpha_v\beta_3$, but at a lower affinity, and possibly other adhesion receptors, showed a probability of CFU formation similar to, but slightly

lower than that of RGD. The increase in the relative likelihood of CFU-AP formation on RGD and even more on C16 to that of RGE was due to their higher ratio of CFU-AP to CFU than that of glass and RGE. Other peptides, YIGSR, EIDGIEL and DGEA, did not support significant CFU formation, as indicated by the low probability of CFU or CFU-AP formation. This could be a result of the low affinity of the peptides as validation results with various cell lines or primary hepatocytes in the previous chapter on these peptide substrates showed only a small degree of adhesion.

The number of subcolony clusters and single adherent cells found on all surfaces in the CFU assay was surprisingly low and the number of single cells adhering was often less than 10 even when 2 million nucleated marrow aspirate cells were seeded. This was unexpected as bone marrow aspirates contain at least some endothelial cells and fibroblasts which express receptors that would bind to, for instance, RGD surfaces. The amount of single cell adhesion was also not substrate-dependent but more dependent on which patient sample was used. These observations led us to hypothesize that marrow cells were shrouded by extracellular matrix proteins as they were aspirated and hence, preventing their receptors to bind to the peptide substrates, thus leading to the small amount of adhesion observed. This issue of matrix protein shrouding is explored and discussed in detail in the next chapter.

5.5.2 Patient variability and evaluation of glass as the gold standard control of CFU assay

As mentioned in previous sections, large patient-to-patient variations were observed in CTP prevalence in marrow and CTP adhesion state even on glass standard control. Previous reports by Muschler et al. showed that the prevalence of potentially osteoblastic CTP in bone marrow aspirate was about 1 in 23,000 nucleated cells (Majors et al., 1997). So when 5 x 10^5 nucleated marrow cells per cm^2 was seeded on a total of 16 cm^2 of glass substrate in our experiments, there should ideally be ~348 CFU-APs. However, from our studies, at this seeding density, the total number of CFU on glass coverslips ranged

from 20 to 80 with a median of only 36.0 ± 8.9. Surprisingly, the median number of CFU stayed approximately the same when the seeding density was reduced to one-quarter of the previous seeding density. Steric hindrance and nutrient consumption might limit the number of CTPs that could adhere and subsequently form colonies on the substrate. Assuming the average size of marrow cells to be 10 μm in diameter, 5 x 10^5 closely packed cells would occupy about 0.5 cm^2. Even though not all the nucleated cells were adherent cells, steric hindrance could still contribute to the saturated number of CTPs when a higher seeding density was used. At the lower seeding density, 1.25 x 10^5 nucleated marrow cells per cm^2, the efficiency of early adherent CFU formation to the total number of CFUs on glass coverslips was 30% higher than when the 4-fold seeding density was used. The increase in efficiency was more than 2 fold for Lab-tek. The total number of CFU captured in the early and late adherent fraction at this lower seeding density was about 40% of the ideal number of CFU-APs based on the prevalence reported by Muschler et al.. Even though the number of CFUs reported in our studies included both AP+ and AP- CFUs, the drastic increase in the efficiency of CTP capture was still apparent when the seeding density was decreased from 5 x 10^5 per cm^2 to at 1.25 x 10^5 per cm^2. The lower total number of CFUs and CFU efficiency observed on glass in our experiments could be partially explained by the use of marrow samples from a pool of older patients in comparison to the studies by Muschler and co-workers. The subjects in our pool were dominated by older patients with arthroplasty and an age-related decline in the number of CTPs in marrow has been demonstrated in the literature (Bergman et al., 1996; Muschler et al., 2001). According to the same report by Muschler et al., the number of colonies was the maximum number of CFU-AP counted between day 6 and 9 so more colonies might have been formed. In addition to age-dependence, the variation observed in CTP prevalence and adhesion characteristics among patients may be due to factors such as gender, tobacco use and menopausal status (Muschler et al., 2001).

These CFU assay evaluation studies showed that glass coverslips did not perform up to expectation as a "gold standard control" in CFU assay. When glass coverslips were compared side-by-side with Lab-tek chamber slides, the median total number of CFUs

per unit area and the median ratio of early adherent CFUs to the total number of CFUs were essentially the same for the two surfaces at the higher seeding density (5 x 10^5 per cm^2). However, at the lower seeding density, the significantly higher ratio of early adherent to total number of CFUs on Lab-tek but similar total number of CFUs for the two surfaces showed that Lab-tek was much more capable than glass coverslips in capturing CTP colony formation. This drastic difference was likely due to the difference in the type of glass that glass coverslips and Lab-tek slides were made of. The glass coverslips used in this study were made of borosilicate glass, composed mainly of silica (70-80%), boric oxide (7-13%) with a small amount of sodium, potassium and aluminum oxide. On the other hand, Lab-tek chamber slides, according to the manufacturer, were made of soda-lime glass that composed of 71-75% SiO_2, 12-16% soda, and 10-15% lime (calcium oxide from limestone or calcium carbonate). The last constituent calcium carbonate itself had been shown to be osteoconductive, as under hydrothermal exchange reaction, calcium carbonate, $CaCO_3$ can be changed to hydroxyapatite, $Ca_{10}(PO_4)_6(OH)_2$, the main mineral of bone (Roy and Linnehan, 1974). In fact, several studies have shown that bone marrow seeded on coralline calcium carbonate consistently showed new bone formation (Okumura et al., 1991; Vuola et al., 1996). Thus, the presence of calcium carbonate in Lab-tek chamber glass slides might have contributed to its enhanced ability in capturing CTP colony formation through unknown mechanisms. From these evaluation and optimization studies of glass as the positive control in CFU assays, we have identified 1.25 x 10^5 nucleated marrow cells per cm^2 to be a more optimal seeding density and Lab-tek glass slide to be a better positive standard control for the CFU assay. These findings of assay optimization were applied to the CFU studies in Chapter 6.

5.6 References

Bergman, R.J., Gazit, D., Kahn, A.J., Gruber, H., McDougall, S. and Hahn, T.J. (1996). "Age-related changes in osteogenic stem cells in mice." Journal of Bone and Mineral Research **11**: 568-577.

Bianco, P., Riminucci, M., Bonucci, E., Termine, J.D. and Robey, P.G. (1993). "Bone sialoprotein (BSP) secretion and osteoblast differentiation: relationship to bromodeoxyuridine incorporation, alkaline phosphatase, and matrix deposition." Journal of Histochemistry and Cytochemistry **41**: 183-191.

Gronthos, S., Simmons, P.J., Graves, S.E. and Robey, P.G. (2001). "Integrin-mediated Interactions Between Human Bone Marrow Stromal Precursor Cells and the Extracellular Matrix." Bone **26**(2): 174-181.

Grzesik, W.J. and Robey, P.G. (1994). "Bone matrix RGD glycoproteins: Immunolocalization and interaction with human primary osteoblastic bone cells in vitro." Journal of Bone and Mineral Research **9**: 487-496.

Lee, K., Deeds, J.D., Chiba, S., Un-no, M., Bond, A.T. and Segre, G.V. (1993). "In situ localization of PTH/PTHrP receptor mRNA in the bone of fetal and young rats." Bone **14**: 341-345.

Majors, A.K., Boehm, C., Nitto, H., Midura, R.J. and Muschler, G.F. (1997). "Characterization of human bone marrow stromal cells with respect to osteoblastic differentiation." Journal of Orthopaedic Research **15**: 546-557.

Muschler, G.F., Nittoa, H., Boehm, C.A. and Easley, K.A. (2001). "Age- and gender-related changes in the cellularity of human bone marrow and the prevalence of osteoblastic progenitors." Journal of Orthopaedic Research **19**(1): 117-125.

Okumura, M., Ohgushi, H. and Tamai, S. (1991). "Bonding osteogenesis in coralline hydroxyapatite combined with bone marrow cells." Biomaterials **12**(4): 411-416.

Roy, D.M. and Linnehan, S.K. (1974). "Hydroxyapatite formed from coral skeletal carbonate by hydrothermal exchange." Nature **247**: 220-222.

Turksen, K. and Aubin, J.E. (1991). "Positive and negative immunoselection for enrichment of two classes of osteoprogenitor cells." Journal of Cell Biology **114**: 373-384.

Vuola, J., Goeransson, H., Boehling, T. and Asko-Seljavaara, S. (1996). "Bone marrow induced osteogenesis in hydroxyapatite and calcium carbonate implants." Biomaterials **17**(18): 1761-1766.

Chapter 6

Design of Bone Marrow Aspirate Treatments to Enhance the Efficacy of Colony Formation

6.1 Introduction

In Chapter 5, peptides that possess the ability to promote osteoblastic colony formation of CTPs from bone marrow were identified using the CFU assay. However, the amount of adherent cells in general was much lower than expected, given the millions of cells per cm^2 seeding density. The lower-than-expected number of colonies and single adherent cells on even RGD surfaces and glass control was a surprise to us since bone marrow aspirates contained cells such as fibroblasts and endothelial cells that express $\alpha_5\beta_1$ and/or $\alpha_v\beta_3$ that recognize the RGD sequence. In fact, in Chapter 4, we have extensively demonstrated that peptide substrates like GRGDSPY supported the adhesion of several cell lines very well, such as wtNR6 fibroblasts and HOS osteosarcoma cells, as well as primary pig MSCs. Therefore, the bioactivity of the substrates was not in question. We thus hypothesized that the small amount of cell adhesion was due to the shrouding of bone marrow aspirate cells by the extracellular matrix proteins they were associated with in their natural microenvironment rich in ECM proteins such as fibronectin, laminin and collagen IV. We hypothesized that when marrow cells were aspirated, the ECM proteins associated with them remained attached, preventing them from recognizing and attaching to the peptides on the test substrates.

Therefore, in this chapter, our first goal was to test the hypothesis of protein shrouding. Fluorescence-activated cell sorting (FACS) was used to assess the profile of ECM proteins association with marrow aspirate cells. The level of ECM protein association of marrow aspirates was compared with cells from cell lines using immunoblotting. As mentioned in previous chapters, since there were very few reports on integrin expression

profile of human marrow connective tissue lineage cells, illuminating the integrin profile of different populations of marrow aspirates is one of the goals here. A single marker that delineates CTPs had not been identified to date, because of the lack of consensus of CTP or MSC phenotype (Gronthos et al., 1994; Pittenger et al., 1999; Minguell et al., 2001; Tocci and Forte, 2003), the broad spectrum of progenitor cells defined as CTPs (Aubin and Heersche, 2000), and the highly variable profile of cell surface antigens (Jiang et al., 2002; Vogel et al., 2003). The combination of $CD45^-$ and $CD105^+$ was chosen due to the general agreement that MSCs lack typical hematopoietic antigen such as CD45. CD45 is a transmembrane protein phosphatase marker for all cells of hematopoietic origin except erythoid cells, platelets and their precursor cells (Thomas, 1989; Trowbridge and Thomas, 1994). Therefore, $CD45^-$ cells were gated to exclude cells of hematopoietic lineage in our analysis. On the other hand, CD105, also known as endoglin, has been quite extensively used as a mesenchymal stem cell marker (Barry et al., 1999; Majumdar et al., 2000). When CD105 is used in combination with other markers, and in particular CD45, it has been demonstrated by several reports to obtain an enriched population of mesenchymal stem cells (Lodie et al., 2002; Meinel et al., 2004), even though CD105 is not specific only to MSCs but also expressed by angiogenic endothelial cells (Duff et al., 2003; Fujiyama et al., 2003). Interestingly, CD105 itself, a receptor for the transforming growth factor-β (TGF-β), had been shown to play a role in mediating cell adhesion, spreading, growth, and proliferation in a RGD-dependent manner (Guo et al., 2004). Even though there were some successes in enriching marrow-derived osteoprogenitors using STRO-1, the surface antigen itself has not been characterized and understood to date. In light of all these, CD45 and CD105 were used in our study to identify an enriched population of CTPs.

Our second objective in this chapter was to design marrow aspirate cell treatments to reduce the amount of matrix molecule association, and thus enhance interactions between marrow aspirates and substrates. The treatments had to be mild so as not to disrupt the adhesion potential of the cells. Simple treatment protocols are also favorable considering the procedure will eventually be done intraoperatively when peptide-comb is

incorporated into scaffolds to be used as bone implants. At that point, marrow aspiration, cell-preloading protein reduction treatments, and marrow cell loading will all be performed in the operation room. Based on these design criteria, three protein reduction treatments were designed. The CFU assay, incorporating the new optimized cell seeding density and gold standard control identified in Chapter 5, was used to evaluate the effectiveness of various treatments on marrow aspirate cells. GRGDSPY substrates were used in this model study. The results of these experiments revealed a partitioning of patient marrow samples into two groups with distinctive CTP behavior and cell integrin expression profile. One of the cell-preloading protein reduction treatments was identified to be effective in one of the two patient groups.

6.2 Materials and methods

6.2.1 Human mesenchymal stem cell (hMSC) line culture and preparation of human marrow aspirates for FACS and immunoblotting

Poietics™ human mesenchymal stem cells, a cell line of normal adult hMSCs, was a gift from the Wells Lab (University of Pittsburgh). The cells were used to validate antibodies used in FACS and for comparison with human marrow aspirates in Western blotting. hMSCs were routinely cultured and maintained in DMEM with 10% FBS, 1mM non-essential amino acids, 2mM L-glutamine, 1mM sodium pyruvate and 100 i.u./mL penicillin and 200 μg/mL streptomycin. Cells were cultured at 37°C with 5% CO_2, fed every 3-4 days and split when they were near confluency after 5 -7 days of seeding. Cells up to passage 10 were used. To prepare cells for FACS or Western blotting, hMSCs were detached from culture plates by trypsin (Sigma) and re-suspended in culture media before centrifugation. The cell pellet collected was then ready for FACS or Western blotting.

Frozen bone marrow aspirates were used for FACS and Western blotting. Bone marrow was aspirated according to the procedure described in Chapter 2 and frozen down in media containing 10% DMSO on the same day of aspiration. Right before FACS or Western blot preparation, cells were quick-thawed and re-suspended in culture media containing 2 units/mL of heparin. For FACS, Buffy coat was isolated by centrifuging marrow cells at 1600 rpm for 10 minutes. After removing the media on the top, the buffy coat was slowly and carefully aspirated into a Pasteur pipette, leaving the red cells behind at the bottom of the tube. The buffy coat was then re-suspended in DMEM containing 0.3% BSA and 2 units/mL of heparin and cell clumps were broken up by passing the cell suspension through a 21G needle multiple times and twice with cell sieves (Falcon). The cells were then processed further for FACS according to the procedures described in the next section.

6.2.2 Fluorescent-activated cell sorting (FACS) analysis of bone marrow aspirates

Buffy coat cells were re-suspended in FACS buffer (Dulbecco's phosphate buffer saline with Ca^{2+} and Mg^{2+} and 0.2% BSA) for staining with antibodies. In brief, cells were stained with the appropriate antibodies for 15 minutes on ice and re-suspended in excess FACS buffer before the cells were pelleted by centrifugation. After FACS buffer was removed, cells were subjected to the next round of staining either with a secondary antibody or the next primary antibody. The staining process was repeated until cells were stained with all the antibodies planned to be tested. CD45 (Cat. # 555481, BD Bioscience, San Jose, CA) and CD105 (Cat. # CBL418, Chemicon, Temecula, CA) antigens were used to define an enriched population of CTPs. Polyclonal antibodies were used to recognize ECM molecules as they were made against whole proteins instead of specific epitopes that may not be available for binding. Anti- ECM protein polyclonal antibodies and anti- integrin monoclonal antibodies used in this study, as well as fluorochrome-conjugated secondary antibodies used for detection were listed in Table 6.1. The activity of all the antibodies towards human ECM proteins and integrins were validated with hMSC cell line. 6-color FACS analyses were performed on marrow cells using a BD FACSCanto flow cytometer. Compensation was done using anti-mouse Ig, κ/negative control compensation particles set (BD Bioscience) and the appropriate antibodies used in this study. Negative controls (cells incubated only with fluorochrome-conjugated secondary antibodies, i.e., with the omission of primary antibodies) were used to set up fluorescence gates. 100,000 events were collected for each sample. Cell clusters and debris were excluded from the analyses by gating on mostly single cells in the forward scatter width (FSC-W) versus height (FSC-H) and side scatter width (SSC-W) versus height (SSC-H) plots. Cells were gated on $CD45^-CD105^+$ and NOT($CD45^-$ $CD105^+$). Cells in both populations were analysed for their expression of ECM proteins and integrins. Data analysis was carried out using the BD FACS Diva software.

Antibodies against ECM molecules		**Binding epitope information, if known**
FN	Rabbit anti- human fibronectin (Chemicon AB1945)	Polyclonal antibodies – target the entire protein.
LN	Rabbit anti- laminin (Chemicon AB19012)	
VN	Rabbit anti- human vitronectin (Chemicon AB19014)	
Col I	Goat anti- collagen I biotin (Chemicon AB758B)	
Antibodies against integrin subunits		**Binding epitope information, if known**
α_2	R-phycoerythrin (PE) anti-human CD49b mAb clone 12F1-H6 (BD Cat. # 555669)	Binds to α_2I, the principle binding domain to collagen but no information on whether they bind to the same residues within the 200 a.a. domain. Blocking effect has not been tested (Cruz et al., 2005)
α_3	Fluorescein isothiocyanate (FITC) mouse anti-human CD49c mAb clone 17C6 (MCA 1948F, Serotec, Raleigh, NC)	Binding epitope and whether it blocks α_3 binding to its ligand is unknown.
α_4	PE anti-human CD49d mAb clone 9F10 (BD 555503)	Binding epitope and blocking effect unknown.
α_5	CD49e clone IIA1 Biotin-conjugated mouse anti-human mAb (BD 555616)	Inhibits $\alpha_5\beta_1$ binding to its ligands (Nhieu and Isberg, 1991; VanNhieu and Isberg, 1993).
α_6	FITC anti-human CD49f mAb clone GoH3 (BD 555735)	May block binding of to laminin P1 and E8 fragments (Sonnenberg et al., 1986; Aumailley et al., 1990).
$\alpha_v\beta_3$	PE anti-human CD51/61 mAb clone 23C6 (BD 550037)	Inhibitory effects on binding to vitronectin (Chuntharapai et al., 1993).
β_1	biotin-conjugated anti-human CD29 mAb clone TDM29 (Chemicon CBL481B)	Binding epitope has not been mapped. Blocking effect unknown.
Secondary fluorochrome-conjugated antibodies		
streptavidin-PE-Cy7 conjugate (BD 557598)		
streptavidin-Alexa 700 conjugate (Molecular Probes Cat. # S21383)		
Alexa 700 goat anti-rabbit IgG (H+L) (Molecular Probes A21038)		
allophycocyanin (APC)-conjugated rat anti-mouse IgM monoclonal antibody (BD 550676)		
FITC Goat anti-rabbit Ig (BD 554020)		
Streptavidin PE-Cy5.5 conjugate (Cat. # SA 1018, Caltag Lab, Burlingame, CA)		
streptavidin FITC conjugate (BD 554060)		
streptavidin PE conjugate (BD 554061)		

Table 6.1 Primary antibodies against ECM molecules and integrins and secondary fluorochrome-conjugated antibodies used in FACS. Binding epitope information was obtained from the literature or from the supplier.

6.2.3 Western blot analysis of protein association

Whole cell lysates of hMSCs or bone marrow aspirates were prepared by lysing a known number of cells prepared as described above in 150mM sodium chloride with 50 mM β-glycerophosphate (pH 7.3), 10 mM sodium pyrophosphate, 30mM NaF, 50mM Tris (pH 7.5), 1% Triton X-100, 2mM EGTA, 100 μM sodium orthovanadate, 1 mM of each of DTT, benzamidine and PMSF, 10 μg/mL aprotinin and leupeptin and 1 μg/mL of pepstatin. Protein concentration of each sample was determined by the bicinchoninic acid assay (MicroBCA™ protein assay kit, Pierce, Rockfield, IL). 5% polyacrylamide gels were polymerized and prepared in house using BIO-RAD's Mini-PROTEAN 3 Cell Assembly kit with Protogel diluted with Protogel resolving buffer (both from National Diagnostics, Atlanta, GA) with Temed (Invitrogen, Carlsbad, CA) and ammonium persulphate (Pharmacia Biotech, Uppsala, Sweden) as the initiator. The stacking gel was prepared with Protogel diluted with Protogel stacking buffer (National Diagnostics) and polymerized with ammonium persulphate. Since the goal was to compare the level of ECM protein associated with different cells or cells subjected to different treatment (as described in the next section), protein lysed from the same number of cells for each sample was loaded on the gel for assay. Prior to loading, cell lysates were boiled in sample buffer to ensure antibody-binding regions were exposed. Approximately 25-40 μg of protein lysate, as well as molecular marker solution (Precision Plus Protein Standards, BIO-RAD), was loaded onto the gel and separated by SDS-PAGE. Proteins on the gel were then transferred to sequi-blot PVDF membranes in Ready Gel blotting sandwiches (BIO-RAD). After blocking with blotto (5% non-fat dry milk) for one hour at room temperature, blots were probed overnight at 4°C in primary rabbit anti-human fibronectin or laminin polyclonal antibodies (Chemicon Cat. # AB1945, AB 19012) at 1:1000 and 1:5000 dilution respectively. Both antibodies were validated for their ability to bind to human fibronectin and laminin. Blots were washed 3 times in TBS-T (20 mM Tris-HCl pH 7.5, 137 mM NaCl and 0.1% Tween 20 (BIO-RAD)) for 5 minutes and then incubated with the secondary antibody ECL™ anti-rabbit IgG, horseradish peroxidase linked whole antibody (1:10000 in blotto, Amersham Biosciences,

Buckinghamshire, England), and finally washed 3 times in TBS-T for 5 minutes. Blots were developed with either Western Lightning Chemiluminescence Reagent Plus (Perkin Elmer, Boston, MA) or ECL Advance™ WB Detection Kit (Amersham Biosciences) and imaged on a Kodak Imagestation 1000 and analysed with the Kodak 1D software.

6.2.4 Cell-preloading protein reduction treatments and CFU assay

Marrow aspirates were prepared as outlined in Section 6.2.1. After preparation, the marrow aspirate cell pellet was divided into five groups for treatments to reduce the amount of cell-associated matrix molecules. Cells in Group A received no treatment. Cells in Group A' were incubated in DMEM containing 0.3% BSA. Group B and C were incubated in PBS with and without divalent ions respectively. 200 μM GRGDSP solution (in PBS with divalent ions) was added to cells in Group D. Each group was incubated in their respective solution for 30 minutes. Afterwards, cells were spun down and the supernatant removed. The pellets were washed again by re-suspending in culture media and then centrifuged. After the second wash, cells were re-suspended and counted using a coulter counter or hemocytometer.

Marrow aspirate samples from four individuals were used to examine the effect of these cell-preloading treatments on protein reduction and colony formation. Freshly aspirated cells were treated with Treatments A, B, C and D as described above. After counting, cells from each group were plated on Lab-tek surfaces, GRGDSPY and plain comb copolymer substrates at 1.25 x 10^5 cells / cm^2 and assayed the same way as the regular CFU assay described in Chapter 5, except at this lower cell seeding density and with Lab-tek as the positive control (Figure 6.1). Frozen marrow samples from the same four individuals were treated with Treatments A, A', B, C and D as described above and the level of fibronectin and laminin associated with the same number of cells from each group was analyzed with Western blotting. Frozen marrow aspirates from Patient 1 and 2 were also analyzed with FACS to compare their ECM protein and integrin expression profile. FACS was performed on fresh aspirate samples from Patient 3 and 4.

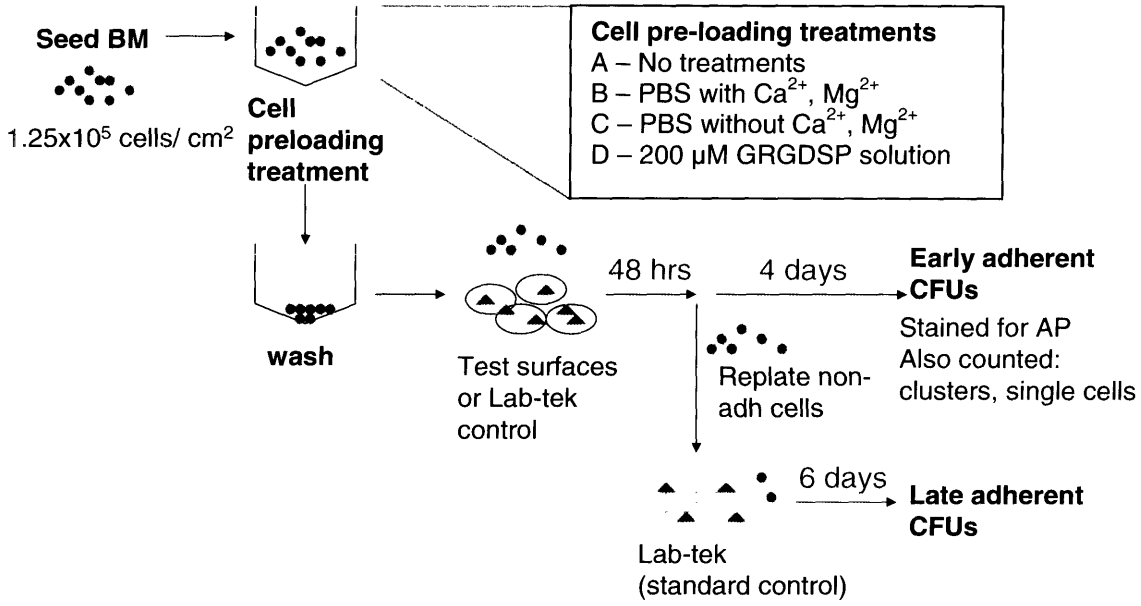

Figure 6.1 Schematics showing the flow of marrow pre-loading treatment and subsequent CFU assay. Marrow aspirates were subjected to various pre-loading treatment in attempt to identify one that could effectively reduce the amount of matrix proteins associated with aspirate cells.

6.3 Results

6.3.1 ECM protein and integrin profile of marrow aspirate cells by FACS

SSC-H vs. FSC-H plots from FACS showed variations in cells in marrow aspirate from different patients. In some patient samples, the lymphocyte and granulocyte populations were more distinct (Figure 6.2a) whereas for some aspirate samples, no clearly-defined population was found (Figure 6.2b). Both of these profiles were normal but their difference showed a large variation in cell sizes and granularities among patient samples as reflected by the different shapes of SSC-H vs. FSC-H plots.

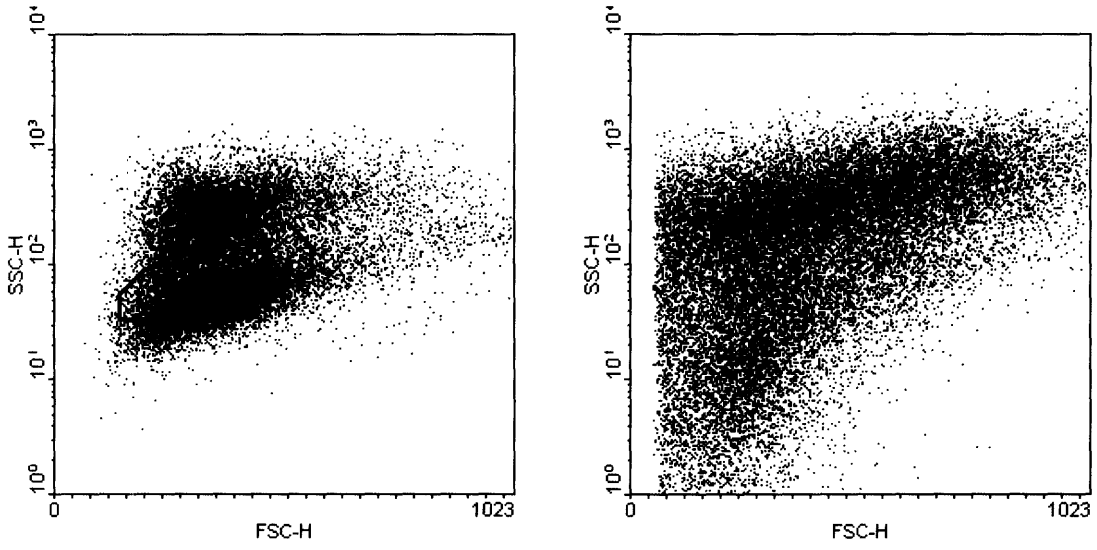

Figure 6.2 Two typical SSC-H vs. SSC-H plots of marrow aspirate cells demonstrated patient variability. **Left (a)** shows distinctive populations of lymphocyte (circle in red) and granulocyte (dotted circle in green), whereas in **(b), right**, there was only one large cell population that was not well defined and with a lot of debris.

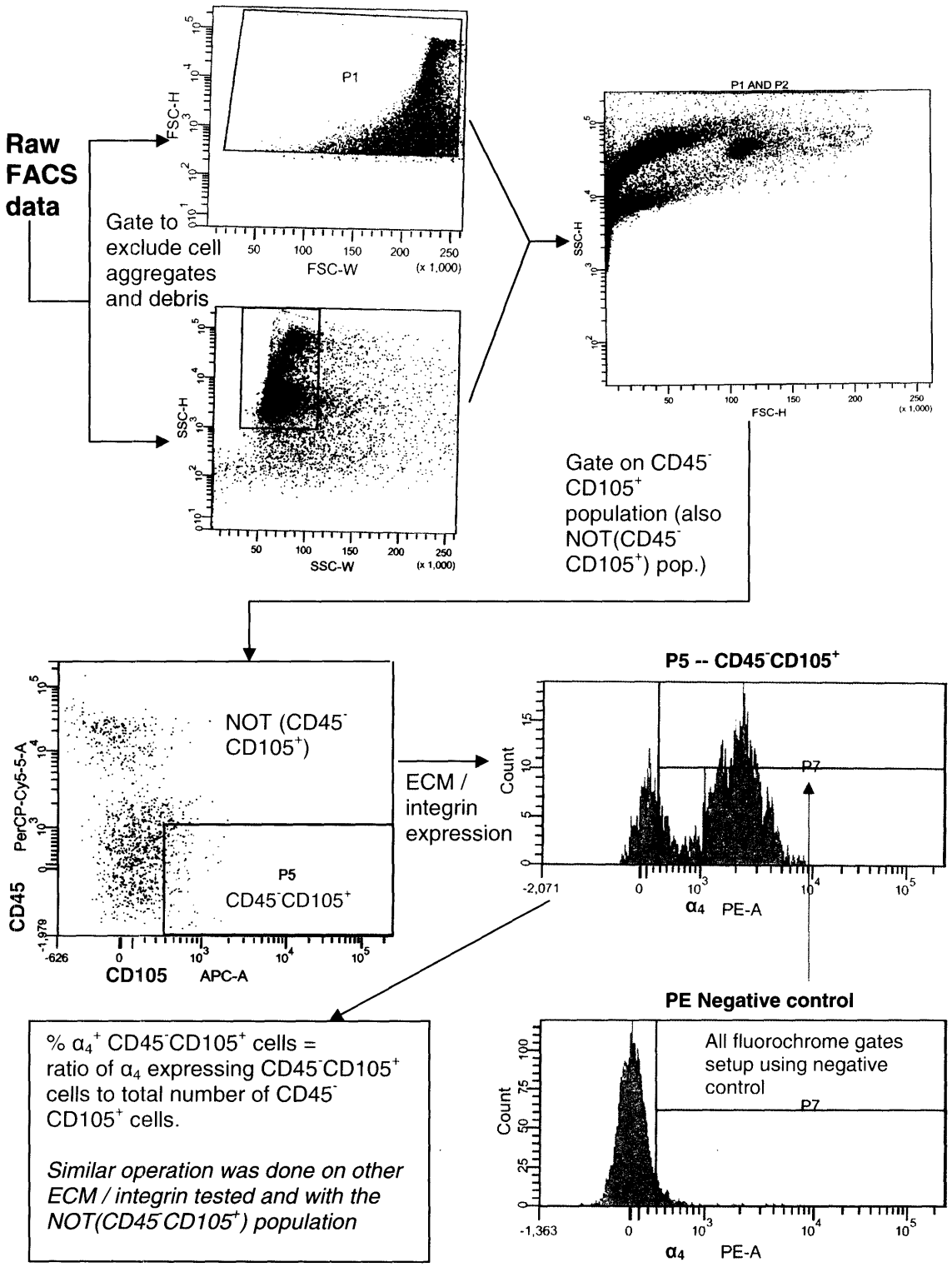

Figure 6.3 An example of how FACS analysis was performed on marrow aspirate cells. The analysis of α_4 expression of $CD45^-CD105^+$ of one patient sample is shown here. Cells incubated with only the secondary antibody (i.e., with the omission of primary antibody) was used as negative controls to set up gates.

CD45$^-$ CD105$^+$ cells only made up of (0.40 ± 0.11) % of the entire marrow aspirate population. This small population was believed to represent an enriched population of CTPs (Lodie et al., 2002; Meinel et al., 2004) and thus matrix molecule and integrin expression of both the CTP-enriched CD45$^-$ CD105$^+$ and non-CD45$^-$ CD105$^+$ populations were compared. Figure 6.4 shows the ECM molecule association profile of marrow aspirate cells. ECM protein association was generally the same for the CD45$^-$ CD105$^+$ and non-CD45$^-$ CD105$^+$ population except for fibronectin, the amount of association of which by CD45$^-$ CD105$^+$ cells ((49.1 ± 11.8) %) were likely to be higher than non- CD45$^-$ CD105$^+$ cells ((28.9 ± 8.25) %) ($p<0.1$).

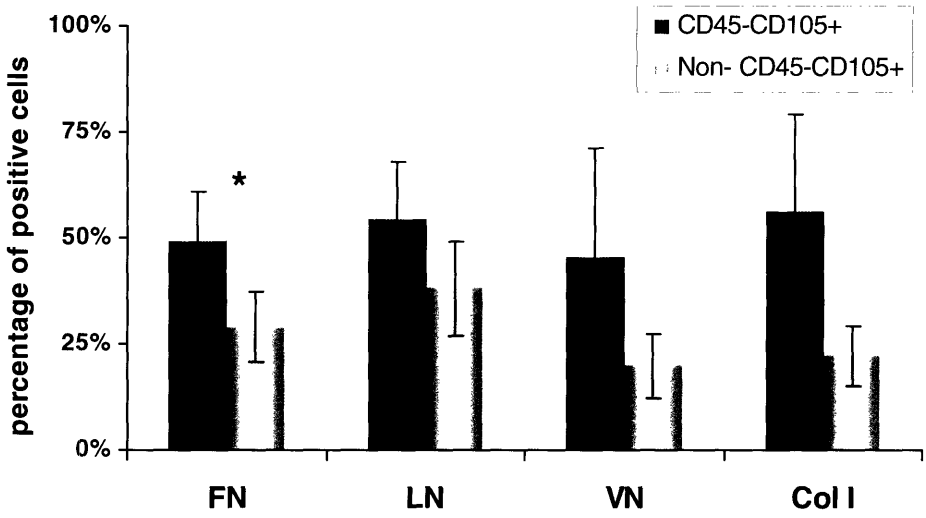

Figure 6.4 ECM association profile of marrow aspirate cells from FACS. Only fibronectin was expressed by a slightly statistically higher amount in the CD45$^-$CD105$^+$ population compared to non- CD45$^-$CD105$^+$ cells (* $p<0.1$, student t-test). The difference in association between the two populations was insignificant for other ECM proteins tested. Data are mean ± SE. n = 6 for FN and LN. n = 3 for VN and Col I.

Like ECM protein association, expression of most integrin subunits was about the same for both the CD45$^-$ CD105$^+$ and non- CD45$^-$ CD105$^+$ populations, except for the α_4 subunit. α_4 was the only integrin subunit that was much highly expressed by CD45$^-$ CD105$^+$ cells than non- CD45$^-$ CD105$^+$ (Figure 6.5). (61.2 ± 8.25) % of CD45$^-$ CD105$^+$ cells expressed α_4 while only (28.9 ± 8.25) % of non- CD45$^-$ CD105$^+$ was α_4^+ ($p<0.005$).

High expression of β_1 (> 60%) was detected in both the CD45$^-$ CD105$^+$ and non-CD45$^-$ CD105$^+$ populations. Although 20-30% of cells express α_5 and $\alpha_v\beta_3$, large variations in expression of both integrins were observed (Figure 6.5). Expression of α_3 and α_6 in both cell populations was negligible.

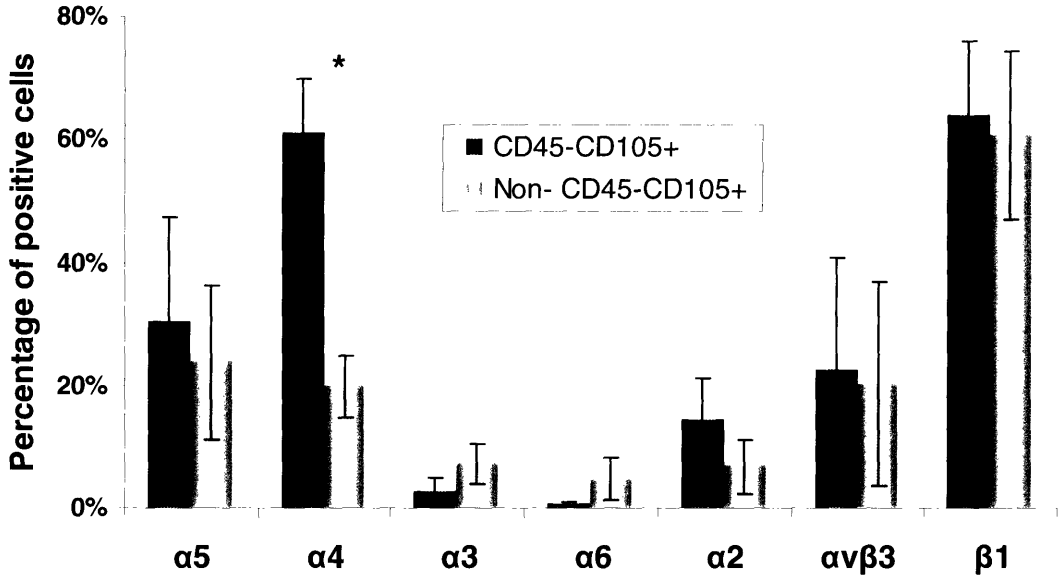

Figure 6.5 Integrin expression profile of marrow aspirate cells from FACS. Data are mean ± SE. α_4 expression was higher in the CD45$^-$CD105$^+$ population (*$p<0.005$). The difference in expression between CD45$^-$CD105$^+$ and non-CD45$^-$ CD105$^+$ populations was insignificant for other integrins. n = 6 for α_4, α_5, $\alpha_v\beta_3$ and β_1. n = 3 for α_2, α_3, and α_6.

6.3.2 Western blotting showed fibronectin and laminin association with marrow aspirate cells

The level of fibronectin and laminin associated with marrow aspirate cells was compared to that of hMSC cell line. When protein lysates from the same number of cells from both types were compared by Western blotting, we saw a much higher level of fibronectin and laminin with marrow aspirate cells. Treatment of marrow aspirate cells with 0.6X trypsin solution (0.3 g/L porcine trypsin and 0.012 % EDTA · 4Na in PBS)

significantly reduced the amount of fibronectin and laminin to a level even lower than that of hMSC cell line (Figure 6.6a and b).

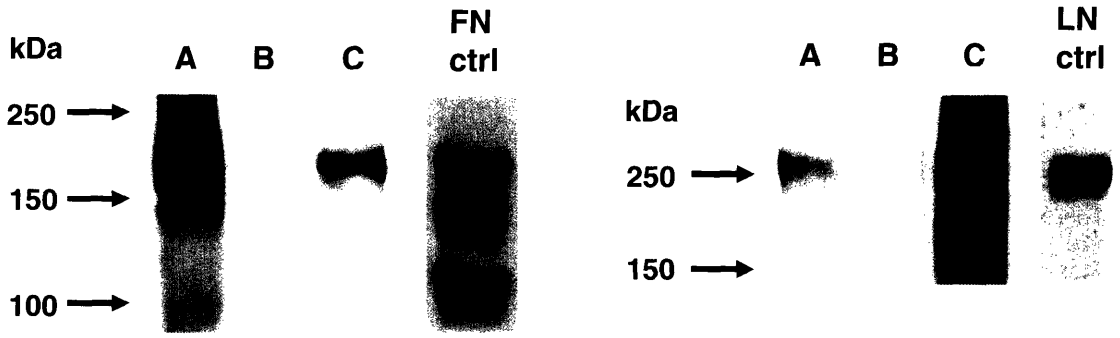

Figure 6.6 Western blot results showed a higher level of matrix molecules associated with marrow aspirate cells than hMSC cells. **Left (a)** fibronectin probed. **Right (b)** laminin probed. Protein lysates from the same amount of cells were loaded and analyzed. Lane A – untreated marrow aspirates. B – marrow aspirates treated with 0.6X trypsin. C – untreated hMSCs. FN ctrl and LN ctrl were commercially available FN and LN proteins. Results of a representative experiment (one of three independent experiments with similar results) are shown here.

6.3.3 Comprehensive study of integrin expression, protein reduction and colony formation of marrow aspirates from four individuals

The effectiveness of the proposed cell pre-loading protein reduction treatments was critically evaluated by their ability to reduce matrix molecules associated with cells and hence increase colony formation in CFU assays. Bone marrow aspirate samples from four individuals were used in this study. Western blots showed that just by washing, matrix molecules associated with aspirate cells could be reduced by a moderate amount. Washing aspirate cells with PBS or GRGDSP solution further reduced the level of fibronectin and laminin (Figure 6.7a). In half of the patient samples tested, the level of fibronectin and laminin was visibily the lowest for cells treated with PBS without divalent

ions (Figure 6.7b) while for the other half of the patients, this further reduction effect was not visible to the eye after the image of the blot was developed.

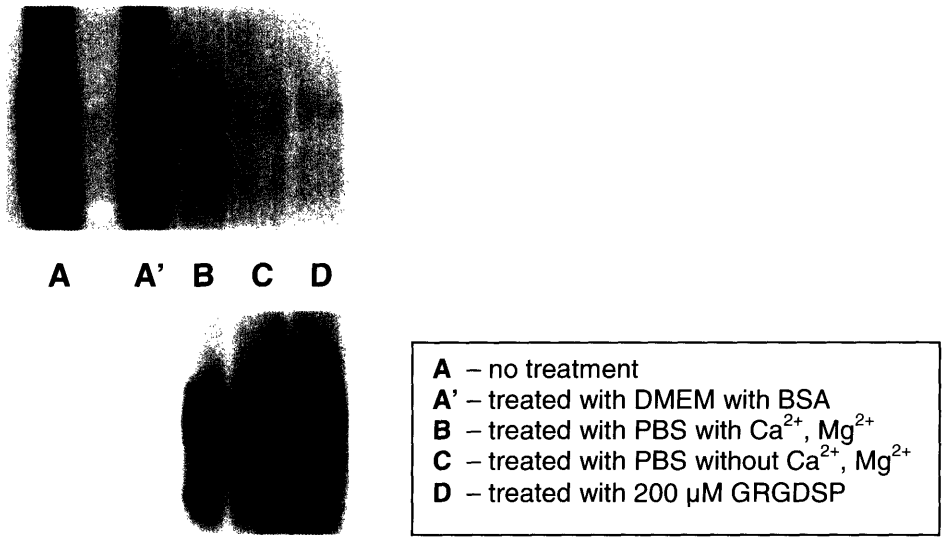

Figure 6.7 Fibronectin level of marrow aspirates treated with various treatments. **Top (a)** The amount of fibronectin associated with marrow aspirates was reduced to a different extent after washing. Letters beside each lane denotes what treatment the cells received before they were lysed. **Bottom (b)** Higher contrast image of Lanes B to D of the image shown in (a). All lanes were loaded with protein lysates from the same number of cells. Blot with laminin also showed a similar trend (data not shown).

CFU assay revealed two different colony formation behavior when marrow aspirate cells handled with various treatments were seeded onto Lab-tek, GRGDSPY and comb substrates. Marrow samples from patient 1 and 3 showed much fewer colony formation than patient 2 and 4 on Lab-tek glass slides (Table 6.1). However, treatment with PBS without divalent ions enhanced CFU formation on RGD surfaces compared to untreated ones for patient 1 and 3. On the other hand, CFU formation decreased after any treatments for patient 2 and 4. Large variation in single cell adhesion but no particular trend was seen for all patients. (data not shown.) Alkaline phophatase expression also

partitioned patient 1 and 3 into the group in which all except one CFUs on Lab-tek surfaces were weak AP^+, while two subpopulations of CFUs, strong AP^+ and weak AP^+ or AP^-, were observed on patient 2 and 4 (Figure 6.9). In addition, CFUs formed on RGD surfaces from patient 1 and 3 marrow cells treated with divalent-ion free PBS were all AP^+. On the other hand, CFUs of patient 2 and 4 on RGD surfaces were all AP^-. A correlation of colony size and AP expression was also observed. CFUs that are AP^- were colonies of smaller size. Strong AP^+ CFUs were usually larger colonies. Some of these strong AP^+ CFUs showed stronger AP staining at the center of the colony and fainter as one goes towards the periphery (Figure 6.8).

		Early adherent colonies						Early adherent colonies			
		A	**B**	**C**	**D**			**A**	**B**	**C**	**D**
Pt 1	Lab-tek	14	10	7	8	**Pt 2**	Lab-tek	36	44	42	43
	RGD	2	0	8	0		RGD	4	0	0	0
	comb	0	0	0	0		comb	1	0	1	0
Pt 3	Lab-tek	4	1	3	0	**Pt 4**	Lab-tek	31	25	18	10
	RGD	0	0	3	0		RGD	7	0	2	0
	comb	1	1	0	0		comb	0	2	0	0

Table 6.1 CFU formation from marrow aspirates pre-treated with PBS with Ca^{2+} and Mg^{2+} (B), PBS without Ca^{2+} and Mg^{2+}(C) and 200 μM GRGDSP solution (D). No treatments were performed on A. Counts of early adherent CFUs from marrow samples from all 4 patients used in this comprehensive study is shown here.

Interestingly, FACS analysis showed a higher percentage of cells that express α_5 and $\alpha_v\beta_3$ in the $CD45^-$ $CD105^+$ and non- $CD45^-$ $CD105^+$ populations for patient 1 and 3 than patient 2 and 4 (Figure 6.10). The higher expression corresponds to the patients with higher early adherent CFU counts on RGD surfaces after divalent-ion free PBS treatment. No significant difference in the percentage of $CD45^-$ $CD105^+$ cells to all marrow cells was observed among the 4 patients. Similar to the FACS results shown in

the previous section, α_4 expression was higher for $CD45^-$ $CD105^+$ cells in 3 out of 4 patients. Table 6.2 summaries all the differences observed between Group I (patients 1 and 3) and Group II patients (patients 2 and 4). However, these trends and differences showed no correlation with patients' age, gender and race (Table 6.3).

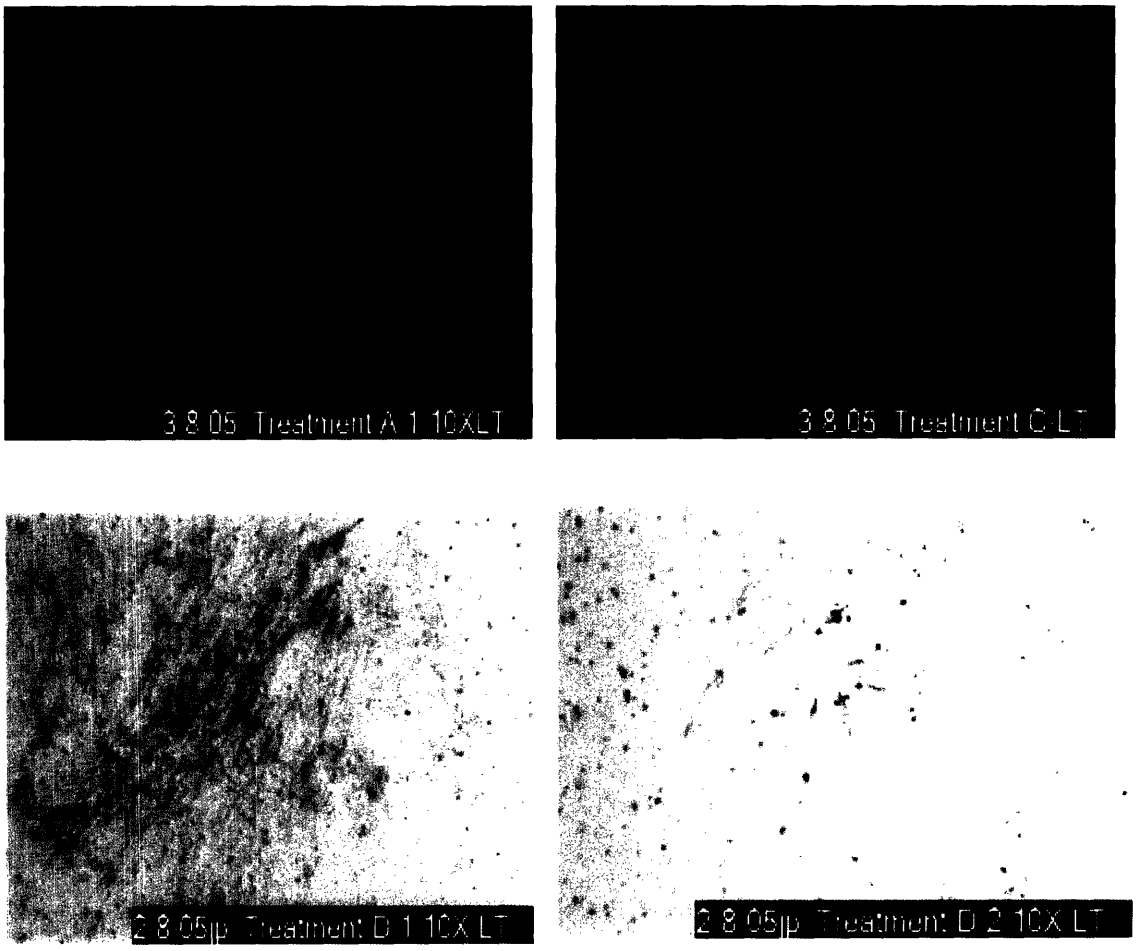

Figure 6.8 Representative images of CFU-AP on Lab-tek surfaces. **Top left (a)** fluorescence image of a typical CFU-AP. AP expression was even across the colony. **Top right (b)** a CFU-AP stained strongly with AP. AP expression was very strong at the center of the colony and fainter as one moved towards the periphery. **Bottom left (c)** bright field image of a large strong-AP^+ CFU. A small colony on the same surface was AP^-. (**Bottom right (d)**)

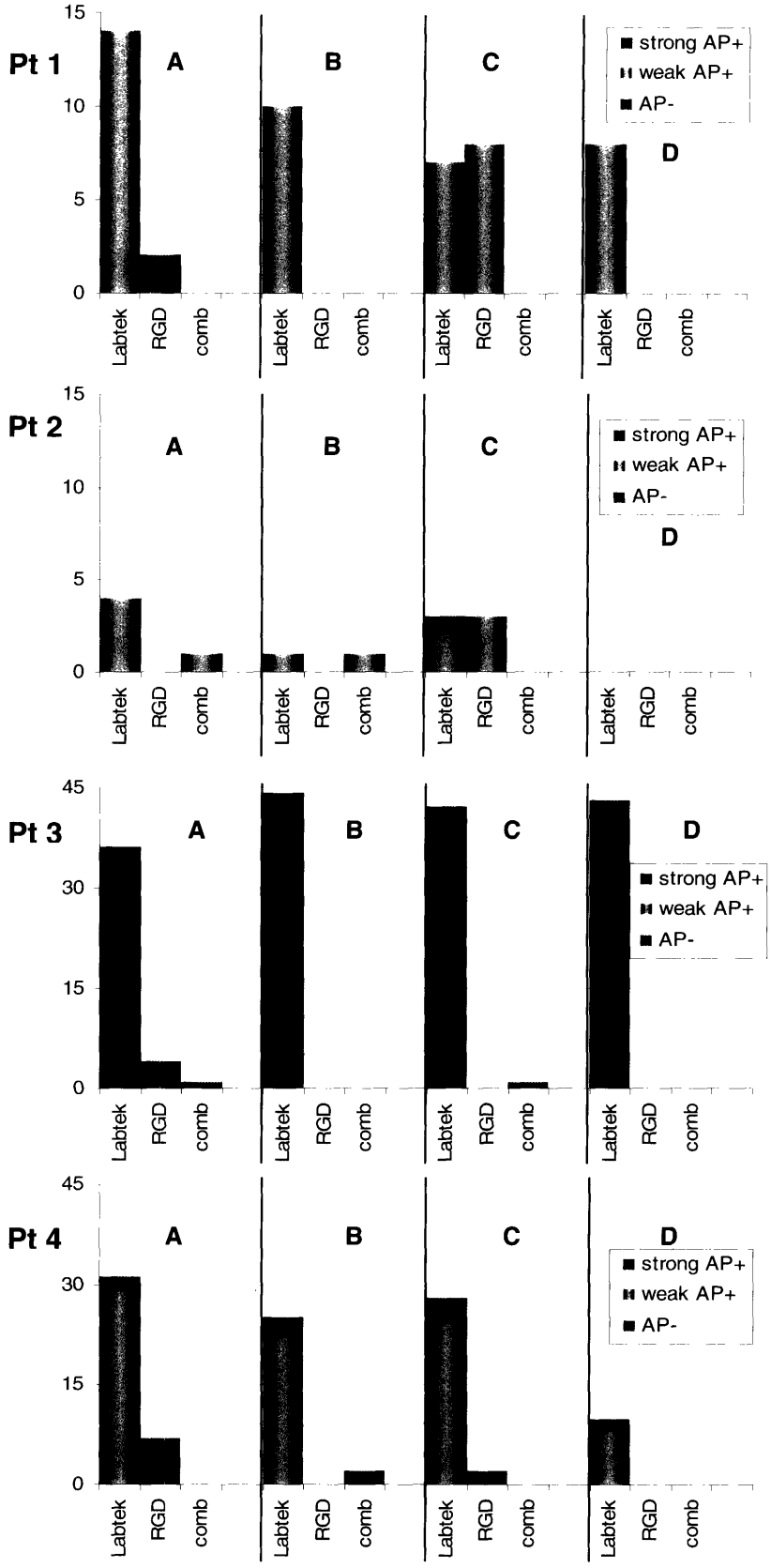

Figure 6.9 CFU-AP formation of marrow samples from all 4 patients after aspirate cells had been treated with divalent ion-containing PBS (B), divalent ion-free PBS (C), and 200 μM GRGDSP solution (D). No treatments were received by the control cells (A) . The total height of each bar shows the total number of CFU formed on that surface and the height of each color showed the AP expression of the colonies as indicated in the legend.

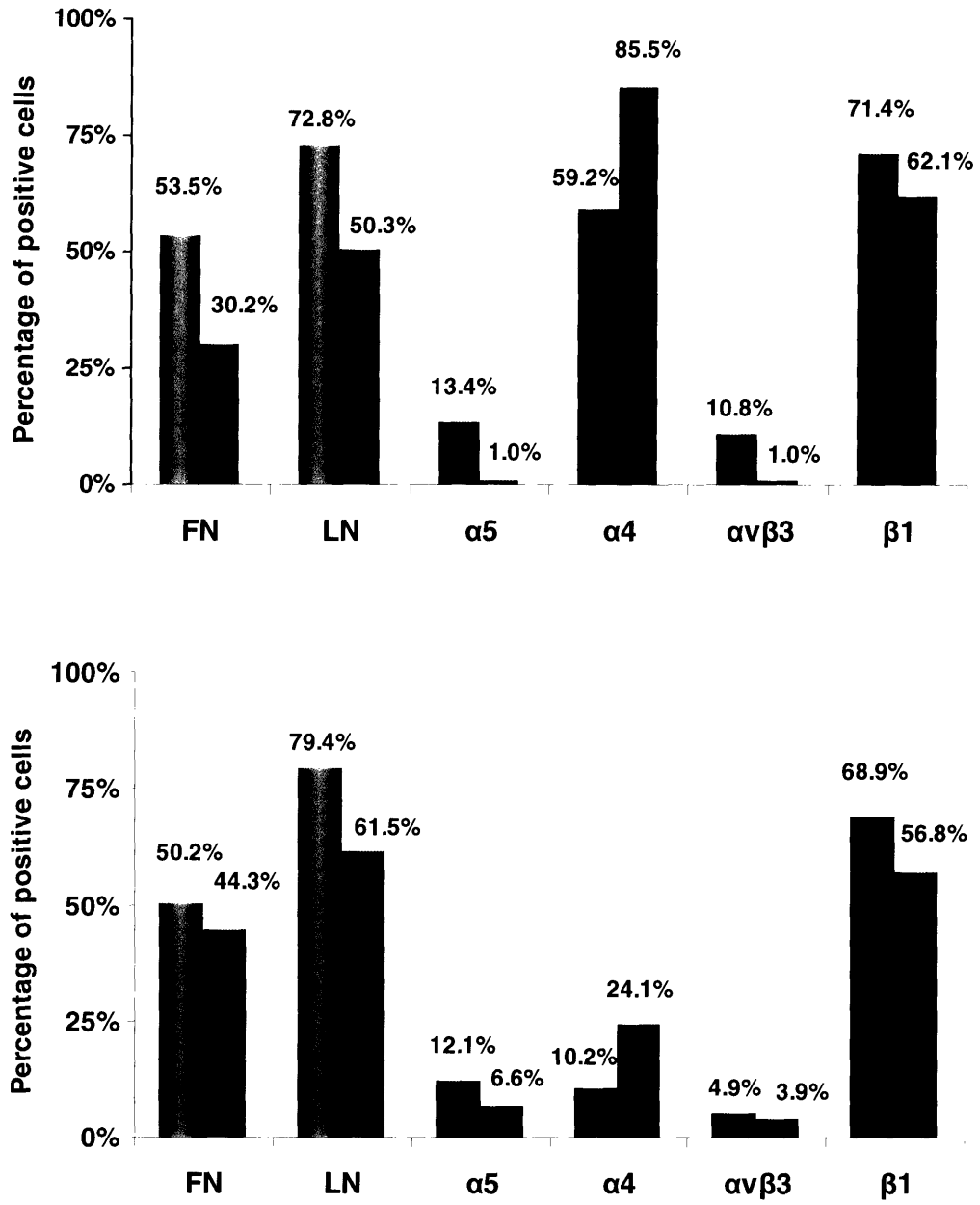

Figure 6.10 Comparison of Patient 1 and Patient 2 ECM protein and integrin expression. **Top (a)** $CD45^-$ $CD105^+$ population. **Bottom (b)** All non- $CD45^-$ $CD105^+$ cells. In each set of 2 bars, all bars on the left (pink) indicate results from Patient 1 and bars on the right (blue) Patient 2. α_5 and $\alpha_v\beta_3$ expression of $CD45^-$ $CD105^+$ cells was about 10-fold higher in Patient 1 than Patient 2. Comparison of Patient 3 and Patient 4 showed similar trend. (Also see Table 6.2)

	Group I (Patient 1 & 3)	**Group II** (Patient 2 & 4)
Number of CFUs on Lab-tek	Low (< 15)	High (20 – 40)
Effect of divalent ion-free PBS treatment on colony formation on RGD surfaces	Drastically increased CFU formation	Decreased CFU formation
Ratio of marrow cells expressing α_5 and $\alpha_v\beta_3$	- Expression of both integrins on Pt 1 cells higher than Pt 2 - α_5 expression on Pt 3 > that on Pt 4 but similar expression of $\alpha_v\beta_3$ by both patient samples	
CFU AP expression on Lab-tek	All CFUs (except one) were homogeneously weak AP^+	2 populations of CFUs for each patient: - weak AP^+ or AP^- - strong AP^+
CFU AP expression on RGD surfaces	All CFUs are AP^+	All CFUs are AP^-

Table 6.2 Marrow aspirates from the 4 individuals tested partitioned into two groups of different CFU formation behavior, integrin expression and AP expression.

	Age	**Gender**	**Race**
Patient 1	56	F	African American
Patient 2	74	M	Caucasian
Patient 3	78	M	Caucasian
Patient 4	73	F	Caucasian

Table 6.3 Age, gender and race information of the four individuals whose marrow aspirates were used in this comprehensive study. All 4 patients were diagnosed with osteoarthritis. No correlation between colony formation experimental results and patient profile was observed.

6.4 Discussion

To understand adhesion and colony formation behavior of CTPs from bone marrow aspirates, FACS analysis was employed to reveal first, what ECM molecules were associated with CTPs and other marrow cells, and second, what integrins these cells express. The $CD45^-$ $CD105^+$ gating was used to identify an enriched population of mesenchymal stem cells or CTPs for reasons described in Section 6.1. Comparing the percentage of marrow aspirate cells that were $CD45^-$ $CD105^+$ ((0.40 ± 0.11) %) with the prevalence of CFU-APs (55 per 1 million nucleated marrow cells) as reported by the Muschler group and the ratio of CFU-APs to CFUs from our data (~ 90%), approximately 1 in 65 $CD45^-$ $CD105^+$ cells might form CFU on Lab-tek surfaces. If indeed as claimed by numerous reports in the literature that CTPs are $CD45^-$ $CD105^+$ as discussed above, the $CD45^-$ $CD105^+$ population provided a significant enrichment of CTPs with colony formation ability (1 in ~ 65 $CD45^-$ $CD105^+$ cells).

A fair portion of both $CD45^-$ $CD105^+$ and non- $CD45^-$ $CD105^+$ populations expresses α_4, α_5, $\alpha_v\beta_3$ and β_1 integrins. Even though large variation in α_5 and $\alpha_v\beta_3$ expression was observed, the expression of the α_4, α_5, $\alpha_v\beta_3$ and β_1 subunits was consistent with previous reports on integrin expression by marrow mesenchymal stem cells or marrow-derived osteoprogenitors (Conget and Minguell, 1999; Gronthos et al., 2001). The large variation in α_5 and $\alpha_v\beta_3$ expression observed was also consistent with the partitioning of marrow samples of the 4 individuals in the comprehensive study. The large difference in the percentage of cells expressing α_5 and $\alpha_v\beta_3$ between in Group I and II patients' marrow cells demonstrated such variability. The variation in α_5 and $\alpha_v\beta_3$ expression was also consistent with the variation in the amount of CFU formation on RGD surfaces.

The α_4 subunit is an adhesion-related antigen of which expression by marrow-derived MSCs or progenitors differed among reports (Soligo et al., 1990; Conget and Minguell, 1999; Franceschi, 1999; Gronthos et al., 2001; Minguell et al., 2001). Our FACS results, however, showed α_4 as the integrin subunit expressed by the highest percentage of

$CD45^-$ $CD105^+$ cells compared to other integrins. (61.2 ± 8.25) % of $CD45^-$ $CD105^+$ cells were α_4^+ and it was the only integrin subunit that showed a significantly higher percentage of positive cells in the $CD45^-$ $CD105^+$ population than non- $CD45^-$ $CD105^+$. Interestingly, in Chapter 5, results from CFU assays showed that two of the three substrates that were the most potent in supporting CFU-AP formation were made of $\alpha_4\beta_1$ peptides. Even though the stellar performance by the 59-mer $\alpha_4\beta_1$ peptide in promoting CFU-AP formation could be due to the higher affinity of the peptide to $\alpha_4\beta_1$ integrins than GRGDSPY to $\alpha_5\beta_1$ or $\alpha_v\beta_3$, the enhancement in CFU-AP formation by the low affinity $\alpha_4\beta_1$ CS-1 peptide still points to the possibility that α_4 may be one of the predominant integrins utilized by CTPs to mediate osteoblastic colony formation.

Consistent with the report by Gronthos et al. (Gronthos et al., 2001), our study showed no measurable level of α_3 on the cell surface of CTPs. However, in contrast to the same report, no expression of α_6 was detected. The expression of α_4, α_5, $\alpha_v\beta_3$ and β_1 by marrow cells in our FACS analysis confirmed our previous choice in Chapter 4 in focusing on $\alpha_4\beta_1$, $\alpha_5\beta_1$, $\alpha_v\beta_3$ as potential integrins to be targeted for the selective adhesion and colony formation of CTPs.

Immunoblotting showed a much higher level of fibronectin and laminin association with marrow aspirate cells than hMSC cell line. These proteins were likely from the microenvironment the marrow cells resided. Collagen IV, fibronectin, laminin had been shown to be in abundance in bone marrow fibrous tissue (Klein, 1995; Lucena et al., 1997). Therefore, when bone marrow was aspirated, these proteins in which bone marrow cells were once embedded were drawn into the aspirate along with the cells. As a result, marrow cells were still in their proteins after they were aspirated. Since our hypothesis was that the small amount of marrow cell adhesion observed was due to the shrouding of bone marrow aspirate cells by a large amount of ECM proteins, the amount of protein associated with marrow aspirate cells and hMSC cell line immediately before seeding onto peptide substrates was assessed. Therefore, protein level of marrow cells was compared with hMSCs detached from culture plates by trypsinizing and re-

suspended in culture media. Although our studies showed that incubation of marrow aspirates with trypsin was effective in reducing the amount of associated fibronectin and laminin, protein-reduction treatments less detrimental were needed to avoid the disruption of the adhesion and differentiation potential of progenitor cells due to their sensitivity to external cues. Therefore, 30-minute incubation of marrow aspirate cells with PBS (with and without divalent ions) and RGD solution was experimented to reduce matrix molecule association with marrow cells. Incubation with RGD solution reduced the amount of fibronectin and laminin associated with aspirate cells to a level similar to the action of trypsin. (data not shown.) Since the level of reduction by RGD and PBS was also similar (and in half of the patients, reduction was even visibly greater when treated with divalent ion-free PBS), we concluded that washing with PBS or RGD solution, but not BSA-containing DMEM, were effective in matrix molecule reduction.

The most striking results from the 4-patient comprehensive study of CFU formation and ECM and integrin expression of marrow aspirate was the partitioning of the 4 patients into two groups with very different cell behavior and expression, but within each group, remarkable consistency was observed. The increase in CFU formation on RGD surfaces by cells treated with divalent ion-free PBS in only Group I patients could be attributed by the higher percentage of α_5 and $\alpha_v\beta_3$ expressing cells in Group I, in particular the $CD45^-$ $CD105^+$ cells. Incubation with divalent ion-free PBS reversed integrin binding to the matrix molecule shroud and therefore, for samples with more cells expressing α_5 and $\alpha_v\beta_3$, more cells would have exposed integrins available for binding after washing. Hence, the increase in adhesion and CFU formation on RGD surfaces was greater for Group I patients. CTP adhesion and colony formation on RGD surfaces could be mediated by a combination of α_5 and $\alpha_v\beta_3$ integrins. GRGDSP has been extensively shown to mediate $\alpha_v\beta_3$ adhesion and validation of GRGDSPY surfaces with CHO-K1 cells which expressed only $\alpha_5\beta_1$ but not $\alpha_v\beta_3$ showed that $\alpha_5\beta_1$ could also mediate adhesion on GRGDSPY surfaces (Figure 6.9). There might be a difference in whether α_5 or $\alpha_v\beta_3$ were utilized by CTPs from each group of patients to mediate adhesion or colony formation, and therefore leading to a difference in AP expression by CFUs on

GRGDSPY surfaces between the two patient groups. (All CFUs on RGD surfaces are AP^+ for Group I and all AP^- for Group II.) In fact, Keselowsky et al. showed that mineralization of MC3T3-E1 immature osteoblasts on fibronectin was inhibited by blocking with β_1 but not β_3 antibodies, suggesting that even though both $\alpha_5\beta_1$ and $\alpha_v\beta_3$ integrins could mediate the adhesion of immature osteoblasts, only $\alpha_5\beta_1$ could mediate the differentiation of these cells (Keselowsky et al., 2005). The possible difference in integrins utilized by marrow cells in mediating adhesion may also contribute to the difference in AP expression by CFUs on Lab-tek by the two patient groups. However, the reasons for the consistent differences observed between the two groups of patients were not known. The difference might be inherent to patient variability.

Treatment of marrow aspirate cells with GRGDSP solution prior to plating on substrates did not enhance CFU formation on RGD surfaces in any marrow samples. RGD peptide solution was effective in reducing the amount of fibronectin and laminin associated with aspirate cells, as shown by immunoblotting. However, even though the two washes after the RGD solution treatment would have removed RGD remaining in the cell media, cell integrins might still be occupied by RGD peptides when the cells were plated on the substrates and thus were inhibited to bind to RGD substrates. All pre-plating treatment of marrow aspirate cells actually decreased CFU formation on Lab-teks for three out of the four patient samples tested. This was likely a result of the reduced protein level after pre-loading treatments. As a result, less protein was adsorbed to Lab-tek surfaces to support the adhesion and colony formation of CTPs. In fact, for three out of four patients, the number of CFUs formed on Lab-tek from marrow aspirates treated with divalent ion-free PBS and GRGDSP solution was lower than that of marrow aspirates treated with divalent ion-containing PBS, implying a higher capability in reducing ECM proteins using divalent ion-free PBS and GRGDSP solution.

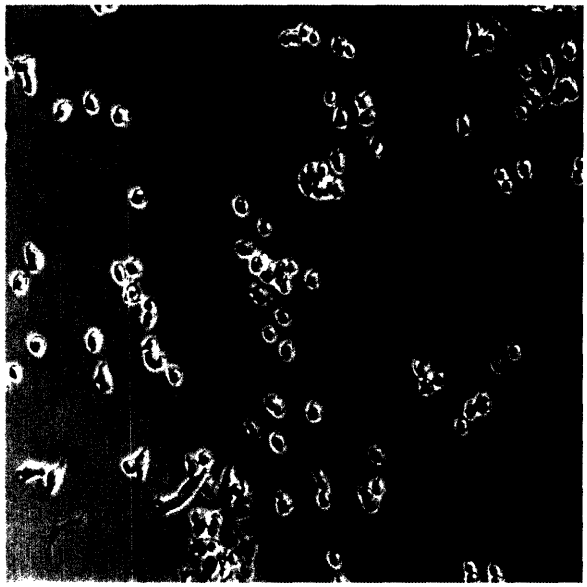

Figure 6.9 Adhesion of CHO-K1 cells on GRGDSPY surfaces. Adhesion on GRGDSPY surface was mediated by $\alpha_5\beta_1$ as CHO-K1 expressed only $\alpha_5\beta_1$ but not $\alpha_v\beta_3$.

In summary, in this chapter, we found that a portion of CTP-enriched $CD45^-$ $CD105^+$ population as well as a portion of all other marrow cells were α_4^+, α_5^+, $\alpha_v\beta_3^+$ and β_1^+, even though we observed a large patient-to-patient variation in α_5 and $\alpha_v\beta_3$ expression. A significant portion of $CD45^-$ $CD105^+$ population was α_4^+, statistically much higher than that of the non- $CD45^-$ $CD105^+$ population. High level of ECM proteins were associated with marrow aspirate cells but various washing treatments could reduce the amount of protein to various extents. Experimental data on integrin expression and CFU-AP formation partitioned patient marrow samples into two groups that showed very different cell behavior and integrin expressions. In one group, the treatment of marrow aspirate cells with divalent ion-free PBS did increase CFU formation as we hypothesized. The consistency within each group of patients suggested that patient variability might not be totally stochastic and could be accounted for.

6.5 References

Aubin, J. and Heersche, J.N.M. (2000). "Osteoprogenitor cell differentiation to mature bone-forming osteoblasts." Drug Development Research **49**: 206-215.

Aumailley, M., Timpl, R. and Sonnenberg, A. (1990). "Antibody to integrin α6 subunit specifically inhibits cell-binding to laminin fragment 8." Experimental Cell Research **188**: 55-60.

Barry, F.P., Roynton, R.E., Haynesworth, S., Murphy, J.M. and Zaia, J. (1999). "The monoclonal antibody SH-2, raised against human mesenchymal stem cells, recognizes an epitope on endoglin (CD105)." Biochem. Biophys. Res. Commun **265**: 134-139.

Chuntharapai, A., Bodary, S., Horton, M. and Kim, K.J. (1993). "Blocking monoclonal antibody to αvβ3 integrin: a unique epitope of αvβ3 integrin is present on human osteoclasts." Experimental Cell Research **205**: 345-352.

Conget, P.A. and Minguell, J.J. (1999). "Phenotypical and functional properties of human bone marrow mesenchymal progenitor cells." Journal of Cell Physiology **181**: 67-73.

Cruz, M.A., Chen, J.M., Whitelock, J.L., Morales, L.D. and Lopez, J.A. (2005). "The platelet glycoprotein Ib-von Willebrand factor interaction activates the collagen receptor alpha 2 beta 1 to bind collagen: activation-dependent conformational change of the alpha 2-I domain." Blood **105**(5): 1986-1991.

Duff, S.E., Li, C.G., Garland, J.M. and Kumar, S. (2003). "CD105 is important for angiogenesis: evidence and potential applications." FASEB Journal **17**(9): 984-992.

Franceschi, R.T. (1999). "The developmental control of osteoblast-specific gene expression: Role of specific transcription factors and the extracellular matrix environment." Critical Reviews in Oral Biology and Medicine **10**(1): 40-57.

Fujiyama, S., Amano, K., Uehira, K., Yoshida, M., Nishiwaki, Y., Nozawa, Y., Jin, D., Takai, S., Miyazaki, M., Egashira, K., Imada, T., Iwasaka, T. and Matsubara, H. (2003). "Bone marrow monocyte lineage cells adhere on injured endothelium in a monocyte chemoattractant protein-1-dependent manner and accelerate reendothelialization as endothelial progenitor cells." Circulation Research **93**(10): 980-989.

Gronthos, S., Graves, S.E., Ohta, S. and Simmons, P.J. (1994). "The STRO-1+ fraction of adult human bone marrow contains the osteogenic precursors." Blood **84**(12): 4164-4173.

Gronthos, S., Simmons, P.J., Graves, S.E. and Robey, P.G. (2001). "Integrin-mediated Interactions Between Human Bone Marrow Stromal Precursor Cells and the Extracellular Matrix." Bone **26**(2): 174-181.

Guo, B.Q., Rooney, P., Slevin, M., Li, C.G., Parameshwar, S., Liu, D.H., Kumar, P., Bernabeu, C. and Kumar, S. (2004). "Overexpression of CD105 in rat myoblasts: Role of CD105 in cell attachment, spreading and survival." International Jouranl of Oncology **25**(2): 285-291.

Jiang, Y., Jahagirdar, B.N., Reinhardt, R.L., Schwartz, R.E., Keene, C.D., Ortiz-Gonzalez, X.R., Reyes, M., Lenvik, T., Lund, T., Blackstad, M., Du, J., Aldrich, S., Lisberg, A., Low, W.C., Largaespada, D.A. and Verfaillie, C.M. (2002). "Pluripotency of mesenchymal stem cells derived from adult marrow." Nature **418**: 41-49.

Keselowsky, B.G., Collard, D.M. and Garcia, A.J. (2005). "Integrin binding specificity regulates biomaterial surface chemistry effects on cell differentiation." Proceedings of the Nation Academy of Sciences of the United States of America **102**(17): 5953-5957.

Klein, G. (1995). "The extracellular matrix of the hematopoietic microenvironment." Experientia **51**: 914-926.

Lodie, T.A., Blickarz, C.E., Devarakonda, T.J., He, C.F., Dash, A.B., Clarke, J., Gleneck, K., Shihabuddin , L. and Tubo, R. (2002). "Systematic analysis of reportedly distinct populations of multipotent bone marrow-derived stem cells reveals a lack of distinction." Tissue Engineering **8**(5): 739-751.

Lucena, S.B., Duarte, M.E.L. and Fonseca, E.C. (1997). "Plastic embedded undecalcified bone biopsies: An immunohistochemical method for routine study of bone marrow extracellular matrix." Journal of Histotechnology **20**(3): 253-257.

Majumdar, M.K., Banks, V., Peluso, D.P. and Morris, E.A. (2000). "Isolation, characterization, and chondrogenic potential of human bone marrow-derived multipotential stromal cells." Journl of Cellular Physiology **185**(1): 98-106.

Meinel, L., Karageorgiou, V., Fajardo, R., Snyder, B., Shinde-Patil, V., Zichner, L., Kaplan, D., Langer, R. and Vunjak-Novakovic, G. (2004). "Bone tissue engineering using human mesenchymal stem cells: Effects of scaffold material and medium flow." Annals of Biomedical Engineering **32**(1): 112-122.

Minguell, J.J., Erices, A. and Conget, P. (2001). "Mesenchymal stem cells." Experimental Biology and Medicine **226**(6): 507-520.

Nhieu, G.T.V. and Isberg, R.R. (1991). "The Yersinia pseudotuberculosis invasin protein and human fibronectin bind to mutually exclusive sites on the α5β1 integrin receptor." Journal of Biological Chemistry **266**: 24367.

Pittenger, M.F., Mackay, A.M., Beck, S.C., Jaiwal, R.K., Douglas, R., Mosca, J.D., Moorman, M.A., Simonetti, S.W., Craig, S. and Marshak, D.R. (1999). "Multilineage Potential of Adult Human Mesenchymal Stem Cells." Science **284**(5411): 143-147.

Soligo, D., Schiro, R., Luksch, R., Manara, G. and Quirici, N. (1990). "Expression of integrains in human bone marrow." British Journal of Haematology **76**: 323-332.

Sonnenberg, A., Daams, H. and van der Valk, M.A. (1986). "Development of mouse mammary gland: Identification of stages in differentiation of luminal and myoepithelial cells using monoclonal antibodies and polyvalent antiserum against keratin." Journal of Histochemistry and Cytochemistry **34**: 1037-1046.

Thomas, M.L. (1989). "The leukocyte common antigen family." Annual Review of Immunology **7**: 339-369.

Tocci, A. and Forte, L. (2003). "Mesenchymal stem cell: use and perspectives." Hematology Journal **4**: 92-96.

Trowbridge, I.S. and Thomas, M.L. (1994). "An emerging role as a protein tyrosine phosphatase required for lymphocyte activation and development." Annual Review of Immunology **12**: 85-116.

VanNhieu, G.T. and Isberg, R.R. (1993). "Bacterial internalization mediated by β1 chain integrins is determined by ligand affinity and receptor density." EMBO J **12**: 1887.

Vogel, W., Grunebach, F., Messam, C.A., Kanz, L., Brugger, W. and Buhring, H.J. (2003). "Heterogeneity among human bone marrow-derived mesenchymal stem cells and neural progenitor cells." Haematologica **88**: 126-133.

Chapter 7

Conclusions and Future Directions

7.1 Conclusions

In *in vivo* connective tissue engineering, the presence of a substrate and an environment inductive to cell adhesion and function is crucial to the success in engineering tissues. In this dissertation, a multi-dimensional approach was taken in an attempt to optimize the molecular design of substrates for the selective adhesion, proliferation and differentiation of connective tissue progenitors from human bone marrow aspirates. We optimized the base substrate material by the critical choice of a highly cell-resistant comb copolymer with sufficient functionalizable sites. When biophysical design was applied to the clustered presentation of peptides, we observed an enhancement of cell adhesion as cell spreading increased on more peptide substrates with a higher degree of clustering. The biochemical design showed that with the right choice of peptides, CFU-AP formation, an indication of CTP adhesion, proliferation and differentiation, could be enhanced. The bone sialoprotein peptide FHRRIKA and peptides that target $\alpha_4\beta_1$ integrins promoted CFU-AP formation. Through a critical evaluation of the CFU assay, we standardized the assay with the better positive control Lab-tek and a lower but more optimal seeding density. The evaluation also revealed the extent of patient variability even on standard controls. In spite of the multi-faceted design of CTP-selective substrates, it was the understanding of marrow aspirate cells through cell studies that led us to explore the possibility of further enhancing colony formation from the angle of marrow aspirate cell manipulation. FACS elucidated bone marrow integrin profile and immunoblotting showed that the high level of matrix molecule association with marrow aspirate cells that could be reduced by washing with PBS and RGD solution. On the other hand, peptide substrates designed earlier in turn allowed us to test whether matrix molecule shrouding

of marrow cells prohibited CTP colony formation. RGD substrates, when used in CFU assays, also revealed the natural partition phenomemon of patient marrow samples according to the expression of marrow cells and colony formation behavior. This could shed light on possible trends in accounting for the huge patient variations observed with bone marrow aspirates. Therefore, this work is an example of how in the optimization of substrates for tissue engineering applications, substrate design and the understanding of the target cells go hand-in-hand. The understanding of cells contributes to the improvement of the design of tissue engineering substrates, which in turn serves as tools to provide a further and more in-depth understanding of the cells of interest. It is our hope that not only the knowledge gained in this dissertation on marrow cells, CTPs in particular, provides a better understanding in this behavior and molecular profile, but the design of the optimized CFU assay with clustered-peptide substrates offers a set of tools for further understanding human bone marrow cells.

7.2 Future directions

The set of tools developed in this dissertation could be applied to study the effect of other adhesion molecules on CTP adhesion, proliferation and differentiation. Adhesion peptides that showed high preferentiality in binding to $\alpha_5\beta_1$ integrins were of particular interest. A recent report showed that blocking MC3T3-E1 immature osteoblasts with β_1 but not β_3 antibodies inhibited the mineralization of the cells on fibronectin, suggesting that even though both $\alpha_5\beta_1$ and $\alpha_v\beta_3$ integrins could mediate the adhesion of immature osteoblasts, only $\alpha_5\beta_1$ could mediate the differentiation of these cells (Keselowsky et al., 2005). A branched $\alpha_5\beta_1$ peptide that consists of both the RGD and PHSRN synergy site from fibronectin, separated by a spacer that consists of 5 glycine and a lysine, has recently been developed in our lab (Ufret et al., 2005). With our FACS data showing a fair portion of CTP-enriched cell population expressing α_5 and the availability of this recently developed peptide with high binding affinity to $\alpha_5\beta_1$, the assays developed in this thesis could be applied to see whether $\alpha_5\beta_1$ substrates could support more colony

formation and osteoblastic differentiation of human marrow-derived CTPs than GRGDSPY surfaces that have higher affinity towards $\alpha_v\beta_3$ than $\alpha_5\beta_1$. This proposed study is one of the many possibilities that the tools and assays developed in this thesis can be used to study the function and behavior of CTPs and marrow aspirate cells.

7.3 References

Keselowsky, B.G., Collard, D.M. and Garcia, A.J. (2005). "Integrin binding specificity regulates biomaterial surface chemistry effects on cell differentiation." Proceedings of the Nation Academy of Sciences of the United States of America **102**(17): 5953-5957.

Ufret, M.L., Richardson, L.B. and Griffith, L.G. (2005). "Multiple Polymer-tethered Ligand Presentation: Fibroblast Adhesion and Signaling by Tethered EGF and Fibronectin-like Branched RGD-PHSRN Peptide." (In Preparation).

Appendix

IUPAC Amino Acids Abbreviations

Alanine	Ala	A
Arginine	Arg	R
Asparagine	Asn	N
Aspartic acid	Asp	D
Cysteine	Cys	C
Glutamine	Gln	Q
Glutamic acid	Glu	E
Glycine	Gly	G
Histidine	His	H
Isoleucine	Ile	I
Leucine	Leu	L
Lysine	Lys	K
Methionine	Met	M
Phenylalanine	Phe	F
Proline	Pro	P
Serine	Ser	S
Threonine	Thr	T
Tryptophan	Trp	W
Tyrosine	Tyr	Y
Valine	Val	V